
Doctoral Dissertations

Student Theses and Dissertations

Spring 2018

The effect of overloading on reliability of wheel loader structural components

Eric Raymond Achelpohl

Follow this and additional works at: https://scholarsmine.mst.edu/doctoral_dissertations



Part of the [Mining Engineering Commons](#)

Department: Mining and Nuclear Engineering

Recommended Citation

Achelpohl, Eric Raymond, "The effect of overloading on reliability of wheel loader structural components" (2018). *Doctoral Dissertations*. 2655.

https://scholarsmine.mst.edu/doctoral_dissertations/2655

This thesis is brought to you by Scholars' Mine, a service of the Missouri S&T Library and Learning Resources. This work is protected by U. S. Copyright Law. Unauthorized use including reproduction for redistribution requires the permission of the copyright holder. For more information, please contact scholarsmine@mst.edu.

THE EFFECT OF OVERLOADING ON RELIABILITY OF
WHEEL LOADER STRUCTURAL COMPONENTS

by

ERIC RAYMOND ACHELPOHL

A DISSERTATION

Presented to the Faculty of the Graduate School of the
MISSOURI UNIVERSITY OF SCIENCE AND TECHNOLOGY

In Partial Fulfillment of the Requirements for the Degree

DOCTOR OF PHILOSOPHY

in

MINING ENGINEERING

2018

Approved

Kwame Awuah-Offei, Advisor
Paul N. Worsey
Samuel Frimpong
Leslie Gertsch
Nassib Aouad

© 2018
Eric Raymond Achelpohl
All Rights Reserved

ABSTRACT

This research attempts to provide a fundamental understanding into the relationship between the productivity of material handling equipment, specifically wheel loaders, and their ability to operate reliably when subjected to high overload conditions. The overall aim is to determine the effect of overloading the bucket on wheel loader reliability. The specific objectives of the research are to: 1) evaluate the effect of overloading the bucket on wheel loader productivity; 2) examine the effect of overloading the bucket on hydraulic pressures in the hoist cylinders (used as a proxy for forces on a wheel loader); and 3) investigate the effect of overloading the bucket on the reliability of structural components of a wheel loader.

To achieve these objectives, the research used data from on-board equipment monitors from the global fleet of ultra-class wheel loaders for a specific original equipment manufacturer to test the various research hypotheses. The data included production data, failure and repair data, and hydraulic cylinder pressures, which were used as a proxy for stresses on structural components. ANOVA and Pearson and Spearman correlations tests were performed on data samples to test the hypotheses. Duty-cycle relationships were established using linear life stress relationships ratios for the wheel loaders structural components. The research showed that, while higher bucket loads increase productivity, there is evidence that they slow down the loading cycle, may be detrimental to productivity. The hoist cylinder pressure increased with increasing payload weight. The reliability of the structural components was similar in both the standard and duty-cycle cases; although, the accuracy of the reliability models increased when the models accounted for duty-cycles.

ACKNOWLEDGEMENTS

The author would like to thank Dr. Kwame Awuah-Offei, principal advisor, for his guidance and assistance during the completion of this dissertation. The author would also like to thank Dr. Paul Worsey for his assistance during the preparation of this dissertation. The author also extends his thanks to Dr. Samuel Frimpong, Dr. Leslie Gertsch, and Dr. Nassib Aouad for their help and guidance in preparing this research.

The author thanks Jesse Dubberly, Product Support Manager, for his support and supervision during the research and writing of the dissertation. Special thanks are extended to Rodney Bull, Vice President and General Manager, Longview Operations and Marr Barr, Engineering Director. The author also extends special to Eric Richter and William De Porter for their input and guidance during the preparation of this dissertation.

More personally, the author would like to thank Russ and JoAnn Achelpohl, his parents, for their continued love, support and editing during my doctoral study. He would also like to thank Rebecca Fikar, his girlfriend, for her constant love and support in returning to graduate school.

Roy Anderson, Andrew Hartford, Steven Jones, and Kevin Sanson for gathering downloads of the wheel loaders operating around the world. The author would also like to thank the following people: my Wheel Loader Product Support team members for their help in the gathering data and assistance in reviewing of the project Lazaro, Gary, Richard, William, Mark, Philip and Melissa. Additionally, thank you to Shirley, Judy, Tina, DeWayne, and Jimmie for their assistance throughout my doctoral study.

TABLE OF CONTENTS

	Page
ABSTRACT.....	iii
ACKNOWLEDGEMENTS.....	iv
LIST OF ILLUSTRATIONS.....	x
LIST OF TABLES.....	xiii
NOMENCLATURE.....	xvii
 SECTION	
1. INTRODUCTION.....	1
1.1. BACKGROUND.....	1
1.2. STATEMENT OF RESEARCH PROBLEM.....	5
1.3. OBJECTIVE AND SCOPE OF STUDY.....	9
1.4. RESEARCH METHODOLOGY.....	10
1.5. SCIENTIFIC AND INDUSTRIAL CONTRIBUTION.....	10
1.5.1. Contribution to Literature.....	11
1.5.2. Contribution to the Mining Industry.....	12
1.6. STRUCTURE OF DISSERTATION.....	13
2. LITERATURE REVIEW.....	14
2.1. OVERVIEW OF THE WHEEL LOADER.....	14
2.1.1. Parts of a Wheel Loader.....	16
2.1.2. Wheel Loader Applications.....	18
2.1.3. Wheel Loader Equipment Selection.....	19

2.2. EARTHMOVING EQUIPMENT DESIGN.....	21
2.2.1. Design Payload Limits	23
2.2.2. Loader Design Modeling.....	27
2.2.3. Design of Equipment for Productivity and Performance	30
2.2.4. Application of Equipment Performance and Productivity	33
2.3. EQUIPMENT RELIABILITY.....	36
2.3.1. Maintenance and Repair Philosophies and Practices	37
2.3.1.1 Run to failure (RTF) maintenance	38
2.3.1.2 Preventive maintenance (PM).....	38
2.3.1.3 Predictive preventive maintenance (PPM) or condition monitoring (CM).....	39
2.3.1.4 Reliability centered maintenance (RCM)	39
2.3.1.5 Establishing inspection / maintenance intervals	42
2.3.2. Equipment Reliability Analysis.....	42
2.3.2.1 Reliability analysis process.....	43
2.3.2.2 Failure analysis	47
2.3.2.3 Distribution analysis	48
2.3.3. Maintenance Plan Schedules	51
2.3.3.1 Time based maintenance intervals / events.....	52
2.3.3.2 Non-time based maintenance intervals / events.....	53
2.3.3.3 Reviewing and optimizing inspection / maintenance intervals and costs associated	54
2.4. EFFECT OF MACHINE OPERATION AND PERFORMANCE ON RELIABILITY	55
2.5. RATIONALE FOR PHD RESEARCH.....	59

3. EFFECT OF OVERLOADING THE BUCKET ON WHEEL LOADER PRODUCTIVITY - A CASE STUDY	62
3.1. INTRODUCTION TO WHEEL LOADER PRODUCTIVITY	62
3.2. EXPERIMENTAL EQUIPMENT & SITES	62
3.2.1. Geology of the Australian Iron Ore Deposits	64
3.2.2. Geology of Australia Bowen Basin Coal Deposits	64
3.2.3. Geology of the South American Iron Ore Deposits	65
3.2.4. Geology of the North American Copper Deposits	66
3.2.5. Geology of the North American Coal Deposits	66
3.3. DATA COLLECTION	67
3.3.1. Step 1: Compile the Wheel Loader Productivity Data	69
3.3.1.1 Data quality control	72
3.3.1.2 Overview of the data	73
3.3.2. Step 2: Preparing Samples for ANOVA Tests	98
3.3.2.1 ANOVA testing of 55 - 60 ton wheel loader class data	100
3.3.2.2 ANOVA testing of 75 - 80 ton wheel loader class data	105
3.4. DISCUSSIONS.....	111
3.5. SUMMARY	114
4. EFFECT OF OVERLOADING THE BUCKET ON BUCKET FORCES EXERTED ON A WHEEL LOADER - A CASE STUDY.....	117
4.1. INTRODUCTION TO FORCES ON A WHEEL LOADER.....	117
4.2. FRAMEWORK FOR INSTRUMENTED WHEEL LOADER CHANNEL DATA REVIEW	118
4.3. DATA ANALYSIS & PROCEDURE.....	123
4.3.1. Step 1: Compile the Wheel Loader Hydraulic Pressure Data	123

4.3.1.1 Data quality control	125
4.3.1.2 Overview of the data	126
4.3.2. Step 2: Correlation Testing	130
4.3.2.1 Pearson correlation analysis	133
4.3.2.2 Spearman correlation analysis	135
4.3.2.3 Kendall correlation analysis	137
4.4. DISCUSSIONS.....	138
4.5. SUMMARY	141
5. EFFECT OF OVERLOADING THE BUCKET ON WHEEL LOADER STRUCTURAL COMPONENT RELIABILITY - A CASE STUDY	142
5.1. INTRODUCTION TO STRUCTURAL COMPONENT RELIABILITY	142
5.2. EXPERIMENTAL EQUIPMENT & SITES	143
5.3. DATA COLLECTION	144
5.3.1. Step 1: Compile Wheel Loader Structural Component Failure Data ..	146
5.3.2. Step 2: Validation of the Structural Case Sample Data	150
5.3.3. Step 3: Perform Weibull Analysis based on Failure Hours	151
5.3.3.1 Presentation of 55 - 60 ton class wheel loader Weibull results	155
5.3.3.2 Presentation of 75 - 80 ton class wheel loader Weibull results	157
5.3.4. Step 4: Perform Standard Weibull Analysis of Structural Component Failure Cases	160
5.3.5. Step 5: Duty-Cycle Reliability Analysis	162

5.3.6. Step 6: Perform Weibull Analysis Based on Duty-Cycle for Structural Component Failure Cases	164
5.3.7. Step 7: Comparing the Standard and Duty-Cycle Weibull Analysis Results	166
5.4. DISCUSSIONS.....	168
5.4.1. Effect of Payloads on the Reliability of Structural Components	169
5.4.2. Effect of Accounting for Payload Duty-Cycle on the Reliability of Structural Components.....	170
5.4.3. Analysis Limitations.....	172
5.5. SUMMARY	172
6. CONCLUSIONS AND RECOMMENDATIONS FOR FUTURE WORK	175
6.1. SUMMARY	175
6.2. CONCLUSIONS.....	176
6.3. CONTRIBUTION OF THE PHD RESEARCH.....	178
6.3.1. Expansion of Research Frontier	179
6.3.2. Contributions to Mining Engineering Practices	179
6.3.3. Dissemination of Research Results	180
6.4. FUTURE WORK.....	181
BIBLIOGRAPHY.....	183
VITA	196

LIST OF ILLUSTRATIONS

Figure	Page
1.1. Repair Cost of Equipment Components	8
1.2. Methodology Used in this Research	11
2.1. Wheel Loader Overview.....	17
2.2. Wheel Loader in Production Operations.....	19
2.3. Recommended Wheel Loader Traffic Pattern.....	20
2.4. SAE Bucket Capacity Examples.....	24
2.5. Dump Height of 55 - 60 Ton Class Wheel Loader over a 240 ton Truck.....	26
2.6. Wheel Loader Lift Arm Force Diagram - Example.....	28
2.7. Example of FEA Model - Stress Changes of Key Nodes.....	29
2.8. Location of Maximum Stress - FEA Model Example.....	30
2.9. V-Shape Loading Pattern.....	32
2.10. Bucket Loading Trajectory Model.....	33
2.11. Sample Wheel Loader Monthly Load Weight Distribution.....	34
2.12. Sample Wheel Loader Monthly Cycle Time Distribution.....	34
2.13. Wheel Loader Monthly Productivity (Sweet Spot) Analysis	36
2.14. Elements of RCM.....	40
2.15. Risk Matrix Example.....	41
2.16. Example of IPSECA Workflow Management Model.....	45
2.17. Assigned Tasks of the IPSECA Workflow Management Model.....	46
2.18. Probability Failure (P-F) Curve.....	46
2.19. Failure Rate Curve Comparison.....	50

3.1. Distribution of 60 Ton WL Class Bucket Tonnage by Load Count.....	74
3.2. Distribution of 55 Ton WL Class Bucket Tonnage by Load Count.....	75
3.3. Distribution of 55 Ton WL Class Bucket Tonnage by Load Count - Coal.....	76
3.4. Distribution of 55 Ton WL Class Bucket Tonnage by Load Count - Metals.....	79
3.5. Distribution of 60 Ton WL Class Cycle Times.....	80
3.6. Distribution of 55 Ton WL Class Cycle Times.....	81
3.7. Distribution of 55 Ton WL Class Cycle Time - Coal.....	82
3.8. Distribution of 55 Ton WL Class Cycle Times - Metals.....	83
3.9. Distribution of 60 Ton WL Class Productivity - Bucket.....	84
3.10. Distribution of 55 Ton WL Class Productivity - Bucket.....	85
3.11. Distribution of 55 Ton WL Class Productivity - Coal.....	86
3.12. Distribution of 55 Ton WL Class Productivity - Metals.....	87
3.13. Distribution of 80 Ton WL Class Bucket Tonnage by Load Count.....	90
3.14. Distribution of 75 Ton WL Class Bucket Tonnage by Load Count.....	91
3.15. Distribution of 80 Ton WL Class Cycle Times.....	92
3.16. Distribution of 75 Ton WL Class Cycle Times.....	94
3.17. Distribution of 80 Ton WL Class Productivity - Bucket.....	96
3.18. Distribution of 75 Ton WL Class Productivity - Bucket.....	97
4.1. Typical Ultra-Class Wheel Loader Lift Arm Arrangement.....	119
4.2. Example of Lift Arm Channel Data for Hoist Cylinders.....	120
4.3. Channel Data from Hoist Cylinder Base Pressure - Underload.....	121
4.4. Channel Data from Hoist Cylinder Base Pressure - Target Load.....	122
4.5. Channel Data from Hoist Cylinder Base Pressure - Overload.....	122

4.6. All Wheel Loader Hoist Cylinder Pressure Samples.....	132
4.7. Loader 8019 All Hoist Cylinder Pressure Samples.....	134
5.1. CMMS Structural Case Data Example.....	145
5.2. Weibull Probability Distribution Plot - Rear Axle 75 - 80 ton WL Class.....	153
5.3. Weibull Reliability Plot - 75 - 80 ton WL Class Rear Axle.....	154
5.4. Weibull Probability Density Function Plot - 75 -80 ton WL class Rear Axle.....	155

LIST OF TABLES

Table	Page
3.1. Ultra-Class Wheel Loaders by Operating Class and Region.....	63
3.2. Ultra-Class Wheel Loaders by Operating Model and Commodity.....	63
3.3. Sample Wheel Loader Production Data - Wheel Loader 8015 Date 1/16/16.....	68
3.4. Sample Wheel Loader Processed Production Data - WL 8015 Date 1/16/16.....	70
3.5. Time Periods for the 55- 60 Ton Wheel Loader Class Datasets.....	71
3.6. Time Periods for the 75- 80 Ton Wheel Loader Class Datasets.....	71
3.7. Breakdown by Bucket Load Weight by Bucket Load Type.....	72
3.8. Bucket Cycle Time Classifications.....	73
3.9. 55 Ton WL Class Bucket Load Groups Averages by Load Type.....	76
3.10. 55 Ton WL Class Cycle Times by Bucket Cycle Category.....	81
3.11. Distribution Modes for 55 - 60 Ton Wheel Loader Datasets.....	88
3.12. 80 Ton WL Class Bucket Load Groups Averages by Load Type.....	90
3.13. 75 Ton WL Class Bucket Load Groups Averages by Load Type.....	91
3.14. 80 Ton WL Class Cycle Time Groups Averages by Load Type.....	93
3.15. 75 Ton WL Class Cycle Time Groups Averages by Load Type.....	95
3.16. Distribution Modes for 75 -80 Ton Wheel Loader Datasets.....	97
3.17. Number of Samples for Wheel Loader Validation Tests.....	99
3.18. ANOVA Results - 60 Ton WL Class - Cycle Time.....	100
3.19. Mean of Cycle Times by Load Type - 55 Ton WL Class.....	101
3.20. Variance of Cycle Times by Load Type - 55 Ton WL Class.....	102
3.21. ANOVA Results of Cycle Times - 55 Ton WL Class.....	102

3.22. ANOVA Results - 60 Ton WL Class - Productivity.....	103
3.23. Mean of Productivity by Load Type - 55 Ton WL Class.....	103
3.24. Variance of Productivity by Load Type - 55 Ton WL Class.....	104
3.25. ANOVA Productivity Source of Variation Summary - 55 Ton WL Class.....	104
3.26. Mean of Cycle Times by Load Type - 80 Ton WL Class.....	105
3.27. Variance of Cycle Time by Load Type - 80 Ton WL Class.....	105
3.28. ANOVA Results Cycle Time - 80 Ton WL Class.....	106
3.29. Mean of Cycle Times by Load Type - 75 Ton WL Class.....	107
3.30. Variance of Cycle Time by Load Type - 75 Ton WL Class.....	107
3.31. ANOVA Results Cycle Time - 75 Ton WL Class.....	108
3.32. Mean of Productivity by Load Type - 80 Ton WL Class.....	108
3.33. Variance of Productivity by Load Type - 80 Ton WL Class.....	109
3.34. ANOVA Results of Productivity - 80 Ton WL Class.....	109
3.35. Mean of Productivity by Load Type - 75 Ton WL Class.....	110
3.36. Variance of Productivity by Load Type - 75 Ton WL Class.....	110
3.37. ANOVA Results of Productivity - 75 Ton WL Class.....	111
3.38. ANOVA Productivity Results Summary.....	112
3.39. ANOVA Cycle Time Results Summary.....	112
4.1. Example - Hydraulic Cylinder Pressures with Production Data.....	124
4.2. Breakdown of Bucket Load Weights by Bucket Load Type.....	126
4.3. Expected Hoist Pressure Readings.....	126
4.4. 75 - 80 ton WL Class Monitoring Data Collection Dates.....	127
4.5. 75 - 80 ton WL Class Wheel Loader Performance Data.....	127

4.6. Hoist Cylinder Base Pressure Dataset - Underload Results.....	129
4.7. Hoist Cylinder Base Pressure Dataset - Target Load Results.....	129
4.8. Hoist Cylinder Base Pressure Dataset - Overload Results.....	130
4.9. Pearson Coefficient Correlation Results.....	135
4.10. Spearman Rank Correlation Results.....	136
4.11. Kendall Rank Correlation Results.....	138
4.12. Summary of Correlation Results.....	138
4.13. Summary of the Hoist Cylinder Hydraulic Operating Data by Bucket Load Type.....	140
5.1. Ultra-Class Wheel Loaders by Operating Class and Region.....	143
5.2. Ultra-Class Wheel Loaders by Operating Class and Commodity.....	143
5.3. List of the Structural Components Examined.....	146
5.4. Example of the Structural Component Dataset - 55 - 60 Ton Rear Axle.....	148
5.5. 55 - 60 ton Class Wheel Loader Expected Component Lives.....	149
5.6. Quantity of Structural Component Cases by Component.....	151
5.7. Weibull Distribution Data - Example.....	152
5.8. Weibull Results Summary for 55 - 60 ton Wheel Loaders Class	156
5.9. Weibull Results Summary for 55 ton Wheel Loaders Class.....	157
5.10. Weibull Results Summary for 75 - 80 ton Wheel Loaders Class	158
5.11. Weibull Results Summary for 80 ton Wheel Loaders Class	159
5.12. Weibull Results Summary for 75 ton Wheel Loaders Class.....	159
5.13. Number of Structural Cases by Wheel Loader Class.....	160
5.14. 55 Ton Wheel Loader Class Weibull Results - Structural Cases.....	161
5.15. 80 Ton Wheel Loader Class Weibull Results - Structural Cases.....	161

5.16. 55 Ton Wheel Loader Class Duty-Cycle Based on Maximum Payload.....	163
5.17. 80 Ton Wheel Loader Class Duty-Cycle Based on Maximum Payload.....	164
5.18. 55 Ton Wheel Loader Class Duty-Cycle Weibull Results - Structural Cases.....	165
5.19. 80 Ton Wheel Loader Class Duty-Cycle Weibull Results - Structural Cases.....	165
5.20. 55 Ton Class Structural Cases Weibull Results - Comparison.....	167
5.21. 80 Ton Class Structural Cases Weibull Results - Comparison.....	167
5.22. Individual 80 Ton Class Structural Cases Weibull Results - Comparison	168

.

NOMENCLATURE

Symbol / Abbreviation	Description
AGGA	Australian Government - Geoscience Australia
AMA	Aggregate Machine Application
ANOVA	Analysis of Variance
CM	Condition Monitoring
CMMS	Computer Maintenance and Management System
CSV	Comma-Separated Variable
EHM	Equipment Health Monitoring
FEA	Finite Elements Analysis
FMEA	Failure Mode and Effects Analysis
FSE	Field Service Engineer
FSR	Factory Service Representative
GSWA	Geological Survey Western Australia
GET	Ground Engaging Tool
IOCG	Iron Oxide Copper Gold
IPSECA	Identify, Plan, Schedule, Execute, Close and Analyze
KMC	Komatsu Mining Corporation
LCD	Loose Cubic Density
LCM	Life-Cycle Management
LoM	Life of Machine
LINCS	LeTourneau Integrated Network Control System
LSR	Life Stress Relationship

MHE	Material Handling Equipment
MTBF	Mean Time Between Failures
MTTR	Mean Time to Repair
NDT	Non Destructive Testing
OEM	Original Equipment Manufacturer
PLM	Production Life-cycle Management
PM	Preventative Maintenance
PPM	Predictive Preventative Maintenance
PRB	Power River Basin
psi	Pounds per Square Inch
RAM	Random Access Memory
RCA	Root Cause Analysis
RCFA	Root Cause Failure Analysis
RCM	Reliability Centered Maintenance
RHM	Remote Health Monitoring
ROPS	Roll Over Protective Structure
RTF	Run to Failure
SAE	Society of Automotive Engineers
st	short ton
TCO	Total Cost of Ownership
USGS	United States Geological Survey
WL	Wheel Loader
3D	3 Dimensional

1. INTRODUCTION

1.1. BACKGROUND

Wheel loaders are used as a preferred loading tool for their mobility, operational flexibility, and comparatively low capital costs (Hartman, 1992). A wheel loader is designed to load a truck or a hopper by driving a bucket into a pile of material, lifting a full bucket, reversing out of the pile, lifting the bucket to dump height while advancing towards the truck or hopper, dumping the bucket, and reversing from the truck while lowering the bucket to return to the pile for another load. The typical cycle time for a loader is 30 - 45 seconds depending on the size of the wheel loader (Heybroek, 2012). Additionally, the goal is to fill the bucket to its designed payload while not overloading it. Typically this “target weight” is 85 -105% of the designed payload (Gurganli, 2016).

Parker Bay estimates the size of the global wheel loader fleet (i.e., 22 ton class machines and larger) at 3,700 active units (Parker Bay, 2017). The global wheel loader fleet capacity is more than 25 billion tons annually. Wheel loaders added an estimated \$100 billion of value to mining operations in 2015 (Shields, 2017) by their abilities to maximize their comparatively-low capital costs and shorter duration maintenance outages coupled with a high degree of operational flexibility and mobility (Hartman, 1992).

Wheel loader costs can be broken down into two separate ownership and operational costs, and these costs account for the machines’ total costs. First, the ownership costs of wheel loaders range from \$2 to \$12 million dollars to purchase depending on the size and configuration of the machine (Ryan, 2016). Second, the operational costs (i.e., fuel, operator labor, maintenance, repair, and rebuilds) can run between \$175 - \$500 per hour depending on the class size of the wheel loader

(Caterpillar, (2), 1997 Caterpillar, (5), 2014 and Fine, 2016). Maintenance, repair, and rebuild costs account for over 30% of the total costs within the mining industry (Montenegro, 2003) (i.e., \$50 to \$175 per hour of operation) (Fleet, 2016). The ability to manage the operating costs of the wheel loader can be achieved by maintaining and reducing these costs through improving the machines' reliability. Saving 5% on the wheel loaders' maintenance cost may reduce the overall operational costs by approximately 2% or up to \$50,000 per machine per year for the first ten years of the machine's life. Improvements can be obtained in many areas: improving the volume of material produced during a defined period of time; decreasing the specific defined period of time; increasing the amount of production time available; and optimizing maintenance and repair time. Normally these forms of improvement are implemented one at a time, or in some cases, a combination of several or all of these factors may be integrated together. Improvement in one or several of these areas has the ability to lower production costs per unit while increasing the number of units produced. The increase in reliability through maintenance plans can increase the number of hours the wheel loader is available to perform its work. Typically these increases are between 50 to 100 hours per year, or 1 - 2 % which can result in additional production capacity of 50,000 to 250,000 tons (Collis, 2016). Once one area has reached an optimized level, the key will be to maintain this level of productive work while still striving to improve other areas.

Reliability is a broad term focusing on the ability of a product to perform its intended function. Mathematically, assuming the system or system component is performing its intended function at time zero, reliability can be defined as the probability that it will continue to perform its intended function without failure in its present

operating context. Reliability is not a function in its own right. It is a performance expectation which pervades all other functions (Moubray (1), 1997). The goal of reliability engineering is to evaluate the inherent trustworthiness of a product or a process, and then pinpoint potential areas for responsible improvement (Moubray (2), 1997).

The potential elimination of all failures from a design is not realistically possible. One purpose of reliability engineering (time zero case) is to identify the most likely causes of failure and address appropriate actions to mitigate the effects of these failure modes. Additionally, reliability engineering consists of a systematic application of time-honored engineering principles and techniques throughout the product's lifecycle. Essential components should be tracked as part of a Product Lifecycle Management (PLM or LCM) program (Weibull.com, 2017). The method to achieve an LCM program is thought to be through the development of a Reliability Centered Maintenance (RCM) plan: a process used to determine what must be done to ensure that any physical asset continues to do what its users want it to do in its present operating context (Moubray, (1), 1997).

The significance of reliability for wheel loaders revolves around a few key factors. These factors are: application; machine availability requirements; and maintenance support plan. First, it is necessary to examine any applications where wheel loaders operate. These applications may include production, waste removal, stockpiling, shipping, and general utility tasks. Caterpillar defines three duty-cycle zones based on the machine's application and the operating conditions (i.e., moderate, average, and severe.) Based on these definitions, mining applications loading shot rock and overburden fall in

the severe duty zone, while stockpile loading is an average usage activity, and shipping and utility operations are considered moderate duty (Caterpillar, (1). 1997). Individual mine haul road and work face conditions may vary and are subject to change throughout any shift depending on weather, traffic, and the utilization of support equipment to up keep their maintenance (Caterpillar AMA, 1998).

The second factor where wheel loader reliability is linked to machine availability is the specific working requirement for the wheel loader, and the fleet to which it is assigned. Most large-scale mines operate multiple fleets where wheel loaders can be planned, scheduled, and rotated through its maintenance requirements while still maintaining its desired level of availability. This is typically 85% - 90% availability for production service machines. Smaller mines operating one or two production fleets may focus on machine reliability while they schedule service to maintain their production goals. Generally, these operations maintain a secondary loader to supplement the production machine during service or downtime events. These secondary units typically are old machines which have been removed from front-line service and are good for part-time or scheduled fill-in work. The reliability of the wheel loader for mines operating only one production machine is paramount. This situation occurs in small production mines, typically when the mine only operates part of the year and can ill afford outages. In this case, if the machine is down, there is no production until the machine is operational again.

Once a downtime event occurs, scheduled or unscheduled, the maintenance support team and its plan affects the reliability of the machine by returning it to service as quickly as possible. Maintenance plans require that the correct people, parts, and facilities

are available to complete their specific tasks promptly. A good maintenance department acts similar to a hospital where the majority of services are taken with routine checks, monitoring, and scheduled repairs based on the equipment's reliability, but it also requires the emergency department to handle unexpected breakdowns.

Reliability affects the ownership and operating costs of a wheel loader in two ways. Specifically, these are the cost of the service / repair, and the production loss occurring from tons not being mined during the machine downtime event. These unscheduled downtime events can increase the operation per unit cost over budgeted / forecasted amounts. Additionally, a rule of thumb for these downtime events is that it can reduce the machine's availability by 0.25% per day based on a 24-hour day mining cycle, which is doubled if the mine only works one shift. Multiple unplanned reliability outages can significantly affect the machine's availability over the course of a year making it difficult to achieve its forecasted operation's targets.

1.2. STATEMENT OF RESEARCH PROBLEM

This research will investigate the effect overloading of the bucket has on a wheel loader's available capacity (i.e., reliability and productivity). This represents a RCM planning and data analysis technique to reduce the overall machine's operating costs (Moubray (2), 1997). With ultra-class wheel loaders only a few events tend to be the primary cause of failure for a component, and overloading of the bucket is perceived to be one of the major fundamental causes of component failure. It is hypothesized that overloading: (1) affects the life expectancy of the structural components of the wheel loader; and (2) is detrimental to the machine's productivity. This study will provide

direction in determining when a structural component is likely to fail and encourage replacement before the actual failure, as part of a scheduled replacement program.

One of the causes of structural component failure on wheel loaders is overloading the bucket during machine operation. The wheel loader is designed to hoist a specified payload. The machine's bucket is sized to accommodate this weight based on the density of material being loaded and the skill of the operator to fill the bucket to the specified payload. Additionally, the structural components are designed to handle slight overloads, typically 105-110% of the maximum payload (DePorter, 2016). Increasing this stress per cycle, through overloading, on a machine may ultimately lead to failure of a component more quickly than if it is operated in a normal to a low stress environment. Mines are also focusing on how to operate at a high productivity level while not constantly pushing the equipment past its designed limits during the machine's estimated life of several million bucket cycles. Continual overloading of the bucket, greater than 110% of design payload, during operations increases the stress per cycle on the machine's structural components, thus reducing the life of each of these components (DePorter, 2016 & Chanda, 2011).

Structural components are tracked through machine operating hours to determine the components' life (Tomlingson (1), 1999). The use of hours to track structural components does not measure how hard the component is actually being used. It is only tracking how long it has been used. Moubray has proposed to supplement the primary unit of measurement (component hours) with other machine units of measures, i.e., number of stress cycles (Moubray (3), 1997).

Equipment maintenance costs and the downtime associated with maintenance and repair activities are a significant concern for any business. In the mining industry over

30% of total costs are related to maintenance (Montenegro, 2003). The availability and reliability of the equipment is key to controlling costs and optimizing the company's return on investment. The proper role of maintenance is to provide the lowest cost in maintenance labor and materials, and to minimize production losses. The goal is to optimize equipment maintenance to achieve the lowest operating costs (Lowrie, 2002).

The components' lives and repair costs are normally the largest single maintenance cost chargeable to any machine. The structural components are part of a group of parts that require significant time and money to repair. Thus, any work which extends the life these components and reduces the amount of time spent on replacements will lead to significant cost savings. The operating conditions and applications affect the component's life and cost the most; abuse of the components though overloading can lead to significant reduction of the structural components lives.

Another significant factor to controlling component repair costs is whether the repair is performed before or after catastrophic failure. Actual repair of a component may cost between 33% - 50% and require less machine downtime and fewer man hours to repair versus the cost of a catastrophic failure, as shown in Figure 1.1 (Caterpillar (2), 2014). The increased costs of a catastrophic failure results from additional damage to the component, secondary damage to other components or system parts, unsalvageable core charges, and / or additional labor hours. Additional operating costs are incurred because of the lost production associated with the increased downtime. Thus, it is important to use optimal component replacement schedules (in the quest to increase component lives) to prevent catastrophic failure.

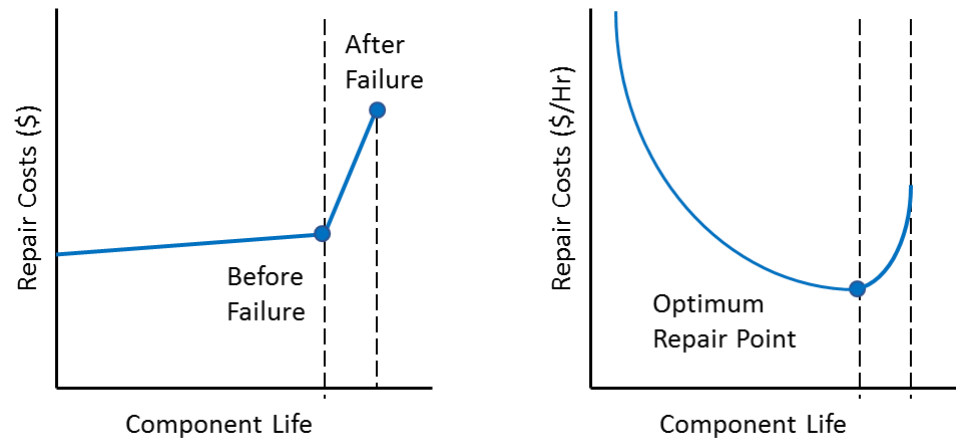


Figure 1.1. Repair Cost of Equipment Components

Production and equipment datasets contain large amounts of production and machine operation data. This data can be used to determine the frequency and severity of bucket overloading as well as the associated stress on the structural components. These datasets give a much broader picture of how hard the machine is working over a longer period and are useful in examining the effect of overloading on productivity and reliability.

Tracking structural components generally takes place in a computerized maintenance management system (CMMS). This system allows for the accumulation of operating hours on components and equipment together as well as scheduling and forecasting maintenance and repair activities (Tomlison (2), 1999). The CMMS also provides a repository for previous component histories and failures. A standard reliability failure analysis involves determining the parameters of a Weibull frequency distribution to determine the probability of failure (Moubray (5), 1997).

Long component lives, time to component failures, and limited fleet size produce issues in this instance in building the datasets on individual components. The resulting

datasets consist of a relatively small number of points, and waiting on the next data point to be reached can take months, or, in some cases, up to a year to occur. These small datasets and resulting analysis can be pushed in order to draw a conclusion, and an additional data point or two may have a significant influence on changing the results.

1.3. OBJECTIVE AND SCOPE OF STUDY

The objective of this PhD research is to examine the effect of overloading the bucket and on the time and likelihood of structural component failure in ultra-class front-end wheel loaders. Specifically, this dissertation strives to:

1. Evaluate the effect of overloading the bucket on wheel loader productivity.
2. Examine the effect of overloading the bucket on forces exerted on a wheel loader.
3. Investigate the effect of overloading the bucket on the reliability of the structural components of a wheel loader.

The first objective will be achieved by analyzing productivity data from a number of wheel loaders from the same manufacturer with machines operating around the world. The goal will be to quantify the cycle time and the tonnage of the wheel loader's bucket loads in order to assess whether different classes of payloads lead to differences in productivity.

The second objective will be achieved by analyzing the data from the wheel loader's on-board equipment monitoring system to determine the maximum forces exerted on specific structural components and match these events to the production data from the first objective. The results will be used to determine the amount of forces the

structural components are being subjected to with different payloads. The goal is to determine whether there are significant differences due to overloading.

The third objective will be achieved by using Weibull analysis performed on the structural components as a predictive tool to forecast future structural component failures based on bucket overload events. The characteristic life value will be calculated from Weibull's prediction of future failures equation from the known failed components. The data analysis from objectives one and two will be used to determine the reliability of the components using Weibull functions. The goal is to determine the time of initial failure for each structural component and by using calculated data to determine the amount of overload events remaining before component failure. This will require modifying the probability of the item failure equation to determine the time at initial failure. The resulting information will be utilized for determining the ability to schedule structural inspections prior to failure and to also increase or decrease the interval of inspections based on operating conditions instead of using only a predefined time interval.

1.4. RESEARCH METHODOLOGY

Figure 1.2 shows the research methodology used to accomplish the three research objectives. Data for this work will be collected from a global fleet of wheel loaders from the same manufacturer.

1.5. SCIENTIFIC AND INDUSTRIAL CONTRIBUTION

This research contributes significantly to both literature and industrial practice. The knowledge acquired is applicable to engineering design, equipment productivity, and

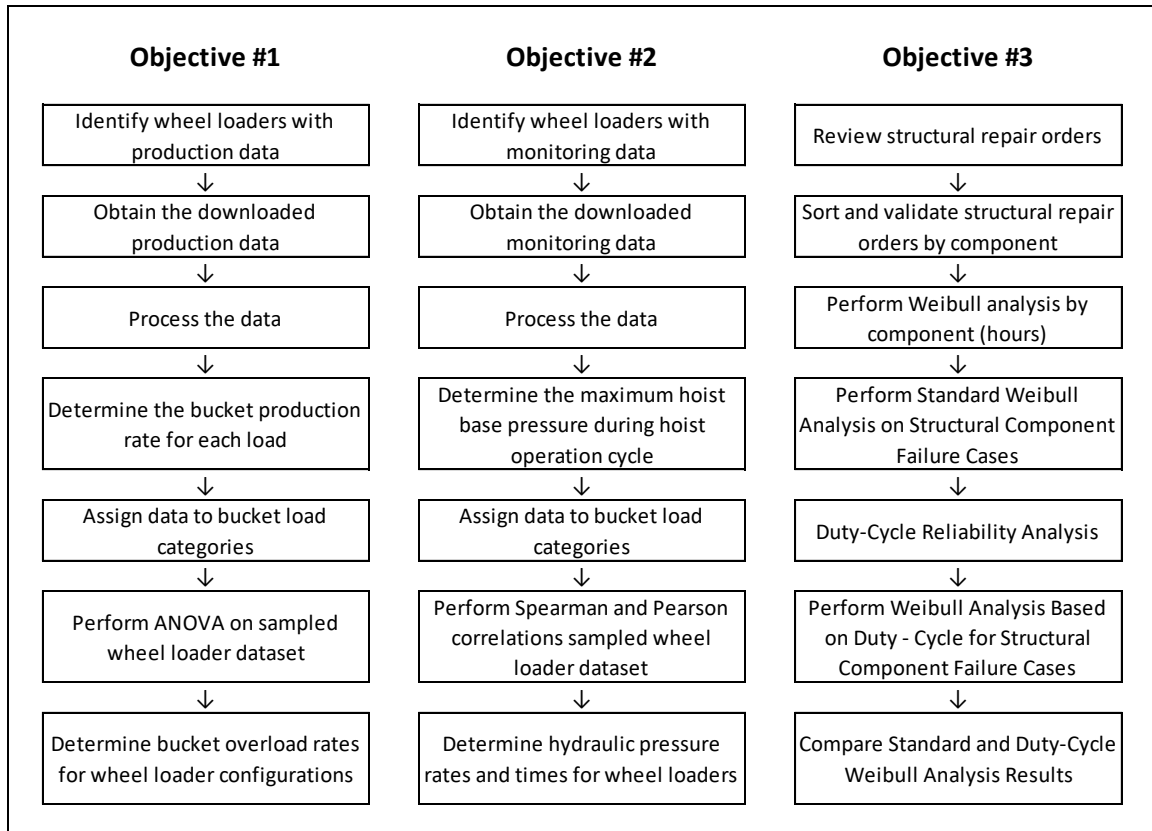


Figure 1.2. Methodology Used in this Research

reliability as well as maintenance, repair, and rebuild planning and execution. This research used multiple techniques including equipment performance studies, statistical data analysis tools, and reliability analysis tools (Weibull distribution characterization and duty-cycle analysis) to facilitate increased wheel loader performance and reliability.

1.5.1. Contribution to Literature. As far as this author can tell, no previous work can be found in the literature that examines the effect of payload (overloading) on wheel loader productivity (tons loader per cycle) and reliability. At least three journal papers can be published from this work, one each from the work in Sections 3, 4, and 5 of this dissertation. There is also opportunity to publish more papers by further research and analysis of the data and results presented in this dissertation.

To the best of this author's knowledge, no research has been published that critically examines the nature and extent of the effect of payloads on cycle time and productivity using real field data. This dissertation examines the nature and extent of these effects. Thus, this will make a significant contribution to the literature.

Again, to the best of the author's knowledge, no work has been published in the literature that scrutinizes the correlation between payload and the hoist cylinder pressure (hoist cylinder pressure can be used as a proxy for the force exerted on the lift arm) with field data (from machines on-board management systems). This successive step of this dissertation investigates the character and the magnitude of this correlation. Thus, the knowledge acquired will establish a consequential addition to the available literature.

Finally, we need a means to account for the wheel loader's duty-cycle (with respect to overloading) in the reliability analysis of its structural components. To the best of the author's knowledge, this has not been done in the literature. This final segment of this dissertation scrutinizes and evaluates classical time based reliability analysis compared to reliability analysis that incorporates overloading. Thus, the end results and their findings will establish substantial contributions to the scholarship available within the literature.

1.5.2. Contribution to the Mining Industry. Components are typically designed to obtain a specific life expectancy (i.e., a maintenance life-cycle). The premature failure of any component leads to unscheduled downtime and additional cost. A machine's structural components can significantly affect unscheduled down time due their long repair times. Mining operations and maintenance groups responsible for wheel loaders use inspections, repair, retrofit, and replacement activities to combat these issues. The

downside of these activities is that they take the wheel loader away from its primary function. Towards this end a successful approach includes acknowledging that each machine cannot be assumed to operate in the same conditions with the same level of operator efficiency (overloading practices). Incorporating the machine's productivity and overloading practices, in addition to current practices, will facilitate guidelines for operations and maintenance departments to optimize the productivity and the maintenance of the machine by creating machine specific inspections and maintenance / repair plans for each machine based on its productivity and loading (overloading) practices. This research will help mines extend component life expectancy and rebuild lives by using machine specific data to drive the wheel loader's overall reliability. In addition, the use of other on-board monitoring system data (i.e., hydraulic cylinder pressures) will be used to confirm the relationship between forces exerted on the wheel loader and its productivity.

1.6. STRUCTURE OF DISSERTATION

This dissertation comprises six sections, including this introductory section. Section 2 covers a detailed review of all relevant literature covering equipment operation and reliability to operational costs, wheel loader productivity and component stress analysis, and RCM plan setup and review analysis. Section 3 focuses on establishing the framework for the wheel loader productivity studies and the results of wheel loader model and configuration. Section 4 discusses work to evaluate the effect of overloading the bucket on the forces applied to the wheel loader. Section 5 chronicles the effect of overloading the bucket on the wheel loader's structural components reliability. Section 6 reports the conclusions of this study and presents recommendations for future work.

2. LITERATURE REVIEW

This section encompasses a comprehensive review of the relevant literature involving earthmoving equipment, specifically wheel loaders with detailed focus on ultra-class wheel loader design, application, reliability, and the effect of machine operation and performance on their reliability. Additionally, the literature review examines maintenance practices for earthmoving equipment specifically, and how these systems are reviewed and revised to improve their performance and minimize any downtime.

2.1. OVERVIEW OF THE WHEEL LOADER

A wheel loader is a mobile piece of earthmoving equipment capable of loading any type of bulk soil (stripping) or rock (ore) in production operations or support capacity in conjunction with another production loading piece of mobile equipment (Kolte, 2015). Wheel loaders have a bucket capacity of up to 70 cubic yards of material (Joy Global, (1), 2016). Additionally, wheel loaders are capable of transporting their payload over short distances, typically less than 600 feet, in order to achieve a productive cost (Komatsu, 2009).

Wheel loaders capitalize on several features over other loading equipment (i.e., hydraulic excavators and electric cable shovels). These characteristics include, but are not limited to, mobility, comparatively low capital costs, operational flexibility, and lower maintenance costs (Hartman, 1992). A wheel loader is very mobile and capable of tramping speeds of 10 - 15 miles per hour compared to other earthmoving loading equipment which generally have maximum tramping speeds of up to 3.0 miles per hour

(Caterpillar (1) & (2), 2015). The wheel loader's rubber tires allow for this speed to travel around the pit with ease to reposition itself from one face to another, or from one bench or pit to another, depending on the mine's production schedule (Gurgenli, 2016). This ability also makes the wheel loader flexible and able to blend out a production face with one piece of loading equipment by tramping from one part of the muck pile to another and back again while maintaining an acceptable production rate. The hydraulic excavator or electric cable shovel would require two or more loading units to accomplish this same task.

Moving a wheel loader to a specific site is easily accomplished by on-highway trucks. Smaller wheel loaders, those with less than a 9 cubic yard capacity, can be moved with one transport truck. Larger wheel loaders, greater than 9 cubic yard machines, may require several transport truck loads to be moved to site. Assembly of the wheel loader on site can take between one to ten days to commission the unit (Fleet, 2017). The mine site should have a shop maintenance area setup and dedicated to work on wheel loaders. Mine maintenance crews work on electric cable shovels and hydraulic excavators in the field or pit and they may only be trammed out for major services or rebuild programs (Caterpillar AMA, 1998).

Wheel loaders have comparatively low capital costs typically, less than \$100,000 per cubic yard of capacity. Hydraulic excavators and cable shovels typically start around \$100,000 per cubic yard of capacity. Wheel loaders have a machine life similar to a hydraulic excavator, which is generally 12 to 20 years depending on the machine's application and the commodity being mined. Electric cable shovels' life expectancy is approximately two times that of the average wheel loader (Caterpillar, (3), 2014).

Wheel loaders' maintenance programs are designed to keep the machines in operation and to ensure warranty coverage. The maintenance programs are designed and scheduled to withdraw the wheel loader from service for only short durations (usually, 12 - 24 hours, i.e., 1 - 2 shifts) for preventative maintenance and inspections every 250 - 500 hours (i.e., every 2 - 4 weeks). Generally, these maintenance programs are divided into modular maintenance schedules, with additional service items or services being grouped onto the base schedule at intervals of 500 hours, 1000 hours, 2000 hours, etc. (Joy Global, 2016). The wheel loader's maintenance philosophy differs from that of the electric cable shovels or the draglines maintenance schedules as these are typically based around longer duration service intervals with longer duration outages (Collis, 2017).

2.1.1. Parts of a Wheel Loader. A wheel loader generally consists of two separate frames (i.e., the front frame and the rear frame) joined at an articulation point in the center of the machine. The operator's cabin sits atop the center of the machine over the articulation point of the wheel loader, as shown in Figure 2.1. The operator controls and monitors the wheel loader's performance from this vantage point. Most wheel loaders are articulated in the middle of their body which separates the frame into two distinct sections, front and rear. The front frame sits forward of the articulation point connecting the bucket to the front frame by the lift arm structure. Typically, the components of the lift arm structure include the lift arms, the bellcranks, and level links. These components are used to manipulate the bucket to gather material from a pile, lift it above the dump point, before placing it into the said dump point (Kolte, 2015). The frame is made to be highly-rigid along with reinforced linkage to resist loading stress and shock

(Komatsu, (1), 1998). The bucket size for each wheel loader is determined by the weight (density of the material it will be expected to handle (Joy Global, (1), 2016).

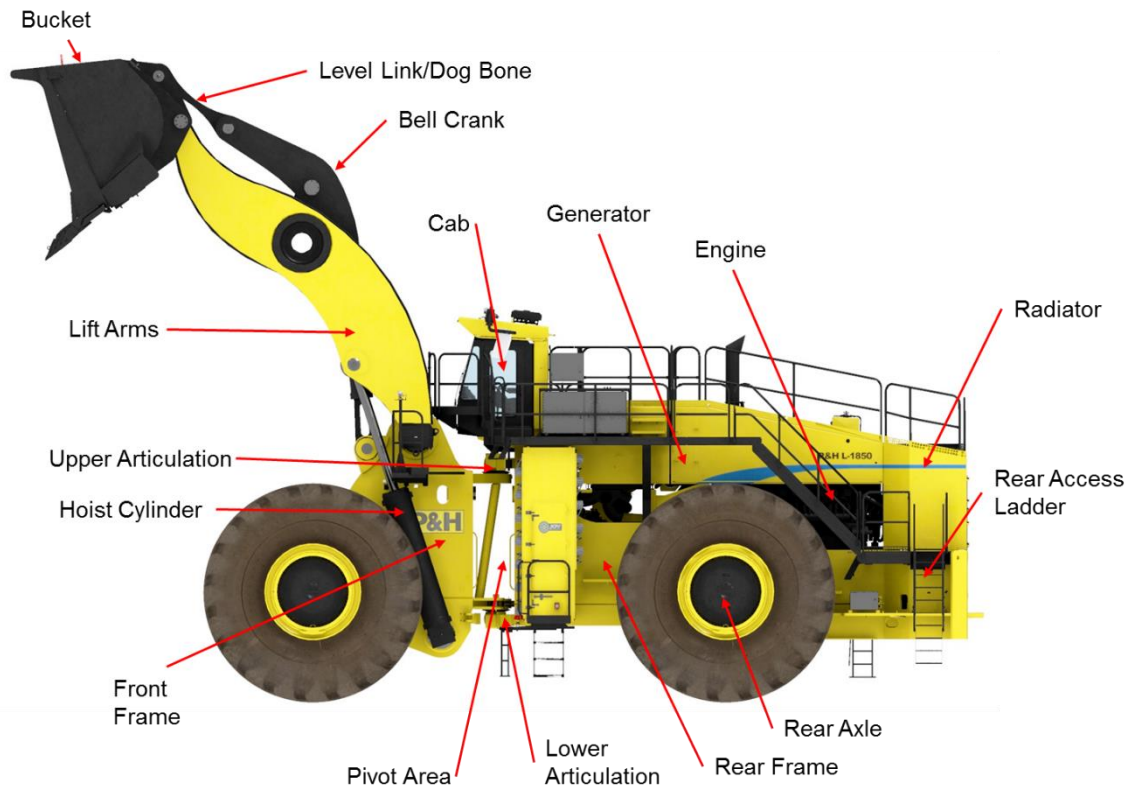


Figure 2.1. Wheel Loader Overview (Joy Global, 2017)

The rear frame (i.e., the half of the wheel loader behind the operator's cabin) houses the machine's power unit, the drive system and other auxiliary systems required for the machine's operation. The wheel loader's power unit, which is generally a diesel engine, is mounted to the rear of the rear frame with the radiator / cooler at the back of the machine to achieve maximum airflow. The drive unit sits forward of the engine, either mechanical, transmission, or electrical, to power the final drive to propel the wheel loader forward or backward. Additional auxiliary systems (i.e., hydraulic / air and

electrical) support the machine's functions. Hydraulic pumps and valves provide flow and pressure to actuate the hydraulic cylinders to hoist and to dump the bucket, and they also control the steering of the wheel loader. The electrical system can also provide power directly to the wheel trough, which is a set of motors.

2.1.2. Wheel Loader Applications. Wheel loaders are rugged all-weather loading tools used in multiple industries and applications. Wheel loaders are utilized in the following industries including, but not limited to, base metals, coal construction, hard rock, industrial minerals, and other industries to load trucks, load and carry material, or load hoppers to transfer material from one area to another. Wheel loaders may work in support roles along with other loading tools (e.g., electric cable shovels, hydraulic excavators, and drills) to prepare, assist and /or clean up their work areas (Barksdale, 1996).

Wheel loaders are optimized to work on level and stable floors with low muckpile profiles. Normally the blasts for loader operations are shot forward and lay out over the bench floor. A photo of a wheel loader doing production loading into haul trucks is shown in Figure 2.2. This floor profile allows for loading the material, while continually cleaning the floor from spillage and loose rocks, without the use of support equipment. Additionally, the muckpile can be blended by loading from two or more areas within the shot area into the same truck. Loaders are capable of tandem loading a truck to decrease the loading time or actually blending the shot material in the truck for further processing (Caterpillar AMA, 1998).

Establishing a good traffic pattern for the haul trucks entering the production face is essential for proper fleet interaction. An example of a recommended wheel loader



Figure 2.2. Wheel Loader in Production Operations (Achelpohl, 2010)

traffic pattern is illustrated in Figure 2.3. An unloaded haul truck enters the production face (dig face) on a separate track from the loaded truck. The haul truck should execute a turn to be able to back into a loading position at the face or to be able to stop short and be prepared to back under the loader as required. In either case, the haul truck operator needs to maintain visual and radio contact to ensure safety of the production crew. After the wheel loader has completed the loading sequence, the truck should exit the production face and travel to the dump area (Caterpillar AMA, 1998).

2.1.3. Wheel Loader Equipment Selection. Selection of a specific wheel loader requires that it be matched to the production requirements of the haulage fleet (i.e., size of the trucks, production rate to feed the hopper, or the load and carry production rate). The wheel loader's buckets should be sized to complete a bucket target load weight and

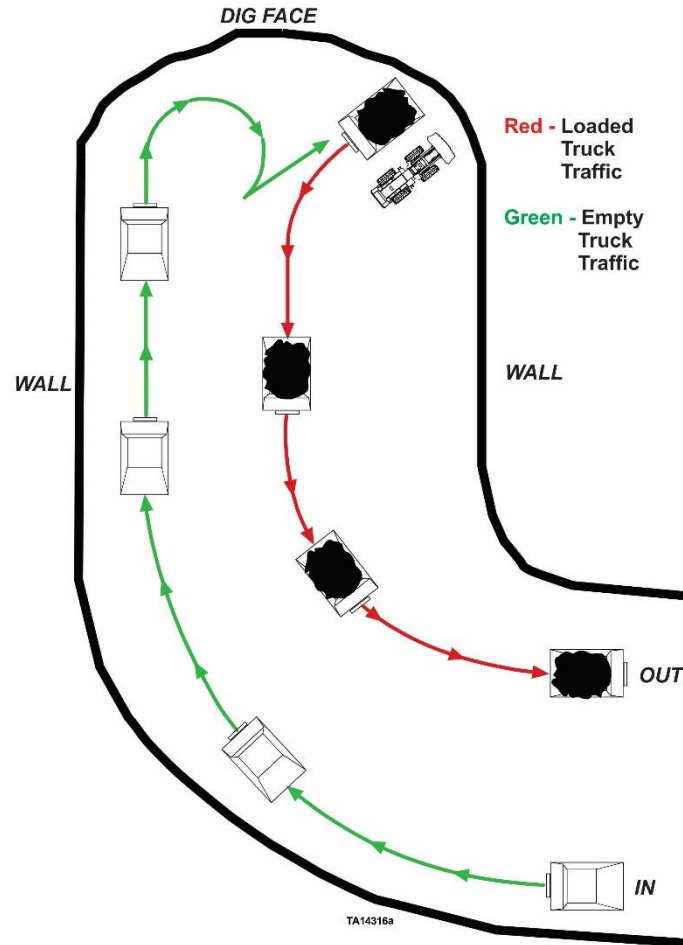


Figure 2.3. Recommended Wheel Loader Traffic Pattern (KMC, 2017)

to cycle the machine in a reasonable time (Barksdale, 1996). The loader is designed to match a truck payload capacity by usually placing 3 - 6 even bucket loads of material into the bed of the truck. Most mining applications accept 3 - 4 loads as being the optimal pass range. This is not to be confused with partial passes if the wheel loader is fully trucked up (Caterpillar AMA, 1998).

The loader is conventionally the limiting factor in any production fleet, as there is usually only one wheel loader for multiple trucks. A mining or application engineer commonly designs excess capacity into all phases of the production system to account for

any and all unforeseen circumstances which can disrupt production. Any excess capacity has to be balanced with additional capital and operating costs for the wheel loader (Barksdale, 1996).

2.2. EARTHMOVING EQUIPMENT DESIGN

Material handling equipment (MHE) are tools to maneuver materials safely, smoothly and directly around a mine site at all times. Earthmoving equipment is designed and acquired in conjunction with the production requirements and cost. The MHE operator's primary goals are safety and control of costs (i.e., create margin). Managers and engineers should put in places processes to control both of these goals. They should also use sensitivity analysis to identify any critical criteria during the selection process and adjust these items based on empirical operating data. (Parsad, 2015). Additionally, examining the equipment's application and operation conditions determine if the selected equipment is optimal for the task. Equipment modification and / or replacement / upgrades may also be required to achieve production goals. The bottom line is that the right system is the one which meets your application's needs at the lowest cost per ton (Caterpillar AMA, 1998).

Wheel loaders conform to several of the Society of Automotive Engineers (SAE) definitions expressed in standards J732, J742, J818 and J1234. These standards focus on quantifying the design parameters of a wheel loader (i.e., hydraulic cycle time for raising and lowering the lift arms and dumping the bucket, breakout force, bucket capacity, dump height, etc.) (Caterpillar (3), 1996).

One area of earthmoving equipment design that has received significant attention in academic literature is estimating the interaction forces between equipment and the soil

/ muckpile. The material's properties such as particle shape, size, size distribution, stiffness, and density affect the dig performance of the equipment's bucket. All of these properties affect the flow of material into the bucket. An example of this would be digging a blasted rockpile using ground engaging tools (GET) such as on a wheel loader's rock bucket. The purpose of understanding all of these properties is critical to preparing and improving the digging conditions at the loading site. Optimal conditions can increase bucket loading efficiency and, therefore the productivity of the earthmoving equipment (Rasimarzabadi, 2016).

Another area that has received considerable concentration is stress estimation for earthmoving equipment. This entails analysis of forces acting on the bucket which transfer through the frame during the multiple processes of the earthmoving equipment to retrieve material from a pile. First is the initial penetration of the pile by the bucket's lip. Second, the bucket is raised via the lift arms and worked back and forth to fill the bucket based on the resistance on the bucket. At this time, the pile or bank may be exerting / transferring additional force onto the machine as material in the pile slides down the pile towards the bucket and the void being created. In the last step, the bucket is lifted, freed of the pile, and begins the hoist procedure to its dump height (Sharata, 2004). Each loading step has its own stress profile. Understanding each step and how one transfers from one to the next is critical. Additionally, the interaction of the pile can come into play with the material's properties discussed in the previous point.

The operator's proficiency is a third area which has received a lot of attention in the literature. Operator practices may lead to inefficient use of earthmoving equipment which leads to increased downtimes which in turn results in higher maintenance costs.

Models are used to determine the optimal operator practices which thus provide an understanding of the impact of operator practices on equipment performance. This measurement of earthmoving equipment performance can be assessed by examining the resistant forces applied to loading the bucket, the digging (bucket) cycle time, and the material produced (payload) (Frimpong, 2010). By using the bucket cycle time and the payload measurement, the equipment's productivity can be calculated to determine how the machine is performing. Operating practices for loading and hauling equipment in mines is a source of significant energy inefficiency based on evidence of energy efficiency and continuous improvement studies. According to Kwame Awuah-Offei (2016) to the best of his knowledge, no one has critically review all these studies to evaluate the extent which an operator's practices affect energy consumption per unit of productivity (Awuah-Offei, 2016).

For this PhD research, the three design elements that are the most critical are payload limits, load and overloading design, and equipment productivity. These are discussed in the next three sub-sections and followed by a discussion of performance assessment.

2.2.1. Design Payload Limits. The design parameter most commonly utilized to select a wheel loader is the lifting capacity of the machine. Buckets are sized and designed according to general types, general purpose, multi-purpose, rock and coal. Rock and coal buckets specify specific applications in which the wheel loader will be used, and they have ground engaging tools (GET) and replaceable liners which are based on the rock's abrasiveness. The GET parts increased weight parts reduces the size of bucket and conversely the payload weight that the machine can hoist (Caterpillar (3), 1996).

The Society of Automotive Engineers (SAE) standard J742 (FEB85) “Capacity Rating - Loader Bucket” defines rating the operating loads and the environment in which they are to be operated. The bucket’s capacity is defined for both struck and heaped loads as shown in Figure 2.4. The struck capacity is the volume contained within the bucket after the load is leveled by drawing a straight edge from the top to the bottom of the bucket. Heaped capacities contain additional material on top of the struck capacity with a 2:1 angle of repose with the struck line parallel to the ground, (SAE (3), 1998 and Caterpillar (4), 2014).

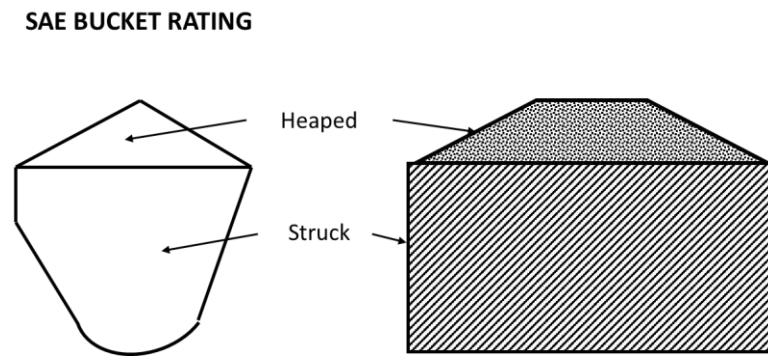


Figure 2.4. SAE Bucket Capacity Examples (SAE (3), 1998)

SAE J732 (JUN92) defines how the hoisting functions of the wheel loader are measured by loading the bucket and transferring the material to another location. The initial force a wheel loader must overcome retrieving material from the muckpile is the breakout force. Breakout force is the maximum sustained vertical upward force exerted 100 millimeters (mm) behind the tip of the bucket’s cutting edge. The wheel loader’s lifting capacity is determined by using the maximum mass at the centroid of an SAE rated bucket volume that can be lifted to the maximum height when applying the

manufacturer's specified working pressure (SAE (1), 1998). Figure 2.5 illustrates both a 60 ton class wheel loader (left) and a 55 ton class wheel loader (right) dumping over the bed of 240 ton class haul truck. The areas to particularly notice are: (1) does the wheel loader have enough reach to place the material in the center of the truck bed or does a special loading sequence (double side loading) need to be set to load the truck; (2) how much clearance does the lift arms have over the truck bed's side rails; is everything there clear.

SAE standard J828 (MAY87) "Rated Operating Load for Loaders" defines the rated operating loads and the environment in which they are to be operated. The rated operating load for an SAE loader is not to exceed 50% of the tipping capacity of the machine, and the hydraulic lift capacity of the machine should be no less than the rated operation load for all lift arm positions (SAE (2), 1998). The bucket should be sized to accommodate the material intended loaded, and a check should be performed to ensure the bucket are sized properly to the bucket's capacity (i.e., volume is multiplied by the loose cubic density (LCD) of the material so that it does not exceed the wheel loaders designed lifting capacity) (Caterpillar (4), 2014). The standard works in conjunction with SAE J732.

Baseline modelling for a wheel loader begins with the design engineer applying the forces of the design payload of the bucket to the machine. A component's life is directly related to the gross machine weight and its associated payload. In theory, the bucket should never be overloaded as this will affect the life of a machines' components by shortening them or degrading them to the point where the machine is unsafe to operate (Fernando, 2011). Mining equipment is designed with a safety factor to account for times

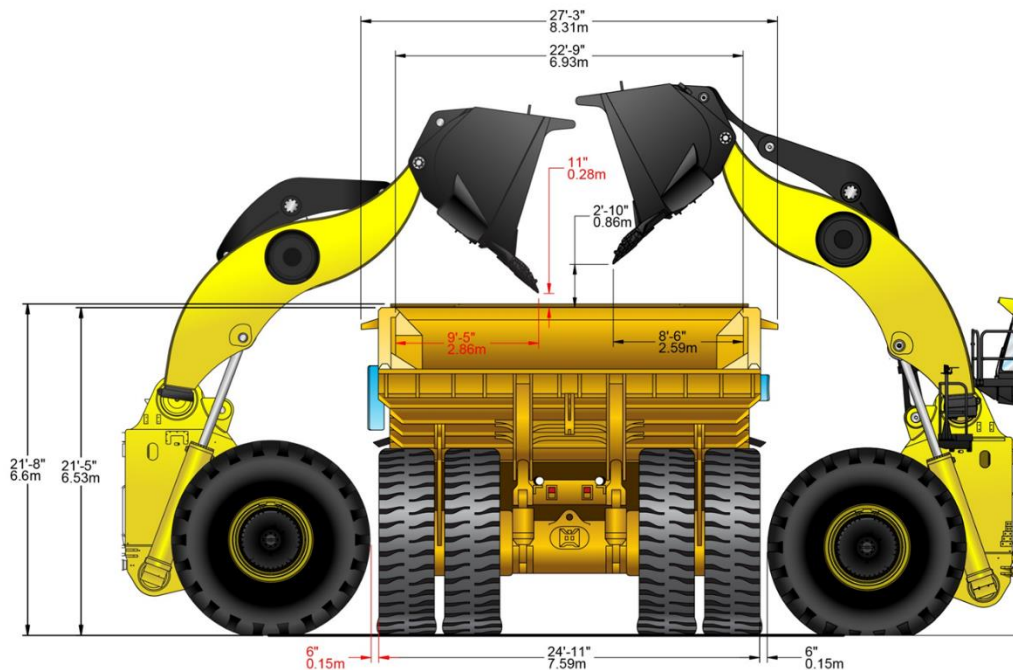


Figure 2.5. Dump Height of 55 - 60 Ton Class Wheel Loader over a 240 ton Truck (KMC, 2017)

where the equipment is pushed over its design limits. These safety limits and overload policies are established to handle the variability and randomness of individual bucket loads as they are difficult to predict and control (Chanda, 2010).

By Caterpillar's 10/10/20 Policy, "the mean of the payload distribution shall not exceed the target payload and no more than 10% of payloads may exceed 1.1x the target payload and not a single payload shall ever exceed 1.2x the target payload." Caterpillar's 10/10/20 policy defines the overload portion between 110% - 120% of the design payload weight and critical overloads are $\geq 120\%$ of the design payload weight (Fernando, 2011). The remaining bucket categories, target loads and underloads, are not as well defined. The target load is generally defined by the mining or application engineer in specifying the fleet's loading tool. The range for the target zone is set around the bucket fill factor. The typical bucket fill factor ranges from 80% - 90% for the fleet (Gurgenli, 2017). The

underloads are any bucket load which is below the target range. Mining operations will adjust these percentages based on their desired metrics to rate the operating performance of their equipment. They usually adjust them within $\pm 5\%$ of these values.

The direct collection of bucket data from wheel loaders is possible through the machine on-board equipment monitoring systems (Caterpillar VIMS, 2017 and Joy Global LINCOS, 2017). These systems provide on-board feedback to the operator on bucket overloads and critical overloads. Additionally, these systems can record and make available, in real time, payload increases for each bucket loads (Chanda, 2010). Acknowledgment and proper actions for the overload alarm information can be useful in preventing further damage to the equipment and its components.

2.2.2. Loader Design Modeling. Design modeling of individual wheel loaders and their components is an on-going process to refine and advance the design of the equipment. Essentially, the design of the equipment is the interdependence between its geometry and its strength parameters on one hand, and the working capacity of the whole machine on the other. The design process involves multi-criteria analysis of a function of many variables which makes the optimization problem a relatively complex and slowly convergent one (Bundy, 1988). A simple force diagram is shown in Figure 2.6 for a wheel loader lift arm design.

A practical wheel loader design is based on machine behavior and visual derivations while seeing that the machine executes its function. Simulating the linkage motion in a 3D drawing finite elements analysis (FEA) program is an instrumental part of the design process. Figure 2.7 is an example of this. The FEA process requires that a

large number of iterations be performed in order to ensure that all criteria are fulfilled, and that there are not adverse results in the calculations (Kolte, 2015).

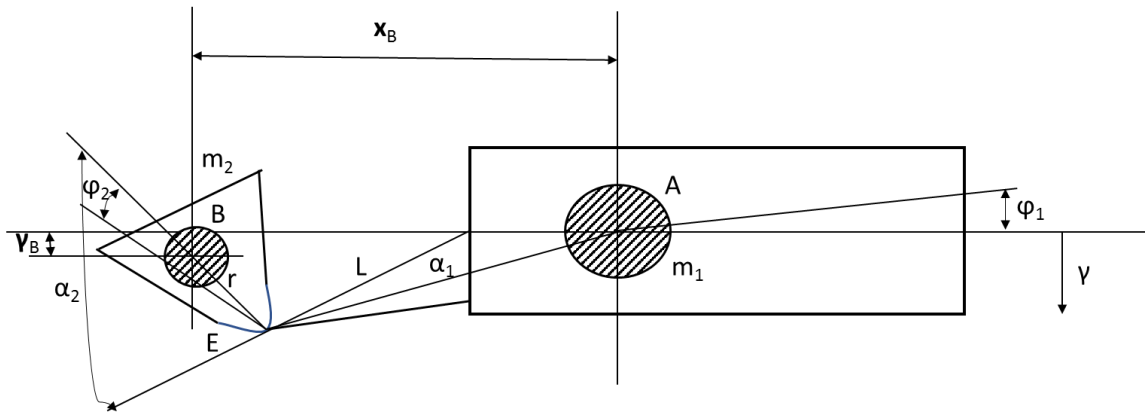


Figure 2.6. Wheel Loader Lift Arm Force Diagram - Example (Kolte, 2015)

Modelling Steps

1. Assembling the components into a current machine (i.e., mating the chassis, the bucket and the lift arms)
2. Motion simulation and parameter verification
3. Performing calculations derived from the first principles

This part of the design requires valid kinematics and dynamics models of the earthmoving machine. Various researchers have modeled the kinematics and dynamics of electric cable shovels (Awuah-Offei, 2011; and Frimpong, 2005) and wheel loaders (Sarata, 2004 and Li, 2015). These kinematics and dynamics models are used to estimate the forces and the stresses on the various components during digging which are then used to evaluate the design using numerical techniques like FEA.

Both the lift arms and the bucket are employed during digging operations.

Operations of both the lift arm and the bucket produces a combination of movements

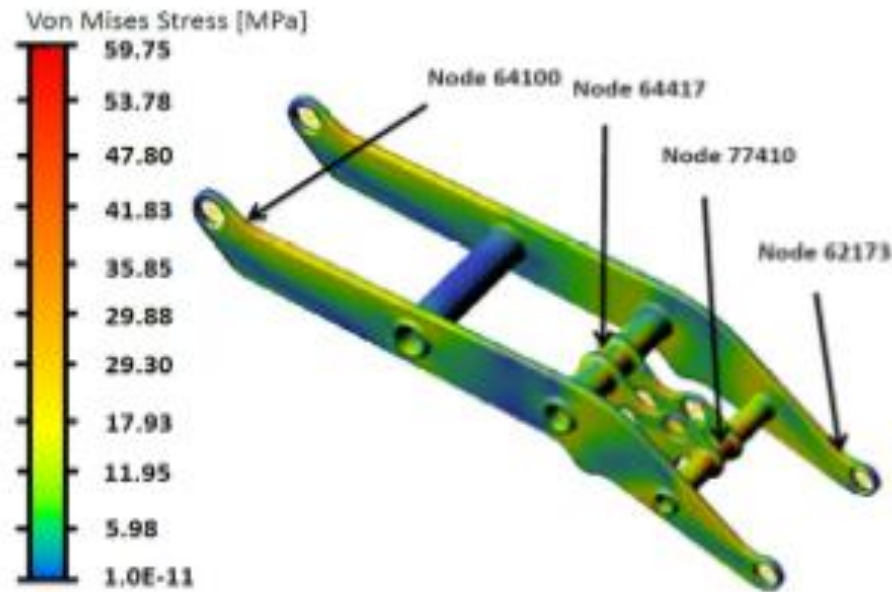


Figure 2.7. Example of FEA Model - Stress Changes of Key Nodes (Napadow, 2013)

during each bucket cycle. The specific force applied to the end of the bucket blade, which balances the forces of the active cylinder and the reactions of the ground equals the digging force (Bundy, 1988). Figure 2.8 exhibits the maximum stress in one of such model iterations. The maximum stress area appears as the red spot at the junction between the lift arm stiffener and the torque tube.

Virtual prototyping combined with FEA can be utilized to estimate the stresses of loading the bucket (Raza, 2013). The loading capacity of a wheel loader is the maximum load generated during operation, which is statically permissible for the machine to carry. This term has been borrowed from the theory of limit load capacity for rigid / plastic bodies. The instance of stability loss due to forces in hydraulic cylinders being exceeded is analog to the plastic flow from the original theory. The resulting analysis equates

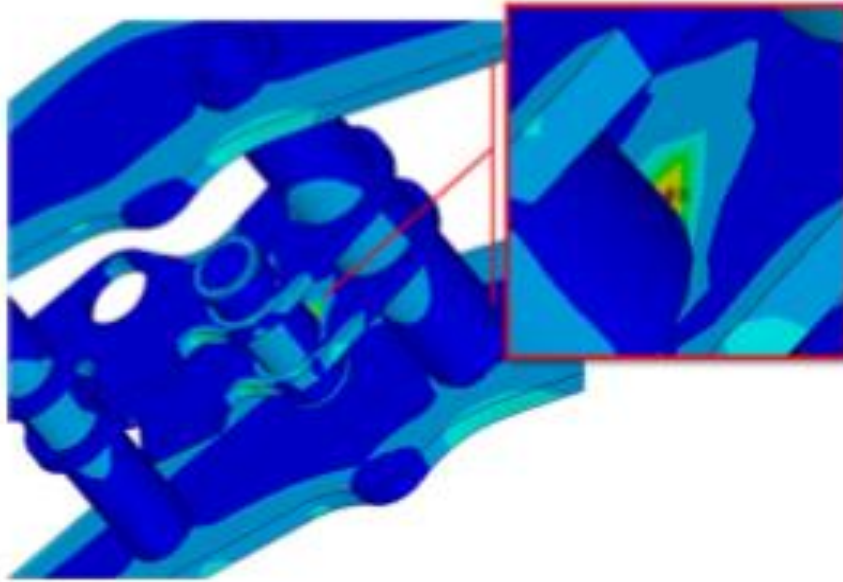


Figure 2.8. Location of Maximum Stress - FEA Model Example
(Napadow, 2013)

equipment geometry and statics, and optimization of the digging forces in the machine working area (Bundy, 1988).

2.2.3. Design of Equipment for Productivity and Performance. The design of the equipment fleet is based on the operational goal to deliver as much material as possible to its destination in the shortest time possible and at the lowest operating cost (Caterpillar (5), 2014). The movement of material from the loading point to the unloading point is accomplished by the mobile equipment fleet (i.e., a wheel loader and a number of trucks). The wheel loader is specified based on the capacity of the bucket, the work cycle of the loader which determines performance, and the ratio of the bucket capacity to the capacity of the truck bed or the hopper (Saderova, 2014). The equipment selection goal of the loading and hauling fleet is to have the right size and the correct number of pieces

available to perform the work in the environment at the lowest cost per ton (Corke, 2006).

Three specifications for selecting a loader (bucket capacity, work-cycle, and bucket to truck bed capacity) are used in matching the wheel loader to the truck fleet to optimize the equipment's efficiency. The wheel loader's bucket should be capable of loading a truck in a reasonable number of (usually 3 - 4) passes (Caterpillar AMA, 1998). The fleet design should be based on both methodical calculation from the OEM performance guides and empirical data from the fleet's proposed operational work area (Saderova, 2014). In loader truck fleets, a common loading pattern for loader-truck operations is the V-shape pattern, shown in Figure 2.9. The five parts of a V-shaped loading pattern are: 1) the loader reverses from the pile creating the first leg of the V; 2) the loader switches direction advancing towards the truck sitting at a slight angle to the pile, 15 - 30 degrees from perpendicular to the pile; 3) dumping the bucket into the bed of the truck; 4) the loader backs away from the truck; and 5) the loader advances into the pile perpendicular to the face for the next bucket (Corke, 2006).

The first step in the loading process (i.e., loading the bucket to its target weight) is the only step which affects the bucket load weight. This step must be executed consistently to achieve the target weight for the haul truck. There are several factors (i.e., swell of the material, muckpile fragmentation, and loading area floor conditions) affect the operator's ability to fill the bucket. Figure 2.10 shows a bucket trajectory model for an even and uniform muckpile. The bucket should be placed on the ground and engage the pile at point A. The bucket penetrates the pile until forward motion is stopped at point B, where the resistance force is increased proportional to increasing the depth of the pile

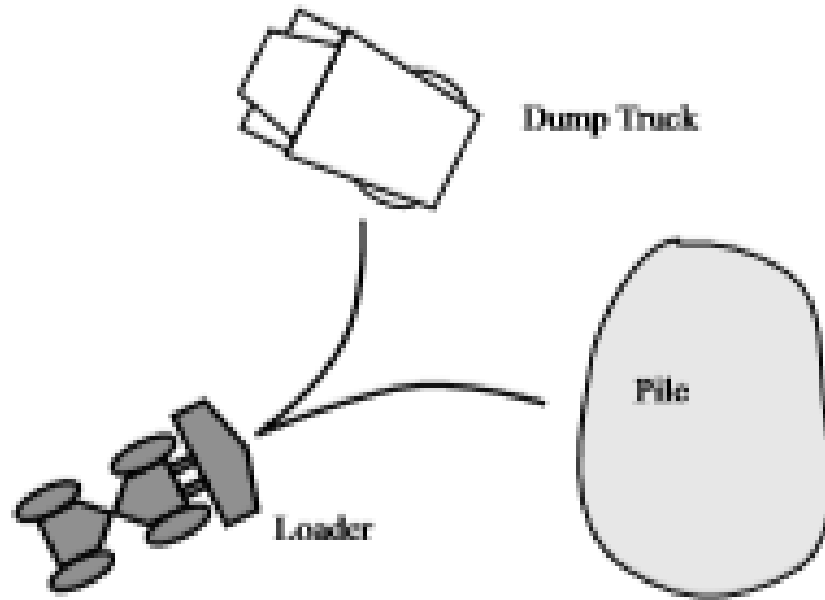


Figure 2.9. V-Shape Loading Pattern (Corke, 2006)

at the tip of the bucket. The bucket can continue to be loaded by raising and working the bucket back and forth to point C, where the resistance force is less. Point D is where the bucket has broken free of the pile and has its bucket load. The cross-sectional areas of point A, B, C, and D are the area for a bucket load (Sarata, 2006 and Corke, 2006). The operator's skill at penetrating the digface and the digability of the pile are critical in loading the bucket to achieve a targeted bucket loading.

All five steps in the bucket loading process contribute to the bucket cycle time. Each operational step in loading the bucket can and should be evaluated to determine its duration in the fleet design. The operational steps should be performed with a minimum of movement and fluidly transitioning from one step to the next (Saderova, 2014).

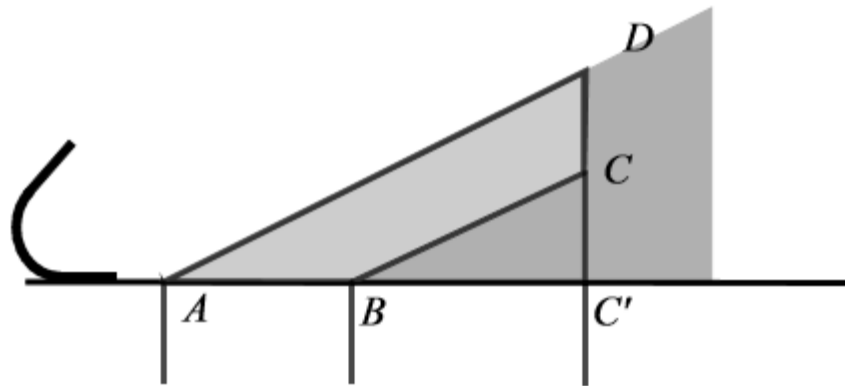


Figure 2.10. Bucket Loading Trajectory Model (Sarata, 2006)

2.2.4. Application of Equipment Performance and Productivity. The combination of the machine performance and the operator's level of skill have the greatest effect on the wheel loaders productivity. Empirical examples for both the bucket load weight and cycle time for a month are shown in Figures 2.11 (load weight) and 2.12 (cycle time) (Joy Global (4), 2016)).

A review of Figure 2.11 shows the distribution of the average weights with a mode of 61 tons, while the design was for 85% of the bucket weight payload (i.e., 60 tons per bucket.) The bucket load weight distribution shows it to be weighted to the left of center. This type of distribution should be expected due to the wheel loaders rated payload. The 7 ton difference between the design bucket payload versus the actual bucket load accounts for over 400 ton per hour or 105,000 tons in lost production and /or roughly an extra 42 hours (8%) of production time, along with \$20,000 of additional costs to achieve the designed specified results.

Figure 2.12 shows the cycle time distribution having a mode of 55 seconds, while the designed cycle time was 45 seconds per bucket. This 10 second difference from the

Load Weight

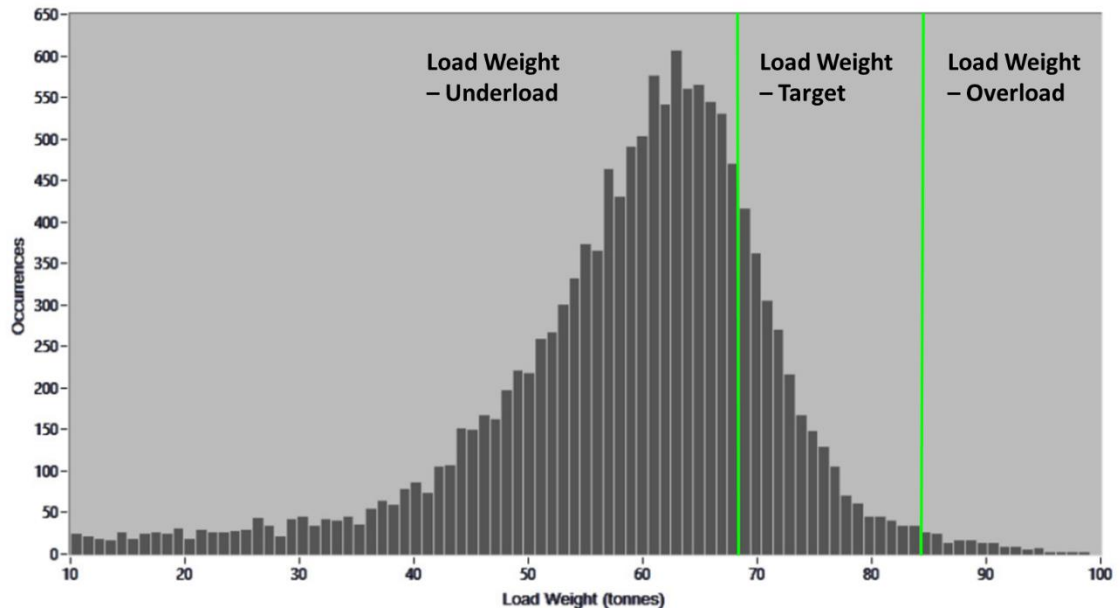


Figure 2.11. Sample Wheel Loader Monthly Load Weight Distribution

Cycle Time

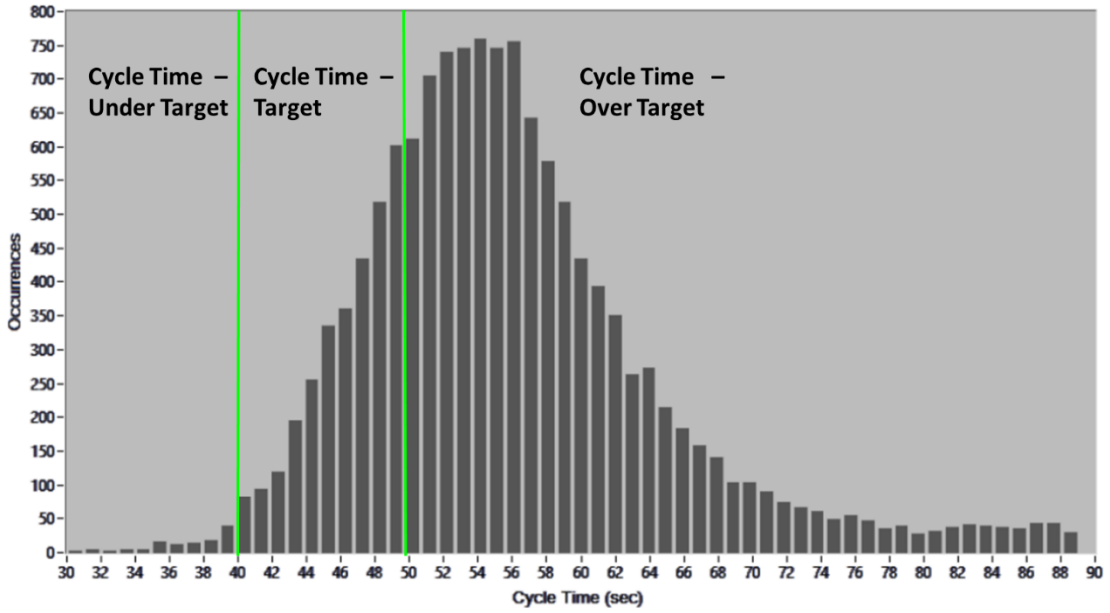


Figure 2.12. Sample Wheel Loader Monthly Cycle Time Distribution

design time to the empirical data shows that the operator is not cycling the machine properly. An evaluation would be a good first step to determine which factors need to be addressed (i.e., operator training, improvement of the loading area, better matching / timing of the haulage units). The extra cycle time results in 34 hours (7%) of additional production and \$15,000 of additional costs.

The combination of the bucket's load weight and the cycle time results equals the wheel loaders' productivity. This is expressed in Equation 2.1. The operator is the person who has the ability to affect the performance of the machine the most. This includes bringing its productivity to between 50% - 120% of its OEM specified performance. The operator can run the machine poorly which cuts its performance in half, or (s)he can operate above its designed limits to increase production levels (Caterpillar AMA, 1998 and Awuah-Offei, 2016). Other factors including operating conditions, mine planning and design, and equipment characteristics also effect the performance of the loading equipment. Examining each of these factors which effect the equipment's performance through the operator is generally the least expensive and the easiest one to change. (Oskouei, 2015).

$$\text{Productivity} = \text{Production (tons)} / \text{Time} \quad (2.1)$$

The combined productivity data from the wheel loaders' bucket and cycle time examples is displayed in Figure 2.13, "Sweet Spot" analysis. This productivity analysis shows the merged distributions together resulting in a weighted scatter plot. The target zones for both the bucket load weight and the cycle time overlay the data in an offset tic-tac-toe grid. The example results demonstrates the effect an operator can have on the

wheel loader's productivity by lowering it 15% due to the underloaded buckets and the slower cycle times. The results show that the majority (75%) of all loads were in the lower right sector, underloaded and over the targeted cycle time. The production fleet, especially the wheel loader, should be constantly monitored to minimize wasted capacity and operating costs (Barksdale, 1996).

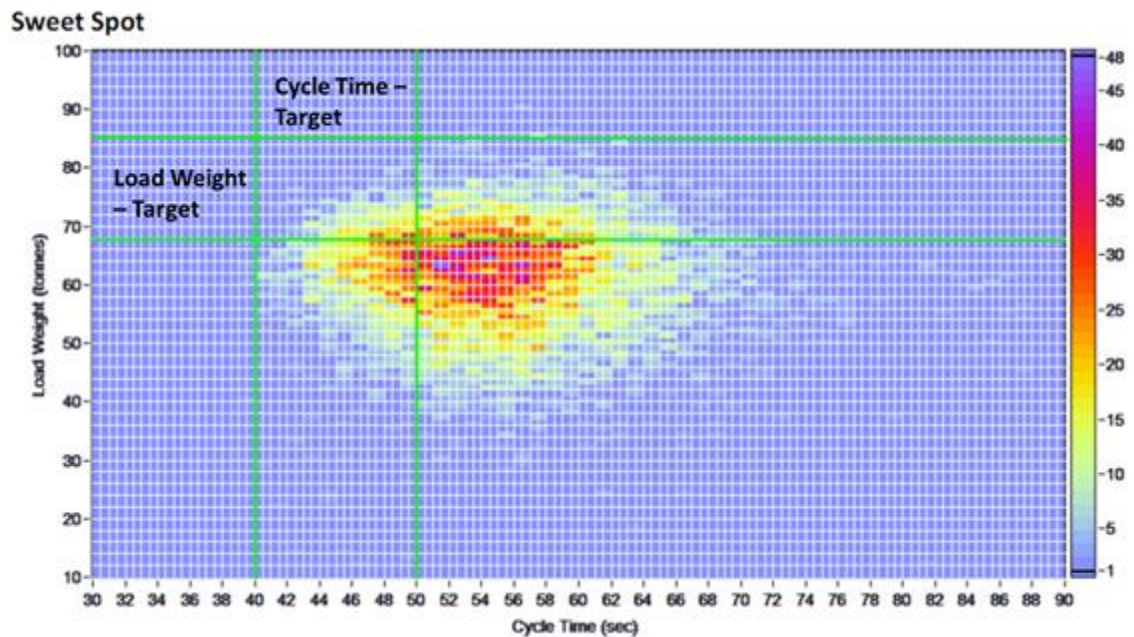


Figure 2.13. Wheel Loader Monthly Productivity (Sweet Spot) Analysis

2.3. EQUIPMENT RELIABILITY

It is the goal of every mine to achieve superior equipment or system reliability. Hence, reliability should be assessed against a set of specifications to ensure the system meets the performance criteria. A production system consists of different types of equipment; all units, components and sub-components must have high availability and reliability in order to ensure a stable and a reliable process (Fredriksson, 2012).

Moubray's view of reliability is that "reliability is not a function in its own right." Instead it is a performance expectation which pervades all of the other functions. It is properly dealt with by handling appropriately each of the failure modes which could cause loss of function (Moubray, 1997). A piece of equipment's reliability can be derived from its design which has been previously discussed, and how well it is maintained resulting in a unit's availability to perform its designed function when scheduled at or below the actual cost of operation (i.e., operating, maintenance and repair costs.)

2.3.1. Maintenance and Repair Philosophies and Practices. Maintenance is the combination of all technical, administrative, and managerial actions during the life cycle of an item which are intended to retain it in or restore it to the state in which it to the state in which it can perform its required function (Fredriksson, 2012). The tasks range from planning, scheduling, preparation, work, clean-up, and completing reports for activities ranging from daily inspections, preventative maintenance services, general repair tasks, component rebuilds to complete unit rebuilds (Wenz, 2013). There are numerous maintenance and repair philosophies and practices and variations of these are utilized to maintain equipment.

- Run to Failure
- Preventive Maintenance
- Predictive Preventive Maintenance
- Reliability Centered Maintenance

These philosophies are developed into maintenance programs and policies which are used to standardize the maintenance of a piece of equipment all the way to an entire fleet. A maintenance program establishes general standards to follow and prescribes the

minimal level of service or inspections to be performed at any point or state in the equipment's life. Individual pieces of equipment may have additional tasks or services added to their schedule based on their individual maintenance requirements (Smith, 2004). A discussion and overview of escalating levels of maintenance and maintenance planning follows.

2.3.1.1 Run to failure (RTF) maintenance. The simplest form of maintenance is run to failure (RTF) maintenance or reactive maintenance. RTF is doing zero preventive or planned maintenance and only repairing or replacing items after failure. This approach does make sense in certain situations (e.g., when inspections will not yield information about using the piece of equipment or component, the time and / or cost of inspections and preventive maintenance cannot be justified, and /or the part may be easy to replace). The use of the RFT maintenance objectives, and not a lack of planning on the part of the fleet / facility management (Eagle, 2017). Manpower shortages and /or lack of a budget for better monitoring and control are by far the most common reasons for selection of this method (Miltitrode, 2008). The RTF maintenance philosophy is the fallback strategy for all the following maintenance strategies. RTF brings the risk of increased repair costs, additional machine downtime, and the possibility of additional system failures to save cost today.

2.3.1.2 Preventive maintenance (PM). Preventive maintenance (PM) programs are designed to avoid equipment failures and to extend the equipment's life (Tomlinsong, (3),1998). PM programs are listed in the maintenance schedule provided in the service or owner's manual with the piece of equipment (Joy Global, (2), 2016). Typically, PM task consist of equipment / system / component inspections, specific testing and condition

monitoring to avoid premature failures. Additional PM items can include the changing of lubricants and filters, adjusting and replacing minor components to extend the life of the equipment (Tomlinsong (3), 1998).

2.3.1.3 Predictive preventive maintenance (PPM) or condition monitoring (CM). Predictive Preventive Maintenance (PPM) or Condition Monitoring (CM) can be a continuation of the PM program which requires additional tools and / or test procedures to ensure the health of the equipment. They utilize specific tools to identify the presence of a failure mode, so that action may be taken prior to total system failure. Examples of condition monitoring tests include: vibration analysis, infrared analysis, thermography, passive ultrasound, motor circuit analysis, lubricant analysis, stress / strain testing, and other forms of non-destructive testing (NDT) (Gehloff, 2013). Depending on the exact PPM test results, additional actions may be required (e.g., additional immediate repairs, scheduling of future repairs for the next scheduled down event, compiling data for trending and future PPM).

2.3.1.4 Reliability centered maintenance (RCM). Reliability Centered Maintenance (RCM) is the process of determining the most effective maintenance approach for a piece of equipment. The RCM philosophy utilizes elements of the maintenance programs described previously in this section. RFT, PM, PPM and RCM techniques can be integrated together to increase the probability that the machine or component will function the required manner over its design life cycle with minimum maintenance. The relationship of the elements in the RCM is shown in Figure 2.14. The goal of an RCM plan is to provide the stated function of the machine with the required reliability and its availability at the lowest possible costs. RCM requires that maintenance

decisions be based on maintenance requirements supported by sound technical and economic justifications (Nowlan, 2002). RCM utilizes the understanding of equipment failures and the root cause of each for each individual failure to improve equipment performance by reducing the maintenance workload and increasing the economic benefit of maintenance by improving the equipment's reliability (Ma, 2014).

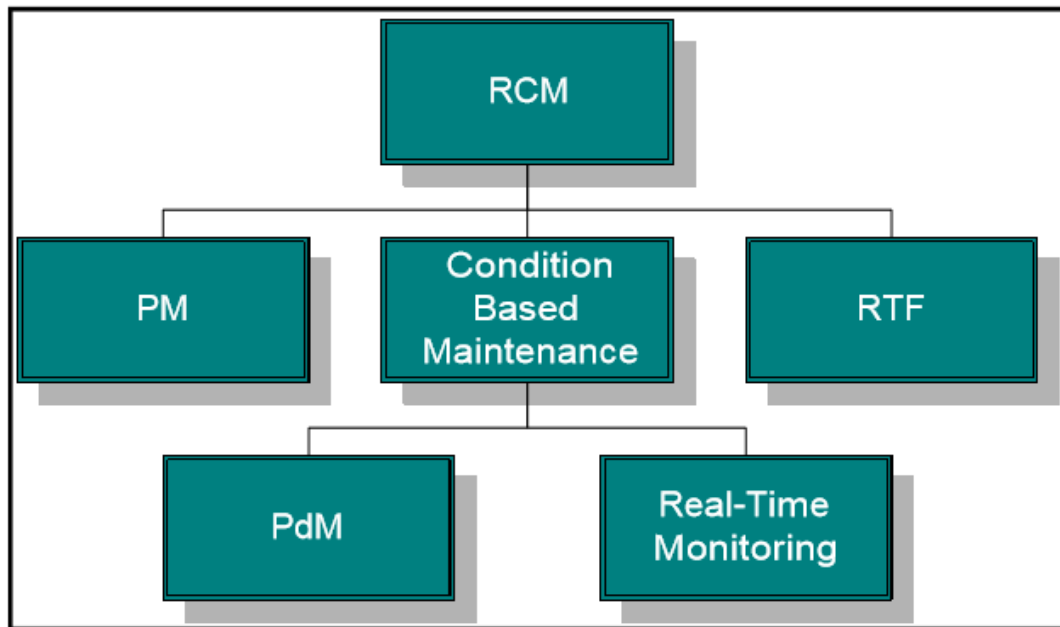


Figure 2.14. Elements of RCM (Nowlan, 2002)

RCM plans ordinarily begin with the examination of the PM, PPM, and RTF maintenance items to identify modes of failure for components and systems on the machine. These failure modes are then traced back to determine their effects on the machine's actual operation. Risk matrixes are used to quantify the severity of each failure mode (Nowlan, 2002). An example of a risk matrixes is shown in Figure 2.15. Most RCM analysis examines the risk of failure via multiple paths. This example uses four

separate risk paths (i.e., safety, environmental, operation, and financial). The assigned risk value for each path is independent of each other based on the exact failure (Reliability, 2015).

		Consequence				
		Very Low (1)	Low (10)	Medium (100)	High (500)	Very High (1000)
Probability	Frequent (5)	5	50	500	2500	5000
	Probability (1)	1	10	100	500	1000
	Possible (0.3)	0.3	3	30	150	300
	Remote (0.1)	0.1	1	10	50	500
	Improbable (0.05)	0.05	0.5	5	25	50

Figure 2.15. Risk Matrix Example (Meridium, 2015)

Following completion of the risk matrix based on the failure mode, plans are developed to mitigate the risk. The maintenance mode is determined depending on the equipment's components having different degrees of reliability and assessing the degree of the hazard. This strategy emphasizes the equipment's reliability and fault consequences as the main basis of the repair strategy. RCM eliminates any unreasonable part from the traditional maintenance mode, and then applies it to equipment maintenance

(Wu, 2014). The removal of non-productive services from maintenance programs reduces the maintenance time and the cost while increasing equipment reliability (Collis, 2016).

2.3.1.5 Establishing inspection / maintenance intervals. The key to establishing inspection / maintenance intervals is to maintain the health of the equipment by minimizing the repair cost with the goal of achieving / extending the machines targeted life. Preventive maintenance, consisting of short- and long-term targets, are essential to move maintenance to a desired level of excellence (Montenegro, 2003). Several maintenance models are classified according to three types of system dependence: 1) economic, 2) structural, and 3) stochastic; where economic dependence occurs when simultaneous maintenance of multiple components can reduce cost; structural dependence occurs when components form a part (often known as a line replaceable unit that is maintained as a single subsystem); and stochastic dependence occurs when the life of one component influence another (Jafary, 2017).

One way to begin establishing the maintenance intervals is from the PM service guide in the OEM maintenance manual (Joy Global (2), 2016). Cost models are another resource and can be obtained from the OEM to provide guidance on the life of major components (Caterpillar, 1996, Caterpillar, (6), 2014 and Komatsu, 2009). These are based on the reliability analysis and design life of the parts and components. The maintenance interval can further be influenced by regional support capabilities, skill level of mechanics and quality of replacement parts (Montenegro, 2003).

2.3.2. Equipment Reliability Analysis. Reliability is the starting point in the reliability potential of a piece of equipment. It is the role of the OEM to understand how the design of the unit, in terms of reliability, will affect the equipment performance under

different operating conditions, how this will affect the installed components, subsystems, sub-components and ultimately, the overall unit reliability (Roux, 2011).

Application and reliability engineers track the performance of the production system to monitor the production units, maintenance, and general health of the system. A system's productivity, the volume of goods produced over a defined period of time, is the unit of measure for most production based systems. The ability to measure, track, and improve the system's productivity is a corner stone of workflow management.

2.3.2.1 Reliability analysis process. Reliability analysis is generally part of a larger asset management process established to monitor and maintain the equipment's health. Asset management is a broad term referring to the systematic and coordinated activities and practices through which an organization optimally and sustainably manages its assets systems. Placing proper asset management systems in a mining environment and implementing the business plan leads to reliable plant and mobile equipment. Then in conjunction with mine planning forecasting, there is no reason why the planned maintenance activities cannot be followed religiously (Stephen, 2013). Six Sigma and lean thinking are processes concerned with improving quality by decreasing variability in the process in order to avoid poor quality or defects (as a form of waste). These processes are completed using workflow models to accomplish the tasks of planning, executing, and analysis (Ross, 2015). An example of a workflow model is the IPSECA (Identify, Plan, Schedule, Execute, Close, and Analyze) workflow management model, and an overview example is shown in Figure 2.16. Each stage of the IPSECA model can be broken down further into a continual loop process (Song, 2017).

The IPSECA workflow management model can be expanded into continuous improvement and sustained maintenance loops, as shown in Figure 2.17. Starting with the “Identify” part of the IPESCA model, a high level work can be prescribed to be completed. After identification of the high level work, detailed planning includes the identified tasks and is followed by scheduling the work, incorporating both resources and the time required to complete the planned tasks. Execution of the detailed plan is based on the scope of the identified work. A work follow-up review of the planning, scheduling, and execution parts of the IPSECA model unites the sustained maintenance loop. The last step analyzes the systems performance, closes the continuous improvement loop, and returns to identifying the new or reoccurrence work items. The use of workflow management models, specifically IPSECA, is one method employed to determine and improve the reliability and equipment health of a piece of production equipment and optimize its application.

One goal of equipment health monitoring (EHM) is tracking the wellness of components to determine their condition and operating health to estimate the Potential-Failure (P-F) curve. Most failure modes provide some sort of warning that they are in the process of failing or failure is about to occur (Moubray (2), 1997). There are three regions shown in the graphical representation of the of the P-F curve displayed in Figure 2.18. The first region shows the time of installation to Point P where it is possible to detect failure by tracking the component. The time between these points is where the component is operating normally within its designed operating parameters. The point to the right of Point P is where the component begins to fail. The purposed of inspections and testing (e.g., oil sampling, vibration analysis, thermal imaging, etc.) is to detect this

initial stage of failure and begin tracking the potential failure. The inspection and sample analysis reports are useful in establishing operating baselines for each component to compare and place in context among its peers (Riddely, 2017). The net P-F interval is minimum interval likely to elapse between the discovery of the potential failure and the occurrence of the functional failure.

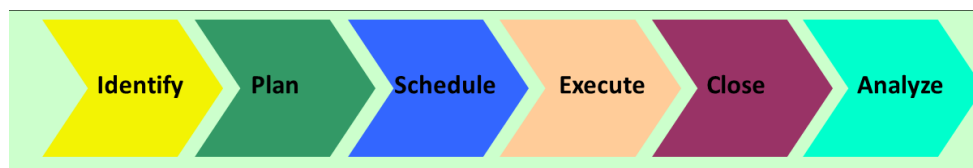


Figure 2.16. Example of the IPSECA Workflow Management Model (Collis, 2017)

Region two of the P to F identifies the potential failure at point P. Point P begins the first stages of failure and predicting the failure mode of the equipment so repairs can be made in a planned manner (Riddely, 2017). This is important in deciding on a component / parts inventory strategy and the allocation of repair personnel. The time between Point P and F can vary independently for each component and failure mode. The time can be very short (i.e., a few hours or days) or in other cases you may have months to plan and take corrective action. Additionally, it is important to determine the P-F interval consistency (i.e., given the failure mode, the time period between the points P and F on the curve and the time interval between the shortest and longest intervals) (Moubray (2), 1997). This is important in the scheduling process and procurement process to get men and materials assigned using the least costly method possible.

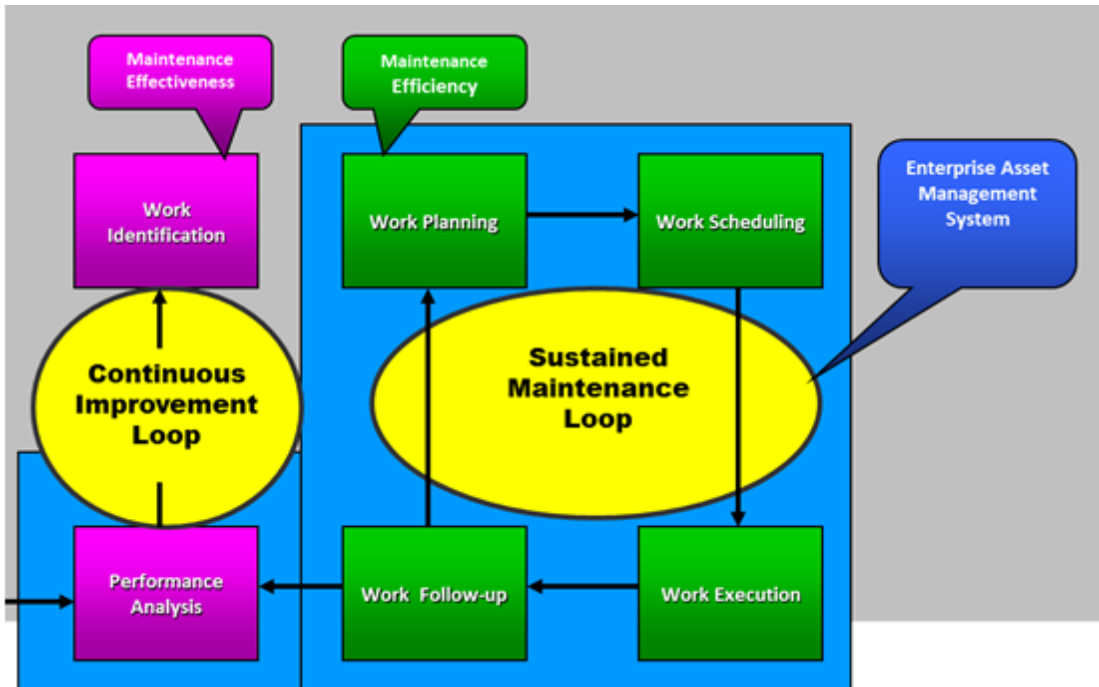


Figure 2.17. Assigned Tasks of the IPSECA Workflow Management Model (Collis, 2017)

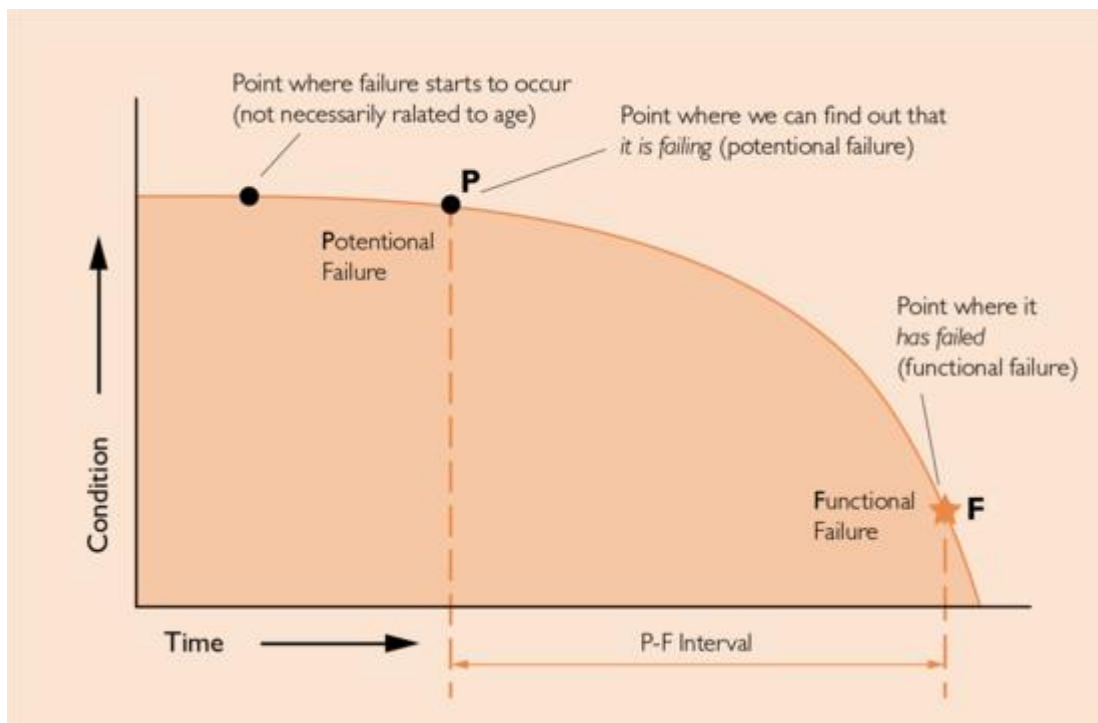


Figure 2.18. Probability Failure (P-F) Curve (Time is not linear in the graph) (Riddely, 2017)

The last region is at point F on the curve, where the functional or catastrophe failure of the component has occurred. Point F generally marks the most downtime and cost for the asset. Additionally, functional failure can cause secondary damage or failure to other systems resulting in additional downtime and expense to correct (Moubray (2), 1997).

2.3.2.2 Failure analysis. There are multiple processes and methods used to identify failures and their causes and work to put in place actions to find, mitigate or eliminate their effects. Two methods are root cause failure analysis (RCFA) and failure mode and effect analysis (FMEA). The RCFA examines the effects of the failure after they have occurred, while FMEA is a proactive approach. Both methods can be used to identify the second region of the P-F curve in order to prevent or delay the onset of Point P, potential failure point of the component.

Root cause failure analysis (RCFA) or root cause analysis (RCA) is a reactive process investigating the incident after it occurs by capturing all factors that affect the operating performance and failure including front line personnel actions, failed part(s), work environment, and work process. The RCFA investigation systematically drills deep into the organization's standards, policies and administrative controls to determine how those elements failed to prevent or eliminated causal factors associated with the incident. The RCFA process is resource intensive and typically reserved for high value casualty incidents where the cost of the investigation is justified in potential savings by prevention of recurrence (Krupa, 2004). RCFA is an efficient process placing priority on the item that experienced failure (Riddell, 2017).

The failure events are mapped to determine their root cause. The map provides a method to assign numeric values to each path to investigate each cause's findings, usually with a frequency distribution of the major root causes. A downside of the RCFA process is lack of follow through on implementing recommendations which address true root causes and prevent future problems. Operations focused on returning their equipment back to service without implementing the root causes leads to repeated failures of the equipment by the same failure modes time over time (Krupa, 2004).

Failure Modes and Effects Analysis (FMEA uses a systematic scientific technique of identifying, analyzing and preventing product and process problems before they occur (Silverman, 2013 & Moubray (4), 1997). FMEA should begin as early as possible, even before equipment is in operation and the process should be reevaluated several times during the equipment's life (Cassanelli, 2006). The failures that occurred should be reviewed and added into each subsequent FMEA process (Silverman, 2013).

FMEA process is composed of several steps. First is evaluation and enumeration of the failure modes of the equipment, subsystem or a part. Second, the engineer should rate the severity of the failure. This can be done with a technique similar to the risk matrix shown in the Figure 2.15 of the RCM section. Third, the engineer should address these failure modes by either eliminating them or protecting the asset from damage in order or severity (Silverman, 2013).

2.3.2.3 Distribution analysis. Conventional reliability analysis can utilize a number of different theoretical statistical distributions to analyze the failure hours of equipment components as a stochastic process. This facilitates changing the component over time due to failure of achieving their change out interval, (Barabady, 2007 &

Dhillon, 2008). Some of the distributions employed are exponential, lognormal, gamma and Weibull family distribution (Das, 2008; Waghmode and Sahasrabudhe, 2010; Barabadi, 2013; Moubray (5). 1997). Each of these distributions have their own strengths and weaknesses when applied to model equipment reliability and the optimal distribution to be used depends on data available for analysis and the particular circumstances (Barabady, 2013).

The Weibull family distributions are by far the most common for reliability analysis (Barabady, 2013). In fact, sometimes reliability analysis is called Weibull analysis. Weibull analysis can be performed on failure datasets such as that for a component or a piece of equipment. Typically, the dataset is constructed around a common factor such as failure mode, though it can be expanded to operating conditions, application, and additional factors (e.g., equipment identification and hours on machine and component at failure). Reliability analysis using a two-parameter Weibull distribution probability density function, shown in Equation 2.2, can be performed using a component failure dataset to determine the mean time between failure (MTBF), characteristic life (η) and the failure pattern of a structural component (i.e. the shape parameter, β) (Moubray (5), 1997). The Weibull distribution is commonly used for its versatility and the ease with which the parameters of the distribution can be estimated (Barabady, 2013 & Usta, 2012).

$$f(t) = \left(\frac{\beta}{\eta}\right) \left(\frac{t}{\eta}\right)^{\beta-1} e^{-\left(\frac{t}{\eta}\right)^\beta} \quad (2.2)$$

The two-parameter Weibull frequency distribution (probability density function) is versatile because of its variety of shapes, which enable it to fit many kinds of product

life data. The distribution is defined by the shape parameter beta (β) and characteristic life (η). Generally, Weibull distribution shapes for the shape parameter, $\beta=1$, is an exponential distribution, or constant (random) failures, shown by the green line in Figure 2.19. When β is between 1 and 4, it represents an observed constant failure rate shown by blue line. Most of the failures will occur in the middle of the components life-span. As β increases towards a value of 4 or higher, wear out failures are observed (yellow dashed line). These should be checked against the design life of the component. Infant mortality (premature) failures are represented by $\beta \leq 1$ displayed in red (Moubray, (5), 1997, & Uptime, 2017).

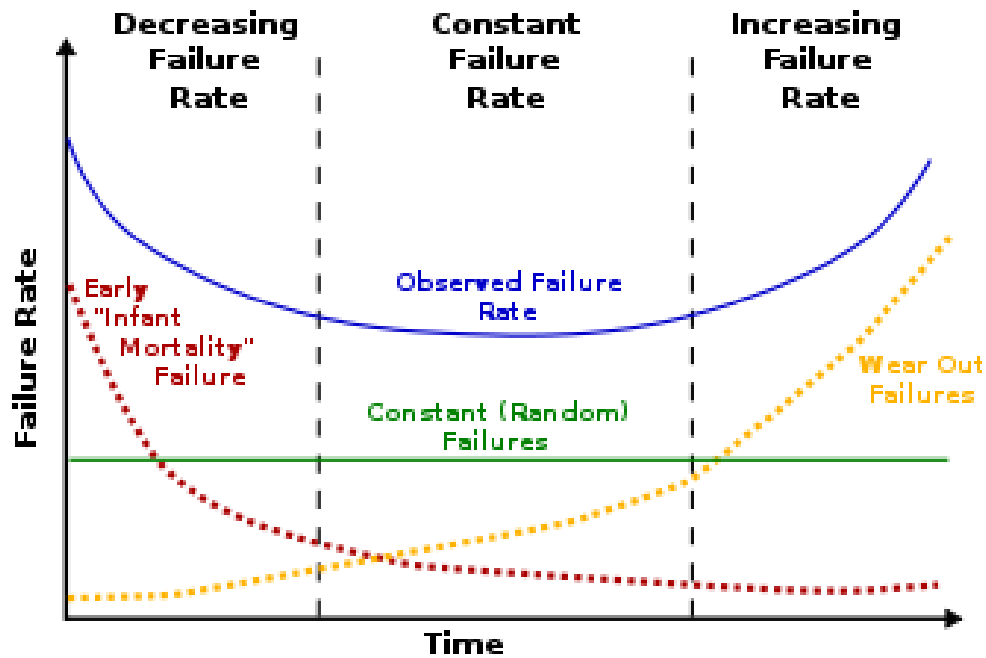


Figure 2.19. Failure Rate Curve Comparison (Uptime, 2017)

The main advantage of Weibull distribution analysis are its versatility (Barabady 2013; Usta 2012). Murphy et al. (2004) documented over 40 distributions used for reliability analysis in the Weibull family distributions. This wide range means that different failure modes can be captured by one of the Weibull family distributions. Even just the two-parameter Weibull distribution can be used to capture a variety of failure modes. Some authors have also pointed out the limitations of the Weibull distribution (e.g., Todinov, 2009)

This work chose to use the Weibull distribution because of its versatility. The candidate knew from his experience working with wheel loader failure data sets that Weibull distributions are able to capture the variety of failure modes. Also, the emphasis of the work was not to overcome the limitations of the Weibull distribution in reliability analysis.

2.3.3. Maintenance Plan Schedules. As part of formulating an effective maintenance plan / strategy, scheduling the tasks is the most important part of the plan's execution. Two types of schedules are typically developed. Both short-interval and global schedules are used to execute the maintenance plan. The short-interval schedule is used to schedule defined routine tasks, (e.g., engine oil change) and its duration (e.g., 250 hours). The schedule is continually updated based on current equipment performance data and the duration of previous service events. Short duration schedules are typically forecast and scheduled out a week to two months in advance. The global schedule has a forward looking focus of typically 6 to 24 months. It examines the long duration non-routine services (e.g., yearly inspections, component replacements, machine rebuilds, or plant shutdown events). Events which are on the global schedule typically require additional

planning to ensure that the required parts are ordered and on-hand before commencing the maintenance activity, scheduling an OEM or specialty contractor to perform the work, and coordination with other departments to assign tasks or make them aware that non-routine work is commencing (Song, 2009). The maintenance plan intervals generally fall into two categories, time based (i.e., hours, days, months, etc.) or event / cycle based.

2.3.3.1 Time based maintenance intervals / events. Time based maintenance intervals measure the service interval by hours run, days, operated, or calendar days (e.g., perform these tasks the 15th of the month). Time based maintenance intervals of tasks are typically based on design criteria or RCM analysis based on the failure range of FMEA analysis as part of the planning / implementation stage for the RCM plan (Huang, 2012). Multiple inspection services or tasks should be scheduled and conducted to detect the failure prior to a catastrophic failure event (Moubray (3), 1997). These inspections should be conducted in the first stage of the potential-failure (P-F) curve, discussed in Section 2.3.2.1.1, prior to detection at Point P. The reason for these inspections is to establish a baseline of what is normal for this specific component and to identify premature failure, based on its populations normal failure window (Moubray, (3), 1997).

Tracking these maintenance tasks generally takes place in a computerized maintenance management system (CMMS). This allows for the accumulation of operating hours on components and equipment together as well as scheduling and forecasting maintenance and repair activities (Tomlison, (2), 1998). The CMMS provides a repository for previous component histories and failures. This information is critical in construction of datasets used in failure analysis tests and updates to the time-based maintenance intervals. Additionally, age replacement PM is developed for both

system availability and expected system cost. The PM interval objective is to optimize the interval and minimized the cost, which also has a two-front purpose to extend the PM or inspection interval while not increasing the likelihood of component failure (Grida, 2012).

A limiting factor to time based maintenance intervals is it takes a simplified approach to scheduling the interval based on the collective failure of the group. This poses a danger to safety critical systems which suffer failures based on overworking the component beyond its designed duty-cycle (Jafary, 2017). This has led to industry looking for additional ways to quantify the duration of the maintenance plan based duty-cycle of the equipment.

2.3.3.2 Non-time based maintenance intervals / events. Non-time based maintenance intervals are gaining acceptance, though require additional resources to track and analyze additional accumulators to either hold off or trigger the maintenance event. Examples of this type of this service intervals follow: 1) the engine service should be scheduled when the engine has accumulated 150 hours of run time above 1500 rpm, or 300 hour of run time whichever comes first (i.e., the engine is operating above the designed duty-cycle of 50% (Cortese, 2016) or 2) a machine structural inspection is scheduled every 500 overloads or 30 critical overloads (Dubberly, 2017). The first example shows a combine PM service scheduled logic where the service could be scheduled earlier based on increased duty-cycle of the machine based on application, operator, or both. The second examples uses just the non-time based accumulators to

schedule the service regardless of time. A structured method is necessary to choose the practices, which will help to achieve the objectives (Montenegro, 2003).

Modern mining equipment is designed with various on-board equipment monitoring systems (e.g., Caterpillar's Product Link and Vehicle Informational Management System (VIMS) (Caterpillar, 2017) and Joy Global's LINCS and PreVail systems (Joy Global LCM, 2017). These systems monitor and report the health of the equipment to the operator through on-board monitors which display the results as well as save and transmit this information from the equipment to the cabin for further analysis. The data currently available from these on-board monitoring systems include production and operating system information.

2.3.3.3 Reviewing and optimizing inspection / maintenance intervals and costs associated. Periodic auditing of maintenance plans is crucial to verify actions are undertaken according to the predicated patterns to bring about the improved results. The audit makes possible the identification of vulnerable points and specify countermeasures for the continuous improvement of the maintenance process (Montenegro, 2003). These plans are reviewed and updated to focus on specific fleets, company goals, or other factors in order to optimize the maintenance of the equipment. These updates focus on the short- and long-term targets are essential to move maintenance to a desired level of excellence (Montenegro, 2003).

As the maintenance practices evolve through the use of RCM and other maintenance philosophies concerning system improvements, maintenance training, work planning, failure treatment and supplier / service purchase agreements (Montenegro, 2003). The key to a successful maintenance strategy is to minimize the downtime, ensure

that the proactive maintenance tasks are properly being used, thus reducing / eliminating the reactive tasks, meaning less failures, minimized downtime events, lowered stress and higher quality, all working to increase profit (Fredricksson, 2012).

Despite the large number of maintenance models and applications, relatively few studies consider the impact of correlation of dependence on the optimality of maintenance policies (Jafary, 2017). Changes to the organization evolve overtime as part of progressive maintenance strategy (i.e., changing practices to increase availability) by reliability predicting failures and maximizing the lives of components help to reduce cost per unit. The consolidation of these gains across the fleet allows for additional lower costs for other equipment or additional operations (Fredricksson, 2012).

2.4. EFFECT OF MACHINE OPERATION AND PERFORMANCE ON RELIABILITY

Most earthmoving equipment structures (e.g., equipment frames) are designed to last until a major rebuild or the entire working life of the machine. The reliability and the remaining useful life of a piece of equipment or its components depend on the stress and its load history. The structures are designed to suffer through loading conditions which are measurable, quantifiable, and not deterministic (Corbetta, 2014). The literature contains work that tries to solve one of multiple specific problems of the real-time prognosis of fatigue-induced damage propagation, and, thus, how to determine the residual amount of life remaining in the structural components (Corbetta et al., 2015).

Corbetta et al. (2015) suggests looking at multiple real-time damage prognoses when dealing with random loading conditions, which are more complicated to model than the constant amplitude fatigue measurements. In cases where the structure is subjected to

random loads, the instantaneous value of the load is unknown, future loads are unknown as well which pose significant challenges. The next case involves uncertainties on the current load conditions. In these cases the load can be equated in statistical terms and estimated using a rainbow method, extracting the mean load and the range. However, rainbow load counting is an approximated extraction of the actual load affecting the damage, which remains unknown. In the third case, retardation and acceleration effects due to the load sequence can be scrutinized. The crack growth accelerates with overload events, thus reducing the life of the structural component(s). In the last case, there remains the uncertainty of future loads where damage may occur and propagation from the current state until a critical condition is reached. For all of these cases, the nonlinearity method of describing damage propagation prevents closed form solutions for the component's residual time (Corbetta et al., 2015).

The forces which earthmoving equipment are subjected can vary greatly depending on the equipment operator (i.e., angle of attack entering the pile, speed entering the pile, and manipulation of the bucket in the pile), site conditions, (i.e., floor conditions, fragmentation size, and pile conditions) (Oskouei, 2014), and environmental factors (i.e., weather, time of day). Examination of wheel loader production data in this study shows all of these factors to be in play. The data shows times of “normal operations” with a few to no overload events occurring for long periods of time, (i.e., multiple days with multiple operators). Conversely, the data also shows localized events with multiple overload events occurring back-to-back or in a small cluster, (i.e., 5 bucket overloads in a 10 bucket sample). In these digging conditions, each hour the equipment operates at a stress level higher than “normal use” or “designed use” is equivalent to

more than one hour of normal use. How much more can be determined by estimating a stress acceleration factor (Li, 2007).

The examination of failure degradation of the structural components follows two paths: (1) gradual failure, where the failure occurs over time and can be tracked and acted upon to correct; or (2) sudden failure, which is generally catastrophic and requires complete replacement of the component (Beganovic, 2017). The stress and load history depends on the duty cycle, which can contribute to structural fatigue leading to failure or to the ultimate failure of the structure. That is, how the equipment is used determines the loads and stresses to which it will be subjected. Current practices for life time assessment are based on conservative design assumptions and simplifications due to uncertainties. This conservative approach potentially leads to under-estimation of actual fatigue life, and over monitoring for failures (Noppe, 2016).

Structural components are monitored via inspections and on-board sensors. First, these inspections range from the daily operator inspections through complete frame inspections (Noppe, 2016 and Joy Global (3), 2016). The effects of the inspections are decreased availability and increased maintenance time to complete the checks. Mobile equipment can be installed with strain sensors for direct strain measurement at critical fatigue locations. The use of these sensors has limitations. The sensors are known to be unreliable over time due to damage from operations, loss of adhesion to the equipment, and maintenance and data analysis requirements (Noppe, 2016 and DePorter, 2017).

For earthmoving equipment, the operator has a significant influence on how the equipment runs and the loads the equipment experiences (Oskouei, 2015). For example, Abdi Oskouei and Awuah-Offei (2015) show significant differences in dragline energy

efficiency due to differences in dumping height, drag distance, and spotting time, among others. Differences in operator practices, such as these, not only affect energy and production efficiency but also affect the loads and the stresses to which the equipment is subjected (Awuah-Offei, 2015). Again, a preliminary review of the production datasets in this research indicates that the loading times vary greatly from one bucket to the next due to the operator's skill level (i.e., amount of distance covered by the loader, the activation of multiple commands, hoisting the bucket and moving the loader, and working the pile in relation to truck).

For loading equipment, the payload is a key indicator of the loads and the stresses the equipment sustains. The frequency of overloading is an indicator of the higher than normal use that the loading machine endures, which could affect the remaining useful life and the reliability of the equipment. Hence, there is reasonable evidence to suggest that the extent of overloading should be accounted for in estimating the reliability of the machine. It is normal practice to use the current overload rate to supplement the time based hours of operation in establishing the maintenance inspection and replacement intervals. This is similar to identifying equipment idling too long and taking corrective actions (Akhavian, 2013).

However, the author did not find any work in the English literature which accounts for using overloading in estimating loading equipment reliability. The ability to issue / reschedule maintenance tasks based on multiple parameters, (i.e., run hours and duty-cycle conditions, bucket overload events) could increase the likelihood of finding structural issues which will increase the equipment's availability. This would be accomplished by tracking the number of overload cycles which would give the

maintenance department the ability to shorten the inspections and service intervals for machines when they are seeing increased high force (stress) events and extending these intervals when these events are occurring less frequently.

2.5. RATIONALE FOR PHD RESEARCH

The rationale for this PhD research is to: (1) improve our understanding of the effect of payload on the forces incident on a wheel loader's liftarms and bellcranks (using cylinder pressures as the proxy for forces); and (2) develop an approach to incorporate overloading (duty-cycle due to payload) into reliability analysis of the wheel loader's structural components.

Reviewing the literature around the first point (the effect of payload on the on the forces incident on wheel loaders) shows that some machines have been instrumented with stress / strain sensors for limited periods of time. The purpose of these measurements were to determine the stresses on the machines structural components in its working environment. While stress /strain sensors provide good data for this purpose, there are limitations of this approach. First, not all machines are instrumented and those that are require additional maintenance to keep the sensors on the machine and downloaded for analysis. Second, the stress data generated is considered proprietary information by OEMs. Hence, the literature does not provide much stress data from wheel loaders operating in the field.

We need an alternate method to provide, say using a proxy that is non-proprietary, to determine the forces exerted on the wheel loader during operations. The hoist cylinders have been identified as part of the wheel loaders liftarms group and are instrumented in the on-board monitoring systems to display the pressures required to lift the bucket free

of the pile and hoist it to the tipping point. These sensors are monitored via the loader's on-board monitoring systems and remote health monitoring (RHM) system (e.g. PreVail). This research seeks to provide a method, based on non-proprietary data, to understand the effect of payloads on forces exerted on the wheel loader during operations.

The second rationale (develop an approach to incorporate payload duty-cycle into reliability analysis of the wheel loader's structural components) was to bridge the knowledge gap between the parameters monitored by RHM systems and the accumulators used to operate preventative maintenance systems in order to increase the equipment's availability. The research is to evaluate the feasibility of developing PM programs based on dual triggers (as opposed to just time) and to transition from the current inspection window of hours to hours and the payload duty cycle (i.e., account for the effect of overloads and critical overload events) without decreasing equipment reliability. Such an approach will allow maintenance engineers to establish PM inspection triggers and to have the service issued in a timely manner that accounts for the variability of the duty-cycle based on loading conditions. To the best of this candidate's knowledge, there is no work that has attempted to account for payload duty-cycle in reliability analysis. And this is not currently part of industrial practice.

Currently, the RHM system (e.g., PreVail) for wheel loaders has limitations and this research is to address and upgrade the some of these items in the system. The RHM systems does not use duty-cycle as monitoring factor in reliability analysis. Additionally, the RHM does not used monitor the relationship of forces (i.e., hoist cylinder pressures) exerted on the wheel loader and the payload being lifted. The knowledge gained from this

research will be used to improve the RHM system to better monitor equipment relating to its application and duty-cycle.

Following completion of this research there will be multiple additional steps required to transition from the results to commercial application. First of these steps will be the new accumulators (determined from this research) will have to be built into the maintenance profiles of new machines in the maintenance system to track the overload events in order to issue structural inspections based on them. Currently, operating machines profiles will have to be edited with these new accumulators to provide the same functionality. Before this is done, there needs to be evidence that these accumulators can improve reliability estimates to justify the cost and effort. This is the focus of this research.

3. EFFECT OF OVERLOADING THE BUCKET ON WHEEL LOADER PRODUCTIVITY - A CASE STUDY

3.1. INTRODUCTION TO WHEEL LOADER PRODUCTIVITY

This section addresses the first objective of this dissertation. The work uses data from 20 ultra-class wheel loaders in mines around the world to examine the effect of overloading the bucket on wheel loader productivity.

Tracking the impact that overloading the wheel loader bucket has on productivity was broken down into three tasks: (1) the raw datasets were separated into four bucket load categories based on their weight percentage: under loads (<85%), target weight (85-105%), overloads (106-120%) and critical overloads (>120%); (2) the production rate for each cycle was determined by bucket categories; (3) the production rates were compared using an analysis of variance (ANOVA) to evaluate whether there is a statistically significant difference between the productivity of different sets of data.

The first step was completed during the analysis of the information by separating the raw data load categories. Each data point was assigned to one of the four categories (under loads, target weight, over loads, critical overloads) based on the weight percentage (ratio of the payload to the rated bucket payload). The second stage determined the productivity of each load based on the cycle time and the payload. In the third step, the datasets were subjected to an ANOVA single factor test to evaluate whether the bucket cycle times and productivity rates were significantly different.

3.2. EXPERIMENTAL EQUIPMENT & SITES

The ultra-class wheel loaders provide a unique fleet to study due to high bucket capacity and small overall population of a few thousand machines operating around the

world (ParkerBayMining, 2016). These wheel loaders operate in mines all over the world in production, stripping, stockpiling, and support roles in all the major mining sectors which include coal, base and precious metals, industrial minerals, and gemstones. Table 3.1 discloses the number of units in this study, commodities mined, regions, and applications in which the ultra-class wheel loaders operate. Table 3.2 details the number of loaders by the commodity they extract during their shift operations. The wheel loaders are matched to haul trucks to provide optimal loading in three to seven passes based on the trucks' payload capacity (typically greater than 240 tons) (JoyGlobal.com). Wheel loaders provide great flexibility to mining operations because they are able to quickly relocate to different faces in the mine, blend ore in the pit, and provide a variety of other tasks (Hartman (1), 1992).

Table 3.1. Ultra-Class Wheel Loaders by Operating Class and Region

Bucket Capacity (st)	Unit in Study	Commodity	Location	Application
60	1	Coal, iron ore, copper, and overburden	Australia, North America, and South America	Production, overburden, and stockpiling
55	8			
80	5			
75	6			

Table 3.2. Ultra-Class Wheel Loaders by Operating Model and Commodity

Class	Commodity			TOTAL
	Coal	Iron Ore	Metal	
55 - 60 ton	5	3	2	10
75 - 80 ton	-	8	2	10
TOTAL	5	11	4	

This is a case study of ultra-class wheel loaders operating in multiple regions around the world mining several different commodities. An overview of the geology of these mining districts follows.

3.2.1. Geology of the Australian Iron Ore Deposits. The largest number of wheel loaders which were studied operated in the iron ore deposits of Western Australia. All five of the 80 ton class wheel loaders and one 55 ton machine and 60 ton class machine operated in this region. The iron ore deposits in this region are banded iron formations. Banded iron formations (BIF) are heavy narrowly banded sedimentary rocks, which alternate with a variety of iron rich layers of fine grained quartz. Common minerals comprising the banded BIF include: hematite, magnetite, siderite, and stilpnomelane. Large BIF also occur in China while smaller deposits are mined in the United States and Canada (GSWA, 2017).

The Hamersley province, known as Pilbara, of Western Australia contains the largest area of banded iron formations in the world. The Pilbara region was discovered in the early 1950s, and the iron was deposited 2.4 billion years ago during the late Archean to the early Proterozoic eras. This region extends over 150,000 square kilometers and contains approximately 300 trillion tonnes of iron. (Morris, 1998).

3.2.2. Geology of Australia Bowen Basin Coal Deposits. Two of the 55 - 60 ton class wheel loaders in the study operate Queensland's Bowen Basin. The deposition in the Bowen Basin began during the Early Permian to the Middle Triassic periods with the concentration coming from two north trending depocenters, the Taroom Trough in the east and the Denison Trough to the west. The deposition in the basin consisted of fluvial and lacustrine sediment and volcanics deposited in a series of half-graben structures in

the east while a thick succession of coals and non-marine clastics were deposited to the west. (A half-graben is a geological structure bounded by a fault along one side of its boundary.) Following rifting, thermal subsidence occurred during the mid-Early to Late Permian period. Foreland loading of the basin spread from east to west during the Late Permian period, which resulted in accelerated subsidence allowing for deposition of material. During the Late Permian a basin-wide event allowed depositions of deltaic and shallow marine sediments, which were predominantly clastic sediments as well as extensive coal formation. Deposited materials were a very thick succession of Late Permian clastics, along with coal deposited during the Early to the Middle Triassic periods. Sedimentation in the basin was terminated by a Middle to Late Triassic contractional event (AG GA, 2017). The coal seams in the basin typically dip steeply and limit surface pits to depths of approximately 300 meters (Hutton, 2009). Hutton (2009) estimated that the resources for this depth are approximately 23,200 million tonnes in 2004.

3.2.3. Geology of the South American Iron Ore Deposits. The remaining six iron ore wheel loaders studied operate in Brazil's Carajas Mineral Province. This district has had several distinct periods of anorogenic ring complex cluster formations. The last formation took place roughly 1.90 to 1.75 billion years ago during the Paleo Proterozoic period, which produced massive iron oxide mineralization. The deposits, which were first thought to be BIF, are actually hydrothermal replacement iron oxide copper gold (IOCG) type deposits. Granitoids seem to be directly associated with the iron mineralization in the province (Lobo-Guerreo, 2008). The Carajas Mineral Province iron ore deposits

make-up an estimated eighteen billion tons of ore with a 66% iron content (Rosi re, 2000).

3.2.4. Geology of the North American Copper Deposits. One of the ultra-class wheel loaders in the study operates in the copper mines of Arizona's porphyry-copper deposits. These are generally associated with intrusive igneous rocks. These deposits were formed below the surface from saline and metal-bearing fluids that were expelled from cooling magma. The saline fluid and heated groundwater interacted with rocks adjacent to the intrusion chemically altering the depositional area of the host rock. The deposit also commonly contains molybdenum and silver as co-products which were introduced via the saline fluids (Allison, 2017).

Erosion and weathering over millions of years exposed these metal deposits. Additionally, weathering further concentrated the copper through secondary enrichment. Pyrite was oxidized, which dissolved in rainwater, then forming an acidic iron sulfate solution which dissolved the main copper-ore mineral, chalcopyrite (copper-iron sulfide). The dissolved copper was redeposited as principally chalcocite (copper sulfide) (Allison, 2017).

3.2.5. Geology of the North American Coal Deposits. Several ultra-class wheel loaders operate in two different North America coal deposits, the Powder River Basin (PRB) of northeastern Wyoming and southeastern Montana (Luppens, 2013), and the coal fields of northwestern Colorado (CGS (2), 2017).

The Powder River Basin coal deposits began sixty million years ago as the bottom of a shallow sea of rich subtropical swampland. The plant layers formed peat beds, which when buried and compressed turned into low-sulfur bituminous and subbituminous coal

strata (Braasch, 2013). The PRB's coal seams are known to be over 100 feet in thickness and are located close to the surface. The PRB basin consists of over forty coal beds, with the most significant resources being the Roland (Baker), Smith, Anderson, Dietz 3, Canyon, Lower Canyon, Werner/Cook, Otter, Gates/Wall, and Rosebud/Knoblock coal beds of the Tongue River Member of the Paleocene Fort Union Formation. The United States Geological Survey (USGS) estimates an in-place resource of 1.07 trillion short tons of coal with actual recoverable coal resources set at a 10:1 stripping ratio which equals approximately 162 billion tons. Luppens (2013) estimated the economically recoverable resources to be 25 billion tons in 2013.

The surface coal deposits of northwestern Colorado are shallow enough to be extracted by open-pit methods. This coal was formed during the late Cretaceous and the Paleocene-Eocene of the Tertiary Period, between 55 to 100 million years ago, to form bituminous coal (CGS (1), 2017).

3.3. DATA COLLECTION

The machine data was collected from wheel loaders with an on-board equipment monitoring system at multiple sites around the world by mechanics, field service engineers (FSE), factory service representatives (FSR), and factory engineers as part of monthly maintenance procedures. One of the technician's duties includes downloading the wheel loader's production data file monthly and posting it online via the OEM's portal or emailing it for review. The production data file was saved by the candidate to a directory on a laptop setup up with the model and loader ID number. The production data file consists of four data columns: event type, data / time, event, and the weight (in tons) of the event. A 30-minute sample of downloaded production data is shown in Table 3.3.

Table 3.3. Sample Wheel Loader Production Data -
 Wheel Loader 8015 Date 1/16/16
 (weight is color coded by load type located in Table 3.7)

Event Type	Date	Event	Weight (tons)
Production	1/16/16 3:01	Bucket Load Weight: 84	84
Production	1/16/16 3:01	Bucket Load Weight: 72	72
Production	1/16/16 3:02	Bucket Load Weight: 79	79
Production	1/16/16 3:04	Truck Load Weight: 235	235
Production	1/16/16 3:04	Bucket Load Weight: 84	84
Production	1/16/16 3:05	Bucket Load Weight: 83	83
Production	1/16/16 3:06	Bucket Load Weight: 78	78
Production	1/16/16 3:07	Truck Load Weight: 245	245
Production	1/16/16 3:07	Bucket Load Weight: 74	74
Production	1/16/16 3:08	Bucket Load Weight: 87	87
Production	1/16/16 3:09	Bucket Load Weight: 75	75
Production	1/16/16 3:10	Bucket Load Weight: 48	48
Production	1/16/16 3:13	Bucket Load Weight: 80	80
Production	1/16/16 3:16	Truck Load Weight: 364	364
Production	1/16/16 3:19	Bucket Load Weight: 77	77
Production	1/16/16 3:20	Bucket Load Weight: 80	80
Production	1/16/16 3:21	Bucket Load Weight: 74	74
Production	1/16/16 3:23	Truck Load Weight: 231	231
Production	1/16/16 3:23	Bucket Load Weight: 78	78
Production	1/16/16 3:24	Bucket Load Weight: 79	79
Production	1/16/16 3:24	Bucket Load Weight: 78	78
Production	1/16/16 3:26	Truck Load Weight: 235	235
Production	1/16/16 3:26	Bucket Load Weight: 76	76
Production	1/16/16 3:27	Bucket Load Weight: 85	85
Production	1/16/16 3:28	Bucket Load Weight: 87	87

The data was downloaded onto a Dell laptop running Windows 7 64-bit operating system. The laptop has an Intel® Core™ i7-4712HQ CPU processor operating at 2.30GHz with 16.0 GB of installed memory (RAM). All of the data files were downloaded, stored, and processed using this laptop during the project. An additional copy of the dataset of files was maintained on a server as backup during the project.

3.3.1. Step 1: Compile the Wheel Loader Productivity Data. After the downloaded information was received or downloaded from the servers, it was compiled with previous downloads from the same wheel loader. Each wheel loader in the study was able to provide one to twenty monthly downloads worth of data. Each download was processed through the use of Joy Global's LeTourneau Integrated Network Control System (LINCS) software versions 2.20 or 3.60. The data was then converted to a comma-separated variables (CSV) file which was used for further processing.

The various monthly downloads were combined into one master machine file. Once the master file was assembled, the first task was to check to see if duplicated events were present in the file. Another check was performed to ensure only single unique events were present in the machine's combined production record. The data was then sorted to produce a list of bucket loads for analysis. The list of bucket loads gives us the basis to make two calculations: (i) estimate cycle time; and (ii) estimate bucket productivity for each bucket in the file. The bucket cycle time and productivity (t/sec) were calculated using Equations 3.1 and 3.2 .

$$\text{Date}_{n+1} - \text{Date}_n = \text{Bucket Cycle Time} * 86400 \text{ seconds} \quad (3.1)$$

$$\text{Weight (Bucket)} / \text{Bucket Cycle Time} = \text{Bucket Productivity} \quad (3.2)$$

Sample results of both calculations can be seen in the Table 3.4. Additionally, the LINCS Bucket Overload channel data, which issues a bucket overload warning to the wheel loader operator, is also displayed in Table 3.4. The resulting dataset became the processed dataset for an individual wheel loader.

Table 3.4. Sample Wheel Loader Processed Production Data -
 WL 8015 Date 1/16/16
 (weight is color coded by load type located in Table 3.7)

Event Type	Date	Weight (tons)	Time (sec)	Warning	Productivity
Production	1/16/16 3:01	84	5.6	Overload	0.73
Production	1/16/16 3:01	72	49.6		1.45
Production	1/16/16 3:02	79	51.1		1.55
Production	1/16/16 3:04	235	110.0		
Production	1/16/16 3:04	84	4.6	Overload	0.73
Production	1/16/16 3:05	83	48.8	Overload	1.70
Production	1/16/16 3:06	78	51.2		1.52
Production	1/16/16 3:07	245	87.8		
Production	1/16/16 3:07	74	4.9		0.80
Production	1/16/16 3:08	87	59.3	Overload	1.47
Production	1/16/16 3:09	75	57.6		1.30
Production	1/16/16 3:10	48	43.0		0.48
Production	1/16/16 3:13	80	194.4		0.41
Production	1/16/16 3:16	364	192.1		
Production	1/16/16 3:19	77	171.1		0.21
Production	1/16/16 3:20	80	55.5		1.44
Production	1/16/16 3:21	74	50.1		1.48
Production	1/16/16 3:23	231	96.0		
Production	1/16/16 3:23	78	4.2		0.78
Production	1/16/16 3:24	79	46.6		1.70
Production	1/16/16 3:24	78	49.1		1.59
Production	1/16/16 3:26	235	117.7		
Production	1/16/16 3:26	76	3.9		0.63
Production	1/16/16 3:27	85	46.5	Overload	1.83
Production	1/16/16 3:28	87	49.7	Overload	1.75

The ultra-class wheel loader data was obtained from the time periods shown in Tables 3.5 and 3.6. The duration covered by the wheel loader datasets ranged from 2 to 24 months, from June 2014 through June 2016, depending on the specific wheel loader reporting. The individual cycles in the data range from 10,000 to 200,000 cycles. The candidate believes the data is adequate given the number of cycles used in the analysis.

Table 3.5. Time Periods for the 55 - 60 Ton Wheel Loader Class Datasets

55 - 60 ton Wheel Loader Class

Wheel Loader	Begin Date	End Date	Duration (months)
6001	Jan-16	Jun-16	6
6011	Dec-15	Apr-16	5
6012	Jun-14	Apr-16	23
6013	Dec-15	Apr-16	5
6014	Dec-15	Feb-16	3
6015	Jan-16	Feb-16	2
6016	Feb-15	Sep-15	8
6017	Feb-15	Sep-15	8
6018	May-15	Jan-16	9

Table 3.6. Time Periods for the 75 - 80 Ton Wheel Loader Class Datasets

75 - 80 ton Wheel Loader Class

Wheel Loader	Begin Date	End Date	Duration (months)
8001	May-15	Sep-16	17
8002	Oct-14	Apr-16	19
8003	Nov-14	Apr-16	18
8004	May-15	May-16	13
8005	Oct-14	May-16	20
8011	Apr-15	Nov-15	8
8014	Apr-14	May-15	14
8015	Aug-15	Sep-15	2
8016	Jan-15	May-15	5
8017	Dec-15	Jan-16	2
8018	Feb-16	Mar-16	2

3.3.1.1 Data quality control. The objective of this analysis is to evaluate the effect of overloading the bucket on wheel loader productivity. Table 3.7 shows the breakdown of bucket load types for the various ultra-class wheel loaders in the study. A series of data checks were performed on each processed wheel loader dataset before proceeding with the analysis.

Table 3.7. Breakdown by Bucket Load Weight by Bucket Load Type
(Joy Global, 2015)

	Model	60 ton	55 ton	80 ton	75 ton
Bucket Load %	Bucket Load Type	Bucket Load Weight (st)			
0 - 85%	Underload	18 - 51	16 - 46	25 - 67	25 - 64
85 - 100%	Target Load	52 - 60	47 - 55	68 - 80	65 - 75
101 - 105%	Target Load	61 - 63	56 - 58	81 - 84	76 - 79
106 - 120%	Overload	64 - 72	59 - 66	85 - 96	80 - 90
120+%	Critical Overload	72+	66+	96+	90+

The first step of the data check was to review each wheel loader's processed dataset to determine if the bucket load is most likely to be a production bucket load, a clean-up load, a test load, or a lift arm articulation / maintenance check. The first data check is to determine whether the bucket load was greater than 30% of the design target bucket weight for the 55 - 60 ton class wheel loaders or greater than 25 tons for the 75 - 80 ton class wheel loaders. Bucket loads which met the above criteria were retained in the dataset for the next data check.

The second data check was based on bucket cycle time. Table 3.8 shows the classification of the bucket cycle times. The average target load cycle time for the 55 - 60 and the 75 - 80 ton class wheel loaders is 40 seconds and 45 seconds per pass,

respectively. If the bucket cycle time was less than 25 seconds or greater than 180 seconds, these loads were also eliminated from the processed wheel loaders dataset.

Table 3.8. Bucket Cycle Time Classifications

Model	60 ton	55 ton	80 ton	75 ton
Bucket Cycle Category	Bucket Cycle Time (sec)			
Very Good	-35	-35	-40	-40
Target Load	35 - 45	35 - 45	40 - 50	40 - 50
Below Target	46 - 60	46 - 60	51 - 60	51 - 60
Need Improvement	60 +	60 +	60 +	60+

Once both data checks are completed, the wheel loader's cleaned dataset was ready for evaluation. The clean dataset was then broken down into sample groups of 10,000 bucket cycles starting with the oldest usable data point and proceeding to the most recent. These sample groups were used to produce the bucket weight, cycle time, and productivity frequency distributions presented in Sections 3.3.1.2.

3.3.1.2 Overview of the data. This section presents an overview of the payload and cycle time data from the different loaders in the study. The data is presented by the classification of loaders used in this study. This provides a quick overview of what is in the processed data prior to the ANOVA tests. The payloads (tonnages) are presented first and then the cycle times. This section is divided into two sections: the first presents the 55 - 60 ton class loaders and the second presents the 75 - 80 ton class loaders.

As shown in Table 3.1, only one 60 ton class wheel loader is included in this study because there are actually only a handful of units with this configuration operating in the global fleet. Figure 3.1 illustrates the operators' ability to fill the bucket to within

the average of number of buckets for the given bucket weight. Loader 6001 operates as a production wheel loader in a Western Australia iron ore mine. The peak (mode) of its distribution is 47 tons per cycle. This is 4 tons less than the minimum target range of 51 - 63 tons. The bucket count exceeds 400 buckets for the range of buckets between 32 - 54 tons. The distribution shows 65% under loads, 34% target weight, 0.7% over loads, and 0.3% critical overloads. The 60 ton class wheel loader configuration dataset will serve as a guide for the three other additional wheel loader configurations presented.

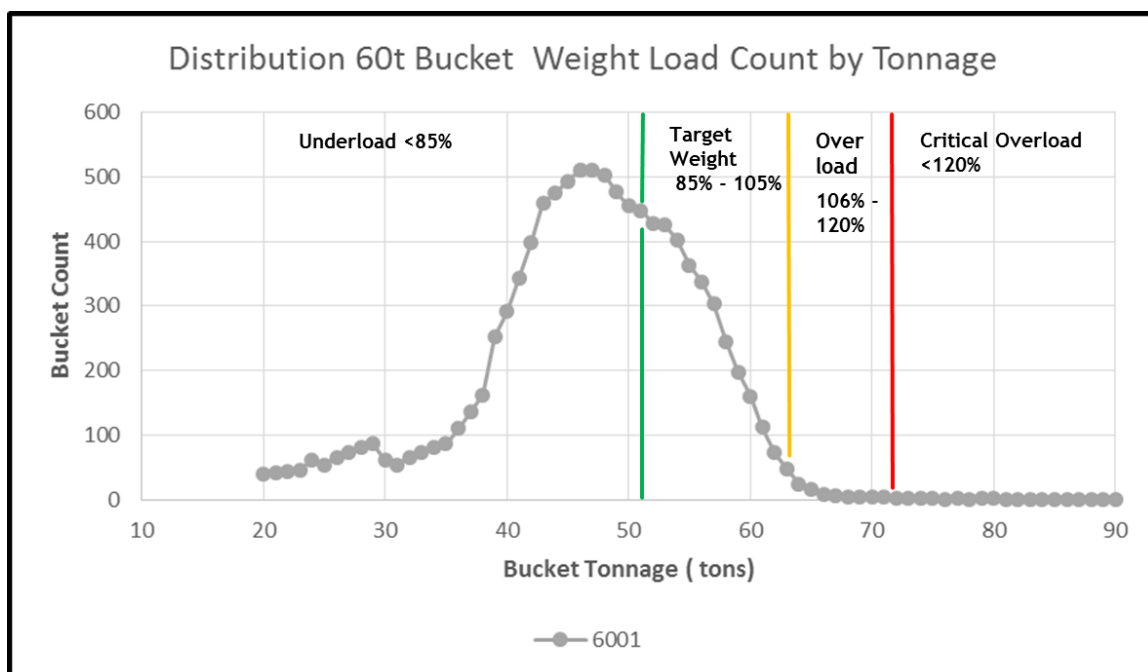


Figure 3.1. Distribution of 60 Ton WL Class Bucket Tonnage by Load Count

There are more 55 ton class wheel loaders in this study than any other class of loaders. Eight machines have reported data for this study. Figure 3.2 shows the bucket weights of all the 55 ton class wheel loaders. This class of wheel loaders can further be broken down into two sub groups by their specific commodities which are coal and

metals (copper and iron ore). The results for the 55 ton class wheel loaders will be discussed within these commodity sub groups.

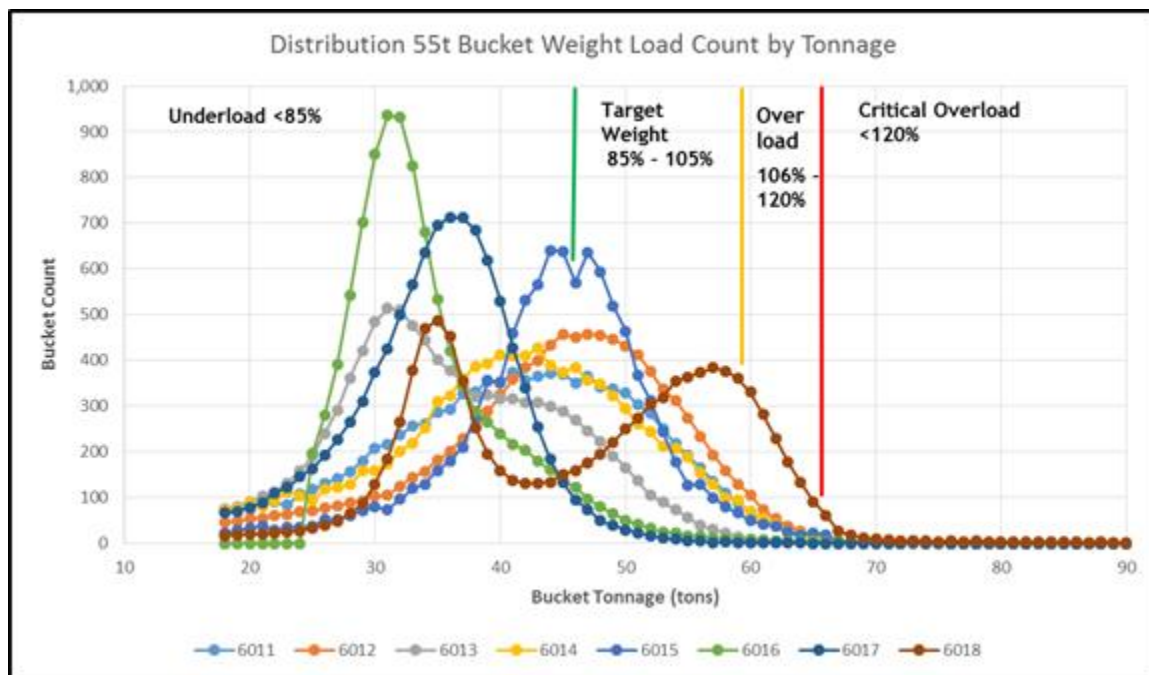


Figure 3.2. Distribution of 55 Ton WL Class Bucket Tonnage by Load Count

The number of bucket loads per group for all of the 55 ton class wheel loaders are displayed in Table 3.9. As shown in Figure 3.2, the fleet results show a wide range of values. These results are attributed to the actual bucket fitted to the specific wheel loader and operator proficiency in being able to fill the individual bucket.

The bucket weight for 55 ton class wheel loaders operating only within coal is shown in Figure 3.3. There are five loaders in this sub group which work in two regions, Australia (4) and North America (1). These wheel loaders perform a variety of tasks including production, overburden removal, site clean-up, stockpiling, and loading coal into the preparation plant for processing. Loaders 6011 and 6014 primarily function as

production machines to extract coal from the face. Both of their distribution curves are very similar and they have modes within one ton of each other: at 44 tons (6011) and 43 tons (6014), respectively.

Table 3.9. 55 Ton WL Class Bucket Load Groups Averages by Load Type

Wheel Loaders								
Bucket Load Category	6011	6012	6013	614	6015	6016	6017	6018
Underload	6,632	5,412	8,569	6,865	5,934	9,448	9,726	4,597
Target Load	3,032	4,089	1,380	2,818	3,789	466	268	3,590
Overload	317	458	47	281	281	47	4	1,666
Critical Overload	19	41	4	36	36	39	2	147

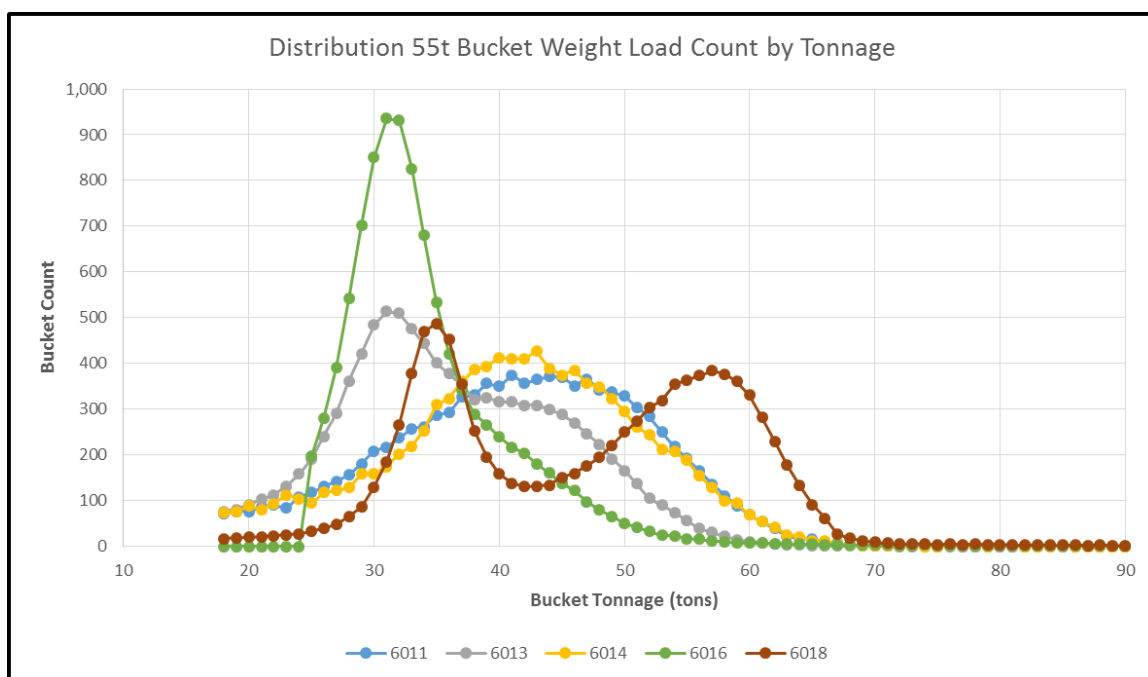


Figure 3.3. Distribution of 55 Ton WL Class Bucket Tonnage by Load Count - Coal

Loaders 6013 and 6016 which are also shown in Figure 3.3 perform multiple duties at their respective sites. Each of these loaders has rock size buckets attached which result in smaller volumes than a traditional coal bucket. Both loaders have distributions that are positively skewed with a inflection point (point where the slope changes) at 38 tons showing bucket loads of mixed material, coal and overburden or just overburden. The amount of time each loader (Loaders 6013 and 5016) spends on each application is shown in the amplitude of the initial peak and flat bulge in the case of Loader 6013 and the change in the right hand tail for Loader 6016 after the hinge point. Examining the area under the curves for both wheel loaders shows Loader 6013 working with coal 61% of the time verses 79% of the time for Loader 6016. Additionally, Loaders 6013 and 6016 spent 39% and 21% of their time working with mixed materials or overburden respectively. The resulting outcomes for all of the 55 ton class wheel loaders are presented in Table 3.9.

Loader 6018 performs two functions as a stockpile / loadout machine and an overburden removal machine. This distinction is displayed in the bimodal (double peak) distribution plot (Figure 3.3). This distribution curve illustrates classic issues with machines operating with bucket specific loads for coal handling. The large volume coal buckets can be easily overloaded when used in an overburden stripping application. Typically, the overburden density can be greater than twice the density of the coal. The distribution curve for Loader 6018 (Figure 3.3) shows the tonnage for the coal loads to be between 25 and 42 tons, and the overburden or mixed materials loads tonnage to be between 43 and 69 tons. Loader 6018 operators overload the bucket at more than five times the rate of any loader studies, and they critically overload the bucket over seven

and a half times the rate of the other loaders studied. If Loader 6018 is compared against the same class loaders operating in metals, the overloads and critical overloads rate drops to three times for both load types.

The three loaders in the 55 ton class wheel loader class study are each operating in different regions around the world. Loaders 6012, 6015 and 6017 comprise two machines which operate in iron ore (one in Australia (6012); and one in South America (6017)), and one machine operating in copper in North America (6015). Loader 6017 is the other iron ore wheel loader. Its operational role is to strip overburden to expose iron ore for production. Comparing the two iron ore wheel loader distribution curves discloses that there is a variance, which is caused by the different material the machines are handling with Loader 6017 peaking at 38 tons loading iron ore versus 47 tons for Loader 6012 loading production ore. The data for Loader 6012 shows a near normal distribution curve. This machine operates in the pit in a typical operation in a production role. Similarly, Loader 6015, which also operates in a production role, has a near symmetric distribution with a mode about the same as Loader 6012. All of the distribution curves for the 55 ton class wheel loaders - metals are shown in Figure 3.4.

The data set also includes data on the cycle time, which reflects the operators' ability to cycle the loader efficiently. There are typically two distinct bucket cycle times in an analysis. The first is the cycle time of moving from the pile to the truck and back again. The second incorporates the cycle of the truck exchange (i.e., one haulage unit leaving the wheel loader filled with material and a second haulage unit moving into position to receive its first bucket of material) (Komatsu, (2), 1998). Typically, this exchange occurs every 4 to 5 bucket cycles and adds between 15 to 45 seconds to the

bucket cycle time for either the first or the last bucket cycle for a truckload (assuming the loader is not matched to fewer trucks than optimal). This exchange time was accounted for in the first bucket cycle by eliminating the truck load event time from the raw wheel loader dataset and recomputed the bucket cycle time in the processed dataset.

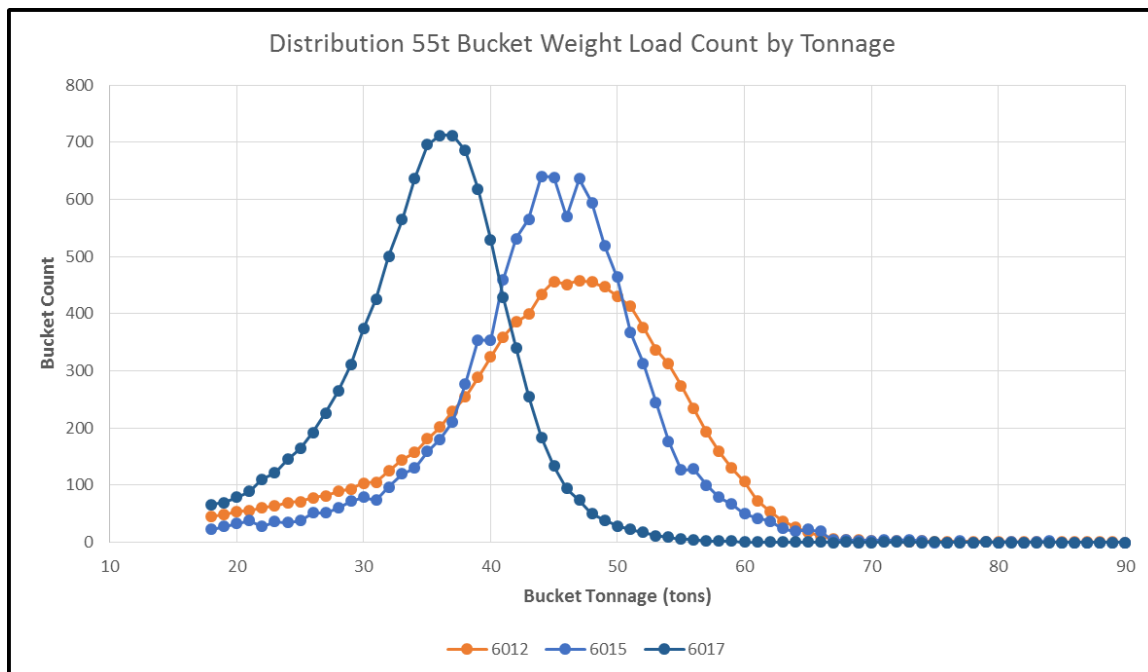


Figure 3.4. Distribution of 55 Ton WL Class Bucket Tonnage by Load Count - Metals

The resulting cycle time distribution, shown in Figure 3.5, comprises all bucket cycles for Loader 6001. The mode of the distribution is 43 seconds per bucket cycle, which is within the target cycle time for a 60 ton class wheel loader. The distribution shows 3% of the cycles under the target time, 41% within the target time, and 56% over the target cycle time for this 60 ton class wheel loader. The right tail of the distribution details the results of numerous loads taking significantly longer than the target cycle time to complete.

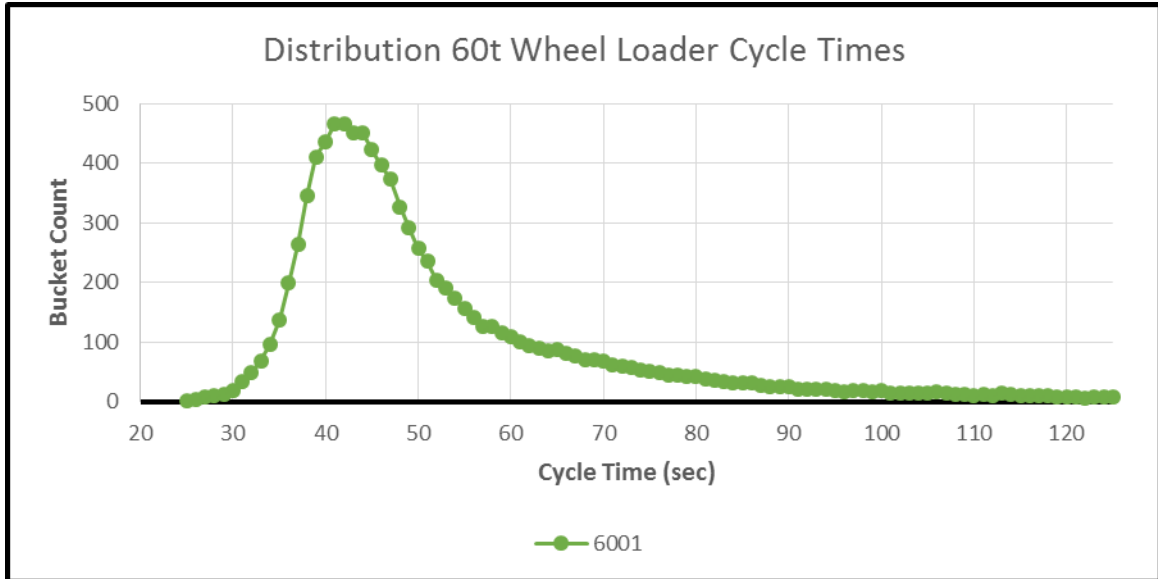


Figure 3.5. Distribution of 60 Ton WL Class Cycle Times

The 55 ton class wheel loader operators are cycling their machines most consistently when they are compared to the target bucket cycle time of seven of the eight loaders presented. They are achieving their peak cycle times within the target windows. The distribution curves, shown in Figure 3.6, for the majority of the machines reveal normal distributions with right side extended tails accounting for increase cycle times relating to change out of haulage units (i.e., truck exchange.) Both wheel loaders, Loaders 6014 (coal) and 6015 (copper) show more linear right hand tails indicating that a couple of factors might be present. These factors include the operator taking additional time to load the bucket, misplacement or further travel to deposit the bucket in the haulage unit, and / or inefficient truck exchange resulting in increased bucket time.

The bucket cycle time group occurrences of the 55 ton class wheel loaders are exhibited in Table 3.10. for Figure 3.6. The Target Load Cycle times range for this class of wheel loaders are from 27% - 58% of the time for the fleet. The wheel loaders

Coal applications for 55 ton class wheel loaders disclose normal distribution operating cycle times for the five machines, excludes Loaders 6012, 6015 and 6017. These are illustrated in Figure 3.7. All the coal sub group of loaders, except of Loader 6011, are operating within the Target Load bucket cycle time of 35 - 45 seconds. Loader 6011 bucket cycle time is at just above the desired time at 46 seconds. Loaders 6016, 6017 and 6018 were able to achieved nearly double the number to target cycle times as the other two loaders in the sub group. Additionally, Loader 6018 exhibits its operators are capable of cycling the machine within the same bucket cycle times, as the unit splits its time between loading coal and overburden applications.

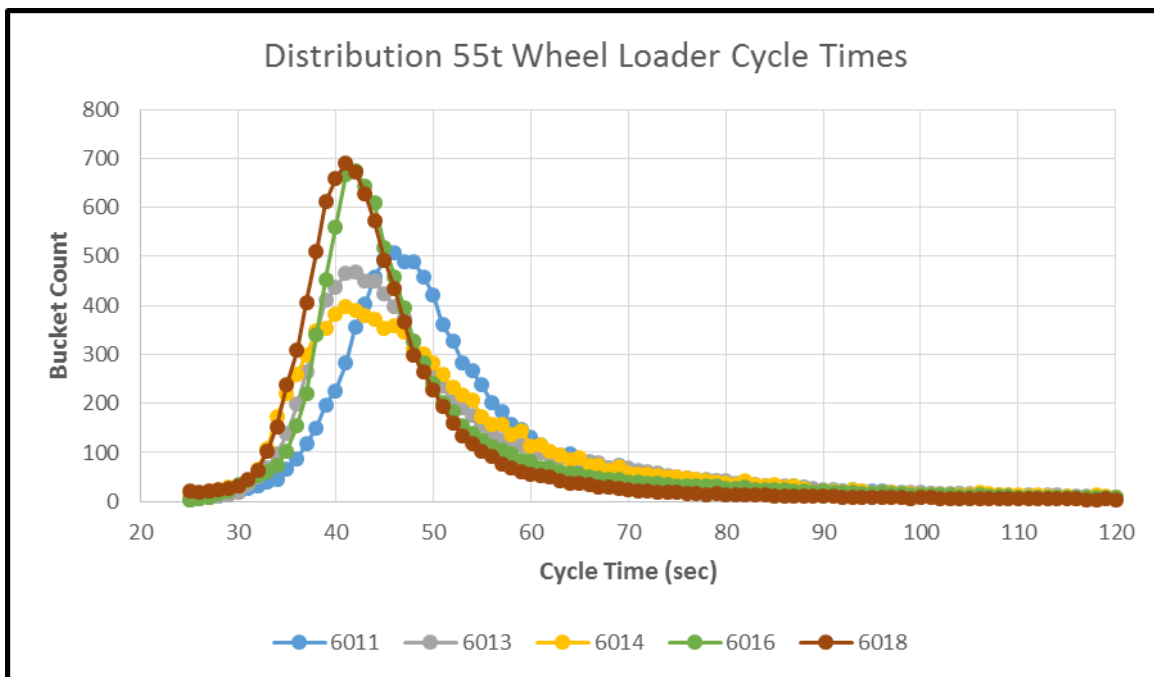


Figure 3.7. Distribution of 55 Ton WL Class Cycle Time - Coal

The results of the cycle time distribution shown in Figure 3.8 shows cycle times 42 - 44 seconds for the three wheel loaders in the 55 ton class. The wheel loaders 6012

and 6017 which operate in iron ore have an average cycle time of 42 seconds and have very similar distribution curves. Wheel Loader 6015 which operates in copper has its peak at 44 seconds with an intensity of 200 loads per group less than the iron ore machines. Additionally, Loader 6015 has a right-side skewed tail starting at a peak of 44 seconds sloping linearly down to 70 seconds. This shows that the operator is taking more time to load the bucket, which may be caused by poorly fragmented material, subpar working conditions, an inefficient operator requiring additional supervision or additional training. Some or all of these factors may be at work in this situation, requiring an application study to determine which or a combination of these factors are at work.

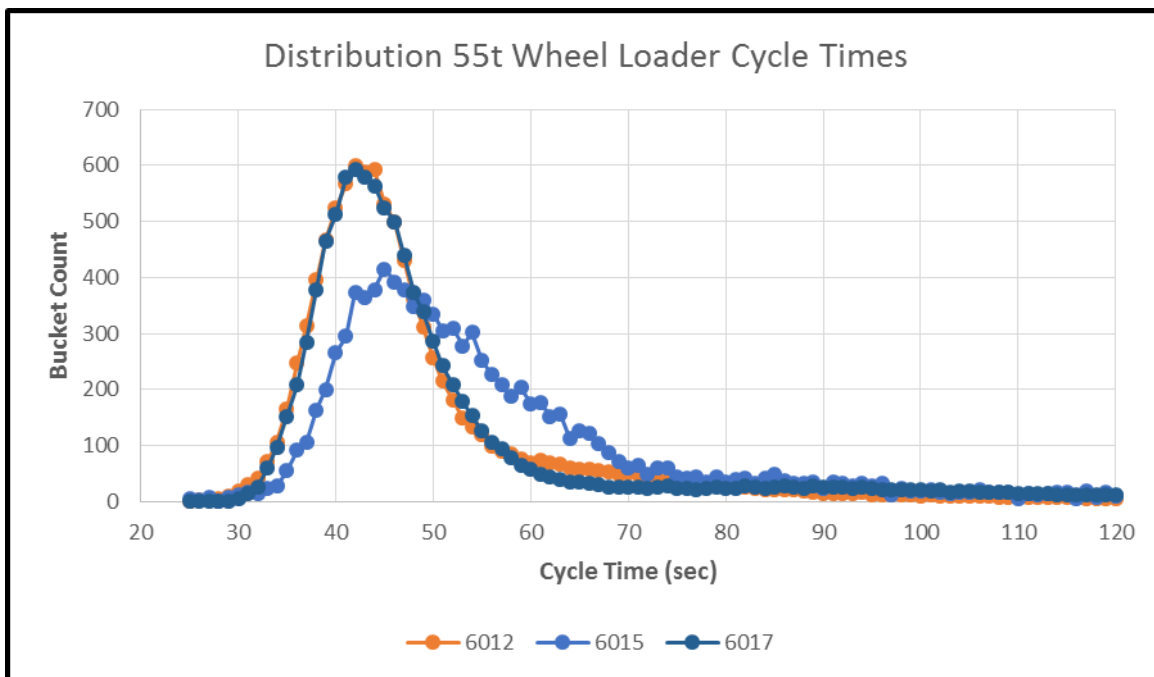


Figure 3.8. Distribution of 55 Ton WL Class Cycle Time - Metals

Bucket productivity is the result of dividing the bucket cycle time into the bucket weight. In this study, bucket productivity is expressed in tons per second, which

corresponds to 3600 tons per hour for a bucket productivity of 1 ton(s) per second. Wheel loaders in the 55 - 60 ton class have a calculated production rate of 3,000 - 4, 000 tons per hour (Fleet, 2017). Wheel loader 6001 has a productivity of 0.77 tons per second or 2,770 ton per hour, shown in Figure 3.9.

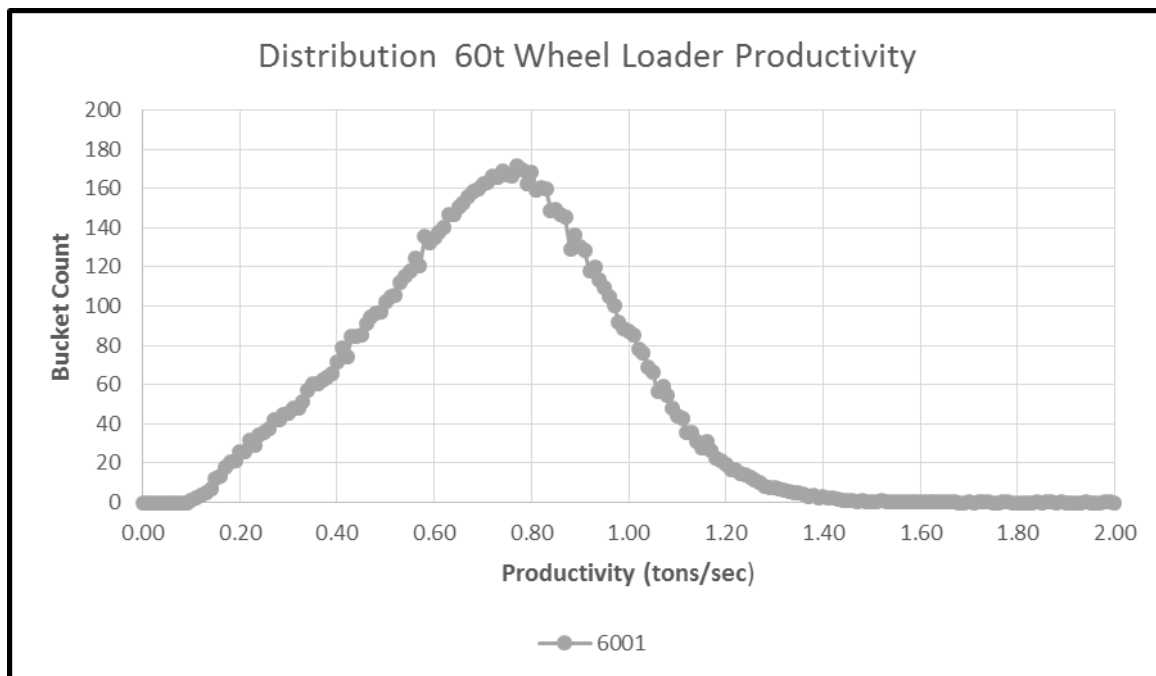


Figure 3.9. Distribution of 60 Ton WL Class Productivity - Bucket

Figure 3.10 shows the distribution for all the 55 ton class wheel loaders' bucket productivities. The wheel loaders in this class have a clearly defined productivity range based on the commodity of material being loaded. The average peak for the coal machines is 0.83 tons per second, while the wheel loader operating in metal shows 0.98 tons per second, or a 600 ton per hour difference. Additionally, two curves show outlier trends in the coal machines. Loader 6016 displays nearly a double bucket occurrence at a significantly lower productivity, and Loader 6018 exhibits a double peak to correspond

with its double peak curve in bucket tonnage pulling double duty-coal and overburden loading applications.

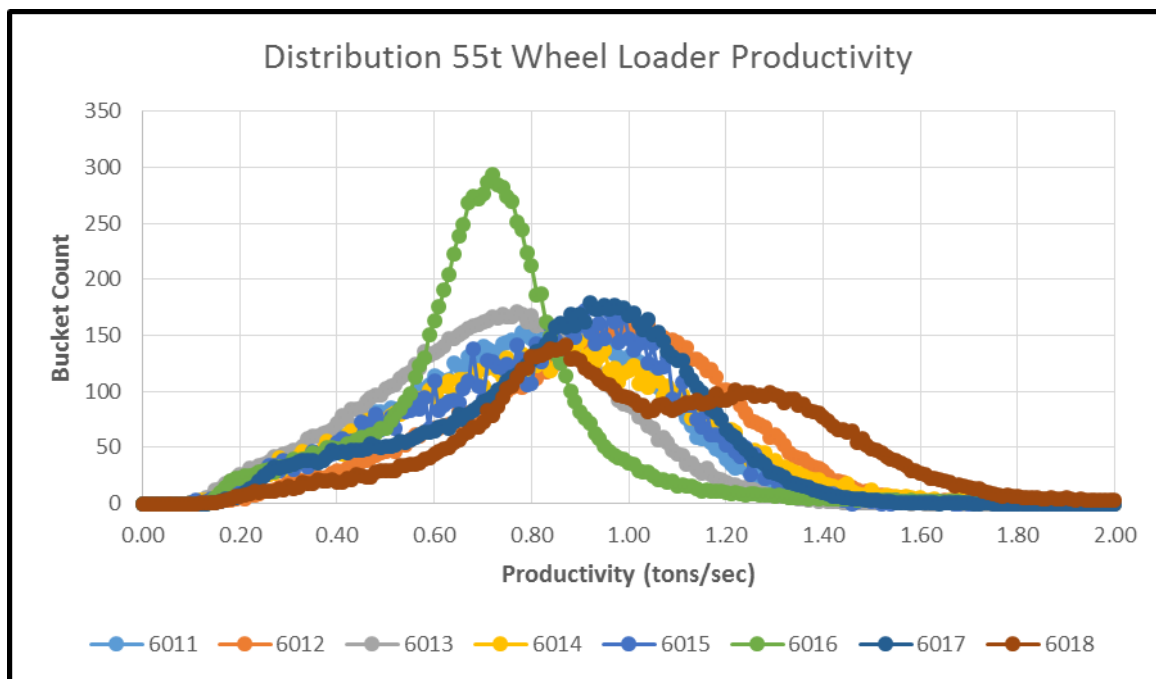


Figure 3.10. Distribution of 55 Ton WL Class Productivity - Bucket

Review of the productivity of the 55 ton class wheel loader operating in coal which is shown in Figure 3.11. Three distinct distribution curves are present. Three wheel loaders, 6011, 6013, and 6014 have similar normal distribution curves with peaks from 0.77 - 0.88 tons per second. The effect of the lower bucket weight combined with a quicker cycle time is able to bring the bucket productivity for Loader 6013 back into a normal operating range of 2,800 to 3,200 tons per hour for these wheel loaders. Loader 6016 displays the effect of the smaller (rock) bucket on a machine primarily being used in a stockpile and preparation plant loader application. This results in productivity being reduced 15% over the average of Loaders 6011, 6013, and 6014. The other extreme is

shown by Loader 6018 with its dual application of loading coal and overburden with a coal bucket. The first peak in the productivity curve loading coal falls in the range of the first three coal wheel loaders at 0.87 tons per second. The second peak at 1.22 tons per second loading overburden is 40% higher than the coal average, although we are starting to see the results of the higher bucket tonnage flatten out the productivity curve around the second peak.

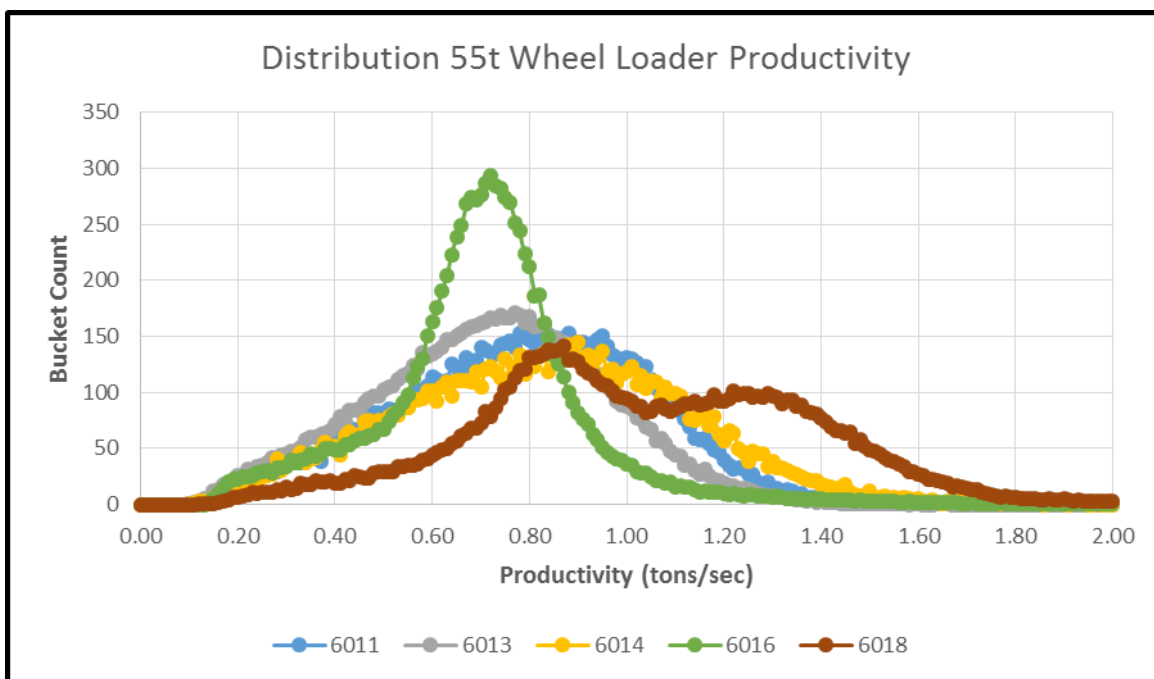


Figure 3.11. Distribution of 55 Ton WL Class Loader Productivity - Coal

The wheel loader operating in the metal mine in the 55 ton class demonstrated similar productivity results which are displayed in Figure 3.12. This specific machine's productivity ranged from 0.96 - 1.04 tons per second or 3,450 - 3,750 tons per hour. The fluctuation in the productivity curve of Loader 6015 is due to the fact that there is only

one group sample for that particular machine compared to sixteen and fourteen group samples for Loaders 6012 and 6017 respectively.

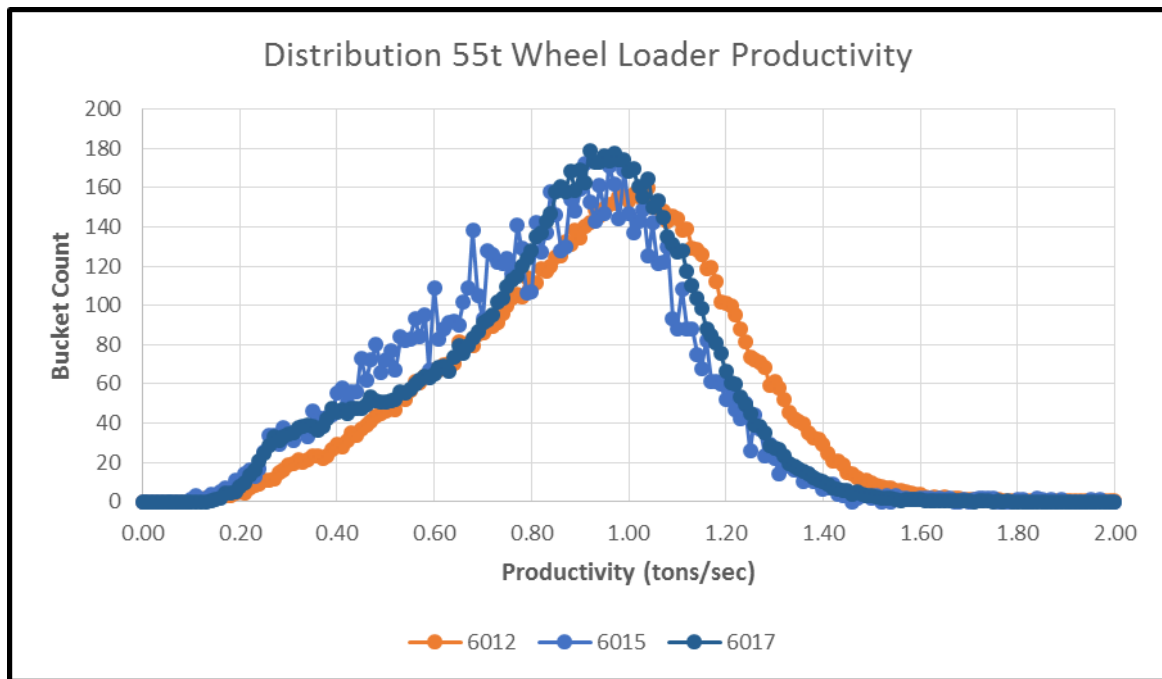


Figure 3.12. Distribution of 55 Ton WL Class Productivity - Metals

In reviewing all the production and productivity data for the 55 - 60 ton class wheel loaders, a couple of items become apparent, see Table 3.11. First, the bucket weight shows that the machines are not being loaded to the wheel loader's target zone based on the machine's designed payload capacity. Only two of the nine loaders studied were able to achieve this parameter, and this includes Loader 6018 achieving this payload capacity only in consistently overloading the machine with a coal bucket moving overburden. The wheel loader operators have shown good skill in being able to cycle the machine within the target cycle time. Eight of the nine wheel loaders studied were in the target zone with the ninth just outside it by a second. This leads to the results that the

wheel loaders operating in metal productivity were 600 tons per hour more productive than their counterparts working in coal. The productivity results show that the variance in bucket weight to be the main difference within the wheel loaders studied.

Table 3.11. Distribution Modes for the 55 - 60 Ton Wheel Loader Datasets

Wheel Loader	Bucket Wt. (tons)	Cycle Time (sec)	Productivity (t/sec)	Commodity
6001	47	43	0.89	Iron ore
6011	44	46	0.88	Coal
6012	47	42	1.04	Iron ore
6013	31	41	0.77	Coal
6014	43	41	0.83	Coal
6015	45	44	0.96	Copper
6016	32	42	0.72	Coal
6017	38	42	0.97	Iron ore
6018	35 / 57	41	0.87 / 1.22	Coal

Peak in the Target Load

The 75 - 80 ton class wheel loaders operate primarily in iron and copper production in Australia and South America. The same testing and evaluation methods were used as that for the 55 - 60 class wheel loaders. The minimum load tonnage and target cycle times were adjusted to account for the 20 ton difference in the wheel loader's capacity.

Figure 3.13 shows five 80 ton class wheel loaders operating in primary production roles in three Western Australian iron ore mines. Loader 8001 operates at one mine, Loaders 8002 and 8003 both operate at a second mine, while Loaders 8004 and 8005 are operating at a third mine.

Wheel loader 8001's operators are loading the bucket to 72 tons per load (mode). This is within the Target Load zone for 80 ton class wheel loaders. Wheel loader 8001 is loading 44% of its buckets in the Target Load zone, while 2% are in the overload category. Additionally, the results show that the other wheel loaders operating in pairs have very similar production results. The mode for Loaders 8004 and 8005 is 62 tons per load. Loaders 8002 and 8003 have similar results with the mode of their distributions being at 62 and 64 tons, respectively. All four of these machines have their modes 4 - 6 tons per bucket load lower than the minimum target load of 68 tons. These loaders are only filling their bucket 19 - 25% of the time in the target load zone, while overloading the wheel loader 0.5 - 1.0% of the time. An interesting note is that wheel loader 8001 is accumulating twice the target loads while keeping overloads at 2% and critical overloads at half the rate of the other wheel loaders in this configuration. All the bucket load category results are presented in Table 3.12.

All of the 75 ton wheel loader class evaluated operate in South America in two different commodities and in a few different roles. The distribution curves are displayed in Figure 3.14. Loaders 8011, 8015, 8017 and 8018 all operate in the same iron ore mine in production roles. Loader 8016 operates in the same iron ore mine in an overburden removal capacity. Loader 8014 operates in a copper mine on the production face in a different region of South America, where it executes both primary loading and support activities for an electric cable shovel.

The analyzed results (Figure 3.14) show that the four iron ore production wheel loaders are all filling their buckets into the target weight range of 64 - 78 tons. These wheel loaders are producing target weight buckets in 36 - 45% of their bucket loads.

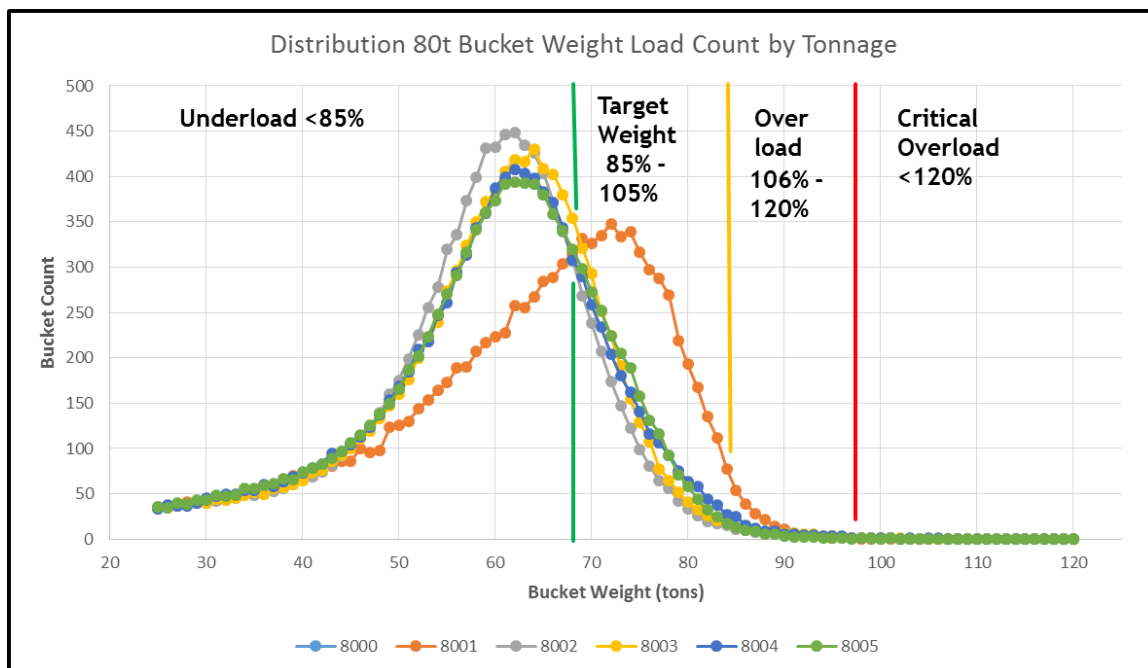


Figure 3.13. Distribution of 80 Ton WL Class Bucket Tonnage by Load Count

Table 3.12. 80 Ton WL Class Bucket Load Groups Averages by Load Type

Wheel Loaders					
Bucket Load Category	8001	8002	8003	8004	8005
Under Loads	5,403	7,999	7,546	7,488	7,428
Target Loads	4,403	1,920	2,358	2,400	2,507
Over Loads	189	70	86	99	59
Critical Overloads	5	12	10	13	6
	10,000	10,000	10,000	10,000	10,000

Wheel Loader 8014 shows a weak performance of 9% bucket loads in the target weight zone. This is due to an improperly sized bucket for its current application. The bucket on Loader 8014 is sized for loading iron ore instead of stripping material. These

The cycle time for the 80 ton class wheel loaders range between 44 - 52 seconds per bucket as shown in Figure 3.15. All of the wheel loaders operating in the 80 ton class operate in the same region and commodity, although the operating method of the haul fleet differs. Loader 8001's haulage fleet is operated by human drivers producing a cycle time mode of 44 seconds per pass. Loaders 8002 and 8003, both at the same mine, have similar cycle times. Their cycle time modes are only one second different from each other at 46 and 47, respectively. Both Loaders 8002 and 8003 operate with a mixed haulage fleet of autonomous and driver-operated trucks. Loaders 8004 and 8005, at the same mine, operating only with an autonomous truck fleet have a cycle time mode at 52 seconds per pass.

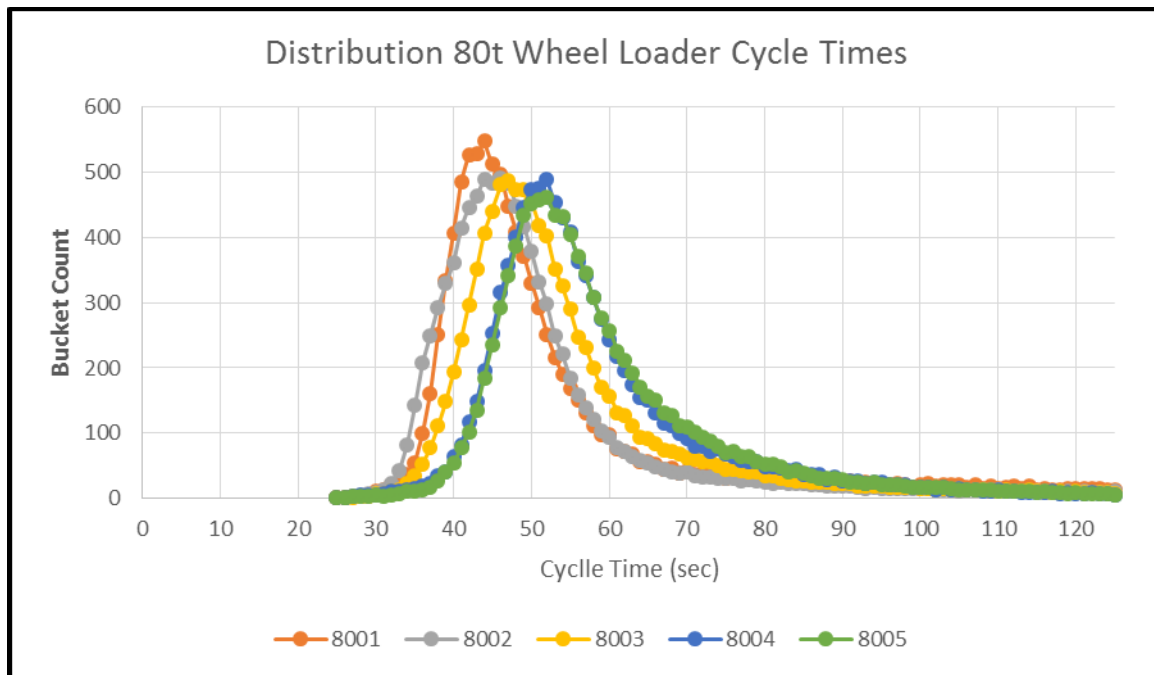


Figure 3.15. Distribution of 80 Ton WL Class Cycle Times

With Loaders 8004 and 8005, one item which was discovered during an application review of the site and pit working conditions is that the wheel loaders were tramming farther than the recommended distance to load the truck. The crew was not updating the position of the wheel loader to account for the movement of the loader across the working face (Komatsu AHS, 2017), which were used to guide the autonomous haulage trucks, or resetting the stop point for the trucks quickly enough. The loaders began performing a short load and carry type operation to load the trucks. This resulted in the 5 - 6 additional seconds per load or 10 - 13% slower cycle times.

The 80 ton class wheel loaders' bucket cycle time summary in Table 3.14 shows that the target load cycle times range between 27% - 51% of the time for the fleet. Wheel loaders operating at or above the target load cycle times account for 37% - 71% of the analyzed loads.

Table 3.14. 80 Ton WL Class Cycle Time Groups Averages by Load Type

Wheel Loaders					
Bucket Cycle Category	8001	8002	8003	8004	8005
Very Good	1,018	1,408	493	191	148
Target Load	5,066	4,881	4,304	2,856	2,694
Below Target	1,708	1,902	2,797	3,788	3,753
Need Improvement	2,207	1,809	2,407	3,164	3,405
	10,000	10,000	10,000	10,000	10,000

Figure 3.16 displays the bucket cycle times of the 75 ton class wheel loaders. Five of the six wheel loaders, which are all iron ore machines, operate in the same mine in South America and have similar cycle times ranging from 52 - 54 seconds. Wheel loader

8016, working in a copper mine in South America, has a cycle time mode that is 5 seconds slower, at 58 seconds, than the iron ore machines. Additionally, the Loader 8016 curve shows a right side tail, while the iron ore wheel loaders have more symmetric distributions.

Cycle time summary for wheel loaders in the 75 ton class is displayed in Table 3.15. This shows that the cycle times for target loads for these machines occur 5% - 23% of the time. This wheel loader class operates above the target load cycle time accounting for 77% - 95% of the time for the loads.

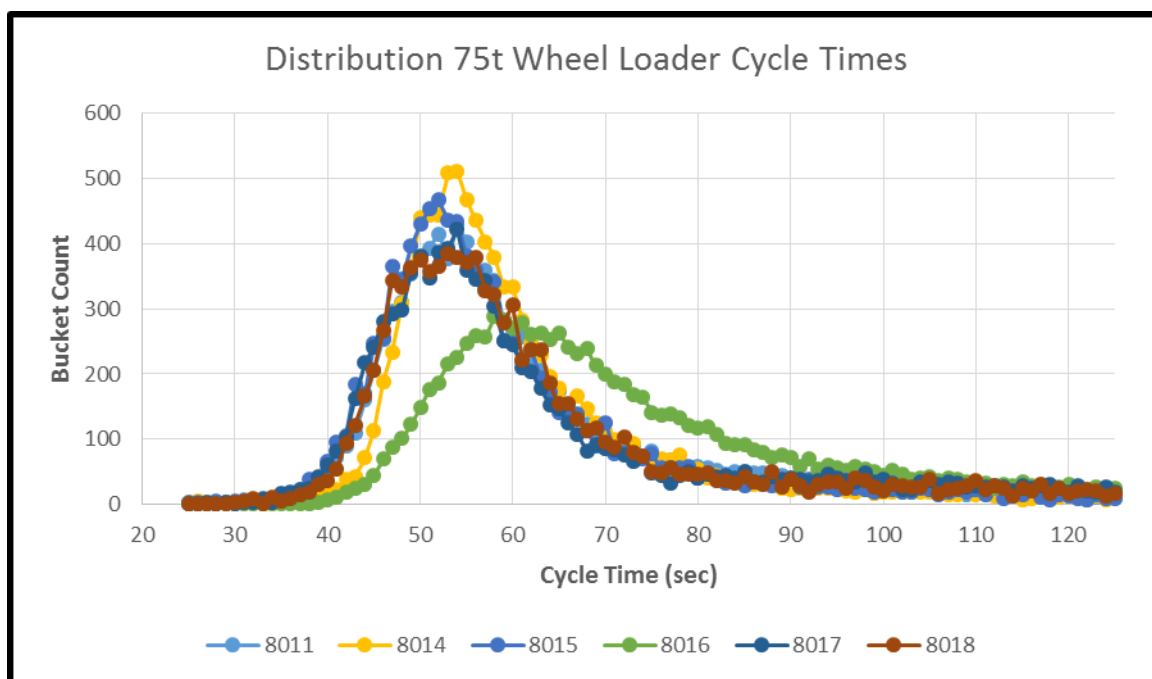


Figure 3.16. Distribution of 75 Ton WL Class Cycle Times

The theoretical (calculated) production rate for wheel loaders in the 75 - 80 ton class is 4,000 - 5,500 tons per hour (Fleet, 2017). Wheel loader 8001 has a productivity of 1.43 tons per second or 5,150 tons per hour (Figure 3.17). The productivity of Loader

Table 3.15. 75 Ton WL Class Cycle Time Groups Averages by Load Type

Wheel Loaders						
Bucket Cycle Category	8011	8014	8015	8016	8017	8018
Very Good	153	72	147	10	150	102
Target Load	2,279	1,839	2,660	664	2,477	2,362
Below Target	3,627	4,266	3,705	2,408	3,397	3,474
Need Improvement	3,906	3,823	3,488	6,918	3,976	4,062
	10,000	10,000	10,000	10,000	10,000	10,000

8001 confirms that the target intervals for the bucket weight and cycle time are achievable over long periods of time. Both are required to maximize wheel loader productivity. Loader 8001 presents a left skewed distribution curve.

Loaders 8002 and 8003, which are at the same mine, are both achieving the same productivity of 1.25 tons per second. This is 12% less than Loader 8001 which is operating in the same region and in the same commodity. Examining the other pair of Loaders, 8004 and 8005, we see a further reduction in the productivity of these wheel loaders at 1.06 and 1.12 tons per second respectively. The reduced productivity of these units is directly correlated to the inability to properly spot autonomous trucks. This mine is 24% less productive than the mine where Loader 8001 operates, or a potential loss of 1,225 tons per hour.

The productivity of the 75 ton class wheel loader mirrors the bucket tonnage distribution curves presented earlier. As a reminder, all of the 75 ton class wheel loaders operate in South America in iron ore and copper mines. Their distribution curves are displayed in Figure 3.18. Loaders 8011, 8015, 8017, and 8018 work in production roles in an iron mine where their productivity is between 1.04 - 1.20 tons per second. Loader 8016's productivity is 0.69 tons per hour. This machine operates in the same iron ore

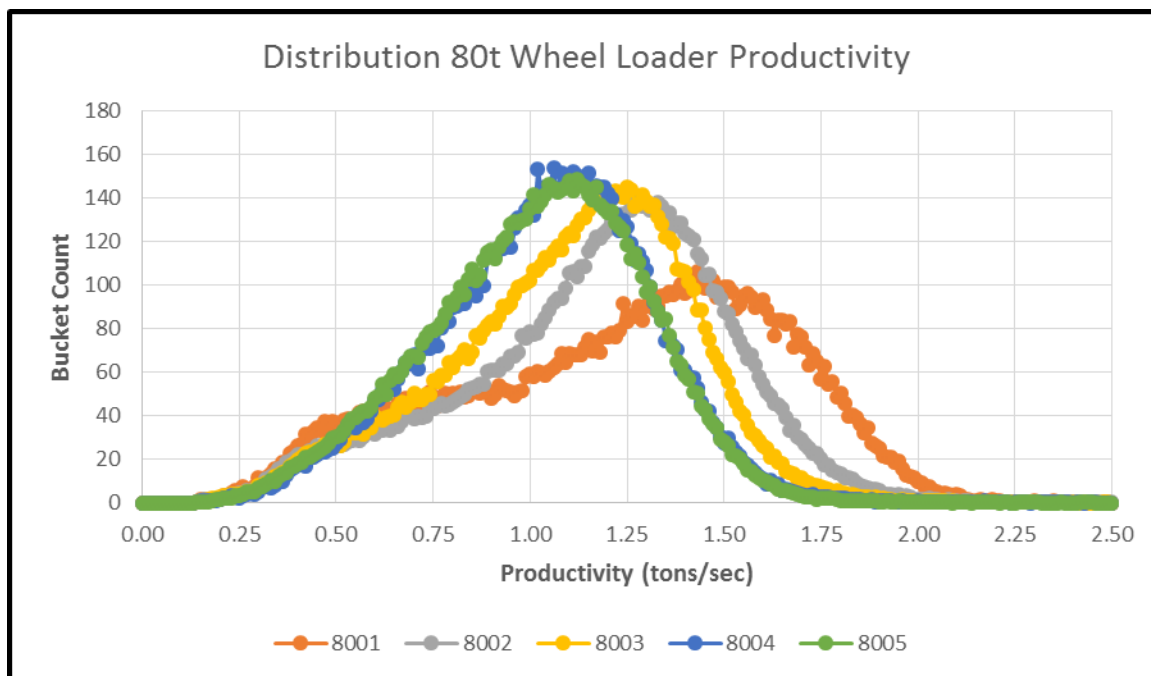


Figure 3.17. Distribution of 80 Ton WL Class Productivity - Bucket

mine as the previous wheel loaders reviewed in this section. The productivity of Loader 8016 shows the effect that the different material densities have on their productivity, as the cycle times for the remaining machines are within 2 seconds of each other. Loader 8014, operating in a copper production and production support activities, shows the effects of low bucket weights and weak cycle times on this machine's productivity at 0.70 tons per second.

Table 3.16 presents an overview of all the 75 - 80 ton class wheel loaders results. The 80 ton class wheel loader shows Loader 8001 achieved both target values in bucket weight and cycle time. Additionally, Loaders 8002 and 8003 achieved bucket cycle times within the target zone. The second wheel loader class, 75 ton, had three machines that realized bucket weights in the target zone. Furthermore, none of the wheel loaders in the

75 ton class were able to achieve cycle times in the target zone. These results also show a wide variance in wheel loader productivities. The productivity of the machines varied almost 100% based on the skill of the operator, the commodity being loaded, and how long it took to cycle the individual wheel loader's bucket.

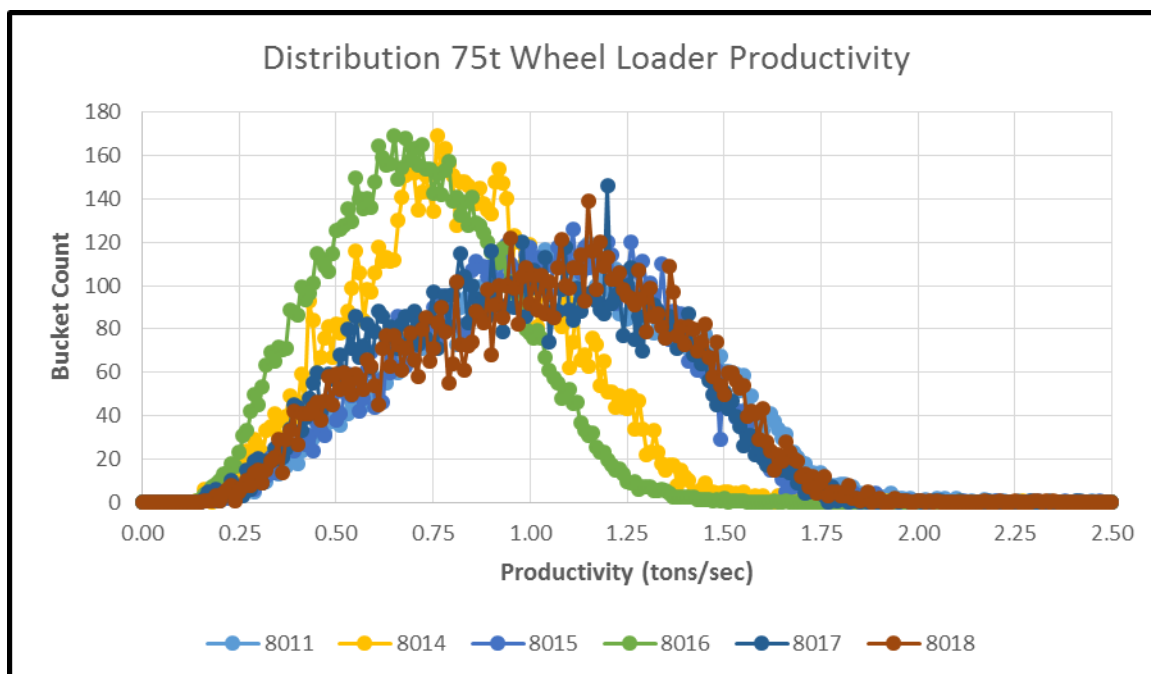


Figure 3.18. Distribution of 75 Ton WL Class Productivity - Bucket

Table 3.16. Distribution Modes for 75 - 80 Ton Wheel Loader Datasets

Wheel Loader	Bucket Wt. (tons)	Cycle Time (sec)	Productivity (t/sec)	Commodity
8001	72	44	1.43	Iron ore
8002	62	46	1.25	Iron ore
8003	64	47	1.26	Iron ore
8004	62	52	1.06	Iron ore
8005	62	52	1.12	Iron ore

Table 3.16. Distribution Modes for 75 - 80 Ton Wheel Loader Datasets (cont.)

Wheel Loader	Bucket Wt. (tons)	Cycle Time (sec)	Productivity (t/sec)	Commodity
8011	69	54	1.04	Iron ore
8014	49	54	0.69	Iron ore
8015	68	52	1.11	Iron ore
8016	51	58	0.70	Copper
8017	64	54	1.20	Iron ore
8018	73	53	1.15	Iron ore

Peak in the Target Load

3.3.2. Step 2: Preparing Samples for ANOVA Tests. The test data was reviewed and sampled to determine the validity of the data. Each of the four ultra-wheel loader classes' datasets was reviewed to determine the quantity of underloads, target loads, overloads and critical overloads. Following this review, it was determined that the overloads and critical overloads would need to be combined to produce larger data samples to in turn produce statistically valid results. This was necessary because of the small number of critical overloads within the datasets.

The test data was reviewed and sampled to determine the validity of the data. Each of the four wheel loader classes' datasets was reviewed to determine the total quantity of underloads, target loads, overloads, and critical overloads. Following this review, it was determined that the overloads and the critical overloads would need to be combined to produce larger data samples to produce in turn statistically valid results. This was necessary because of the small number of critical overloads within the datasets.

Each of the wheel loaders' datasets was organized into underloads, target loads, and overloads (which includes the critical overloads). The number of overload samples in

each dataset determined the number of samples for each test. The Excel random number generator was used to randomly select the same number of samples from each of the other three load types as the number of overload samples. The additional step was to ensure that the list contained no duplicate samples. Table 3.17 shows the number of samples obtained from the underload, target load, and overload datasets.

Following the completion of the list, the complete line of sample data was used for Single Factor ANOVA testing (Gitlow, 2005). The ANOVA procedure compares the means of the groups which is achieved by analyzing three variances: the variance among groups, the variance within the group, and the total variance. The ANOVA tests were used to test the null hypothesis (H_0) against the alternative (H_1) shown in Equations 3.3 and 3.4, respectively.

Table 3.17. Number of Samples for Wheel Loader Validation Tests

Wheel Loaders	# of Samples
55 ton	800
60 ton	250
75 ton	300
80 ton	1000

$$H_0: \mu_{\text{underloads}} = \mu_{\text{target loads}} = \mu_{\text{overloads}} \quad (3.3)$$

$$H_1: \text{Not all the populations means are equal} \quad (3.4)$$

Two different ANOVA tests were performed on each wheel loaders' dataset to evaluate the cycle time and the productivity for each wheel loader within the four individual machine classes. The results of the ANOVA tests will be discussed in the next

two sections. Additionally, the significant figure (α) of 0.05 was used as the cutoff point in all of the ANOVA tests (Rumsey, 2015).

3.3.2.1 ANOVA testing of 55 - 60 ton wheel loader class data. Starting with the 60 ton class wheel loaders, a single wheel loader dataset exists for this machine configuration. Loader 6001's results are in Table 3.18. The data has similar average cycle times for the underloads (51.1 seconds), target loads (52.3 seconds), and overloads (52.3 seconds). The ANOVA test results show that there is not enough evidence to reject the null hypothesis. Thus, we have to conclude that there is no statistically significant difference between the mean cycle times of the three load types for Loader 6001.

Table 3.18. ANOVA Results - 60 Ton WL Class - Cycle Time

SUMMARY STATISTICS						
<i>Groups</i>	<i>Count</i>	<i>Sum</i>	<i>Average</i>	<i>Variance</i>		
Underloads	250	12775	51.10	368.48		
Target Loads	250	13084	52.34	552.38		
Overloads	250	13071	52.28	627.77		

ANOVA						
<i>Source of Variation</i>	<i>SS</i>	<i>df</i>	<i>MS</i>	<i>F</i>	<i>P-value</i>	<i>F crit</i>
Between Groups	244.16	2	122.08	0.2365	0.7895	3.0078
Within Groups	385610.78	747	516.21			
Total	385854.93	749				

Tables 3.19 and 3.20 shows the mean and variance, respectively, of the cycle times of the 55 ton wheel loader class machines, with eight machines reporting data for primary analysis. The outcome of the ANOVA analysis is presented in Table 3.21.

Loader 6015 did not have a sufficient number of overload values as compared to the other wheel loaders datasets and was, thus, excluded from the ANOVA test. Six of the seven wheel loaders reporting data in this class show enough evidence to rejected the null hypothesis ($p\text{-value} < 0.05$). Their average cycle time increases with respect to tonnage. The last wheel loader's (Loader 6018) results show the $p\text{-value}$ was greater than the α value used, indicating that we cannot reject the null hypothesis for this machine.

Table 3.19. Mean of Cycle Times by Load Type - 55 Ton WL Class

Wheel Loader	Load Types		
	Under	Target	Over
6011	56.9	57.8	62.4
6012	49.1	54.8	57.9
6013	55.4	60.6	63.5
6014	53.7	57.3	59.6
6015	Insufficient Data		
6016	51.6	57.2	47.4
6017	54.0	54.0	66.0
6018	48.5	49.5	49.1

The ANOVA results for the 60 ton class wheel loader's productivity are displayed in Table 3.22. Wheel Loader 6001's statistics show a mean productivity of 0.86 tons / second (underloads), 1.18 tons / second (target loads), and 1.36 ton / seconds (overloads). The productivity averages are in increasing order from underloads to overloads as expected. The ANOVA results show that there is enough evidence to reject the null hypothesis.

Table 3.20. Variance of Cycle Times by Load Type - 55 Ton WL Class

Wheel Loader	Load Types		
	Under	Target	Over
6011	639.7	348.4	529.1
6012	332.7	505.6	546.4
6013	594.6	521.6	612.3
6014	509.9	565.6	644.6
6015	Insufficient Data		
6016	481.1	583.9	407.0
6017	518.5	542.5	991.7
6018	332.8	356.2	402.4

Table 3.21. ANOVA Results of Cycle Times - 55 Ton WL Class

ANOVA - Cycle Time Results			
Loader	F	F-critical	p-value
6011	13.8965	2.9995	0.0000
6012	34.7599	2.9995	0.0000
6013	23.3226	2.9995	0.0000
6014	12.5312	2.9995	0.0000
6015	Insufficient Data		
6016	39.2047	2.9995	0.0000
6017	55.7622	2.9995	0.0000
6018	0.6167	2.9995	0.5398

Tables 3.23 and 3.24 shows the mean and the variance, respectively, of the productivity for the 55 ton wheel loader class. The mean productivities show that there

are clearly defined breaks in the productivities rates between the Underload, Target Load, and Overload load types. This is similar to the 60 ton class productivity.

Table 3.22. ANOVA Results - 60 Ton WL Class - Productivity

SUMMARY						
<i>Groups</i>	<i>Count</i>	<i>Sum</i>	<i>Average</i>	<i>Variance</i>		
Underloads	350	302.88	0.87	0.07		
Target Loads	350	413.09	1.18	0.09		
Overloads	350	474.42	1.36	0.12		

ANOVA						
<i>Source of Variation</i>	<i>SS</i>	<i>df</i>	<i>MS</i>	<i>F</i>	<i>P-value</i>	<i>F crit</i>
Between Groups	43.18	2	21.59	226.1927	2.25E-82	3.0043
Within Groups	99.92	1047	0.10			
Total	143.10	1049				

Table 3.23. Mean of Productivity by Load Type - 55 Ton WL Class

Wheel Loader	Load Types		
	Under	Target	Over
6011	0.69	0.94	1.08
6012	0.83	1.03	1.19
6013	0.69	0.92	1.08
6014	0.74	0.99	1.16
6015	Insufficient Data		
6016	0.70	1.00	1.58
6017	0.81	1.02	1.10
6018	0.79	1.16	1.39

The 55 ton wheel loader class, ANOVA productivity analysis results are given in Table 3.25. There is enough evidence to reject the null hypothesis for all the 55 ton class wheel loaders with enough data to perform the analysis. Again, Loader 6015 did not have a sufficient number of overload values compared to the other wheel loaders' datasets and was excluded from the ANOVA test.

Table 3.24. Variance of Productivity by Load Type - 55 Ton WL Class

Wheel Loader	Load Types		
	Under	Target	Over
6011	0.05	0.05	0.08
6012	0.05	0.07	0.12
6013	0.05	0.06	0.10
6014	0.06	0.08	0.12
6015	Insufficient Data		
6016	0.03	0.10	0.19
6017	0.06	0.07	0.14
6018	0.04	0.07	0.12

Table 3.25. ANOVA Productivity Source of Variation Summary - 55 Ton WL Class

ANOVA - Productivity Results			
Loader	F	F-critical	p-value
6011	533.8625	2.9995	0.0000
6012	337.2589	2.9995	0.0000
6013	442.5103	2.9995	0.0000
6014	412.2871	2.9995	0.0000
6015	Insufficient Data		
6016	1442.1497	2.9995	0.0000
6017	193.4389	2.9995	0.0000
6018	948.1146	2.9995	0.0000

3.3.2.2 ANOVA testing of 75 - 80 ton wheel loader class data. The wheel loaders in the 80 ton class have their cycle time mean and variance, respectively, displayed in Tables 3.26 and 3.27. Only two of the five wheel loaders (8001 and 8003) in this class follow the trend of increasing cycle times as payload increases. The other three wheel loaders did not follow this trend. Loader 8002's target load mean time was the fastest of the three load categories, and Loaders 8004 and 8005 sample datasets produced results opposite to the expected result.

Table 3.26. Mean of Cycle Times by Load Type - 80 Ton WL Class

Wheel Loader	Loads		
	Under	Target	Over
8001	47.3	60.2	62.5
8002	53.6	51.3	51.5
8003	54.2	54.9	60.2
8004	59.7	56.7	53.4
8005	61.2	60.2	59.6

Table 3.27. Variance of Cycle Time by Load Type - 80 Ton WL Class

Wheel Loader	Loads		
	Under	Target	Over
8001	1222.2	909.4	845.2
8002	474.4	429.6	553.8
8003	300.5	339.9	423.5
8004	357.8	406.9	587.1
8005	404.1	355.5	375.6

For all the 80 ton class wheel loaders except Loader 8005, there is enough evidence to reject the null hypothesis. Loader 8005 produced a p-value of 0.1762, as shown in Table 3.28.

Table 3.28. ANOVA Results Cycle Time - 80 Ton WL Class

ANOVA - Cycle Time Results			
Loader	F	F-critical	p-value
8001	67.9357	3.9171	0.0000
8002	3.3525	3.9171	0.0351
8003	30.3877	3.9171	0.0000
8004	2324.7090	3.9171	0.0000
8005	1.7373	3.9171	0.1762

The mean and variance of cycle time for the 75 ton class wheel loaders are shown in Tables 3.29 and 3.30, respectively. Loaders 8014 and 8016 did not have a sufficient number of overload values compared to the other wheel loaders' datasets in this class and were excluded from the ANOVA test. Loaders 8011 and 8017 data meet the expected result of average cycle time increases as the bucket weigh is increased. Loaders 8015 and 8018 had their average cycle times out of order in their specific results.

The ANOVA analysis results for the 75 ton wheel loader class (displayed in Table 3.31), exhibits a two-way split of the results. For two wheel loaders, there is not enough evidence to reject the null hypothesis; for another two wheel loaders, there is enough evidence to reject the null hypothesis. For Loaders 8011 and 8018, there is not enough evidence to reject H_0 with p-values at 0.1679 and 0.5036, respectively. For Loaders 8015

and 8017, there is sufficient evidence to reject the null hypothesis based on their ANOVA results.

Table 3.29. Mean of Cycle Times by Load Type - 75 Ton WL Class

Wheel Loader	Load Types		
	Under	Target	Over
8011	64.0	65.8	67.4
8014	Insufficient Samples		
8015	64.0	63.6	69.4
8016	Insufficient Samples		
8017	64.9	71.5	75.8
8018	65.8	68.0	66.5

Table 3.30. Variance of Cycle Time by Load Type - 75 Ton WL Class

Wheel Loader	Load Types		
	Under	Target	Over
8011	544.8	521.9	571.0
8014	Insufficient Samples		
8015	591.5	485.4	561.1
8016	Insufficient Samples		
8017	649.6	1011.5	859.7
8018	608.0	762.5	555.8

The five wheel loaders in the 80 ton wheel loader class have their mean and variance displayed in Tables 3.32 and 3.33, respectively. The productivities averages

show the clearly defined breaks in the productivity rates between the Underload, Target Load, and Overload load types. This is similar to the 55 and 60 ton class productivity statistics. Table 3.34 shows the ANOVA results, which shows that for all 80 ton class wheel loaders there is enough evidence to reject the null (H_0) hypothesis.

Table 3.31. ANOVA Results of Cycle Time - 75 Ton WL Class

ANOVA - Cycle Time Results			
Loader	F	F-critical	p-value
8011	1.7876	3.0043	0.1679
8014	Insufficient Samples		
8015	6.7490	3.0043	0.0012
8016	Insufficient Samples		
8017	12.5606	3.0043	0.0000
8018	0.6864	3.0043	0.5036

Table 3.32. Mean of Productivity by Load Type - 80 Ton WL Class

Wheel Loader	Loads		
	Under	Target	Over
8001	1.05	1.42	1.50
8002	1.13	1.32	1.53
8003	1.09	1.23	1.41
8004	0.98	1.20	1.39
8005	0.95	1.21	1.32

Table 3.33. Variance of Productivity by Load Type - 80 Ton WL Class

Wheel Loader	Loads		
	Under	Target	Over
8001	0.13	0.16	0.24
8002	0.10	0.12	0.27
8003	0.08	0.09	0.23
8004	0.07	0.08	0.16
8005	0.06	0.07	0.16

Table 3.34. ANOVA Results of Productivity - 80 Ton WL Class

ANOVA - Productivity Results			
Loader	F	F-critical	p-value
8001	317.1514	2.9987	0.0000
8002	251.0378	2.9987	0.0000
8003	201.8676	2.9987	0.0000
8004	415.6726	2.9987	0.0000
8005	372.0415	2.9987	0.0000

For the 75 ton wheel loader class, the productivity statistics are shown in Tables 3.35 and 3.36. Again, the means and variances show the clearly defined breaks in the productivity rates between the Underload, Target Load, and Overload load types. These results are similar to the other wheel loaders' classes presented in this study. Loaders 8011 and 8017 results are very similar as both loaders operate in the same mine in production applications. The summary of the 75 ton class wheel loaders' ANOVA

results, (shown in Table 3.37), confirms that all 75 ton class wheel loaders had enough evidence to reject the null (H_0) hypothesis.

Table 3.35. Mean of Productivity by Load Type - 75 Ton WL Class

Wheel Loader	Load Types		
	Under	Target	Over
8011	0.87	1.18	1.36
8014	Insufficient Samples		
8015	0.87	1.20	1.30
8016	Insufficient Samples		
8017	0.86	1.15	1.23
8018	1.10	1.18	1.36

Table 3.36. Variance of Productivity by Load Type - 75 Ton WL Class

Wheel Loader	Load Types		
	Under	Target	Over
8011	0.07	0.09	0.12
8014	Insufficient Samples		
8015	0.07	0.08	0.10
8016	Insufficient Samples		
8017	0.08	0.13	0.14
8018	0.11	0.10	0.11

Table 3.37. ANOVA Results of Productivity - 75 Ton WL Class

ANOVA - Productivity Results			
Loader	F	F-critical	p-value
8011	226.1927	3.0043	0.0000
8014	Insufficient Samples		
8015	206.4689	3.0043	0.0000
8016	Insufficient Samples		
8017	113.5374	3.0043	0.0000
8018	54.7568	3.0043	0.0000

3.4. DISCUSSIONS

All but two of the twenty wheel loaders studied in this case study conformed to the Caterpillar 10/10/20 rule, which states that not more than 10% of the loads should exceed 110% of the design weight, while no loads should exceed 120% of the design weight. In examining eighteen of the wheel loaders in this group, all but one wheel loader kept their overload occurrences below 5% of their load count and their critical overloads at less than 0.5%.

Loaders 6018 and 8011 violated the Caterpillar 10/10/20 rule. Loader 8011's operators overloaded this wheel loader 11.5% of the time exceeding the 10% occurrence criteria of the Caterpillar 10/10/20 rule. Loader 6018 violated both sections of the rule by overloading the machine 18.1% of the time with 1.5% critical overloads. This is more than four times greater than any other wheel loader in the study. Loader 6018 is a wheel loader configured to load coal, and splits its duty-cycle stripping overboard.

The results of the ANOVA analysis shows that in most cases, there is a statistically significant difference between the cycle times and the productivities of the

loaders when the bucket is overloaded compared to when it is loaded within the target payload range. The productivity ANOVA results, given in Table 3.38, show that for all four wheel loader classes the null hypothesis was rejected for all machines' datasets. There exists a significant difference between the bucket productivity for underloads, target loads, and overloads for all the wheel loaders in the study.

In the cycle time ANOVA, a mixed result was observed for the wheel loader data. For a majority, twelve of seventeen machines, of the wheel loaders there was enough evidence from the data to reject the null hypothesis, while there was not enough evidence to reject the null hypothesis for the remaining five wheel loader, as shown in Tables 3.39.

Table 3.38. ANOVA Productivity Results Summary

Wheel Loader Class	H ₀	H ₁	Insufficient Data
55 - 60 ton	-	8	1
75 - 80 ton	-	9	2
	-	17	3

Table 3.39. ANOVA Cycle Time Results Summary

Wheel Loader Class	H ₀	H ₁	Insufficient Data
55 - 60 ton	2	6	1
75 - 80 ton	3	6	2
	5	12	3

Further review of the cycle time ANOVA analysis results show that twelve of the seventeen loaders in the group showed a pattern of increasing cycle times for greater

bucket weights (i.e., it took longer to overload the bucket than to target load the bucket) The 55 ton, 75 ton, and 80 ton class wheel loader datasets each had at least two sample datasets which followed this pattern. Additionally, the five other datasets did not follow this pattern and had their underload, target load, and overload cycles times similar with no clear distinction by bucket load type or out of sequence (i.e., the overload cycle time was less than the target load cycle time.) These results show that each wheel loader class had at least one machine where the null hypothesis was valid, with the 75 ton class group having two wheel loader meeting this criteria.

These results indicate that while there is strong evidence that overloading the bucket will increase the productivity, it is also possible that overloading slows down the rate of loading. This may be why the cycle time ANOVA results are not as clear as the productivity results. Thus the gains in productivity may not be commensurate with the increased payloads.

Additionally, the case study shows areas for improvement across the fleet to improve each wheel loaders' productivity. The results show the bucket weight is the defining factor for wheel loader productivity (assuming the bucket is not overloaded). All four wheel loader classes need to improve their perception of bucket weight / bucket fill factor. The fleet cycle time is a secondary factor to improve the productivity of the wheel loader fleets. The 55 - 60 ton class wheel fleet consistently achieved their target cycle time of 35 - 45 seconds. The 75 - 80 ton class wheel loader fleet also needs to improve their cycle times to their target level of 40 - 50 seconds by cycle. In the 75 ton class wheel loader fleet there are three machines (Loaders 8011, 8015 and 8018) whose bucket

capacity were in the target load range, but their cycle times need to have a 20 -30 % improvement to reach the middle of the cycle time target zone.

The case study confirms the industry's general belief by operators that they can produce more if the bucket is overloaded. Continual overloading of the bucket can be a negative factor for the health, reliability and productivity of the wheel loader. Repetitive overloading of the bucket increases the likelihood of failure on the structural components and other systems, which could lead to their premature failure. This will be discussed in Sections 4 and 5.

The analysis in this section may have certain limitations. These include the fact that the analysis does not explicitly account for the effect of the type of commodity the loaders are operating in, operator skill level, bucket configuration, or working conditions. All these factors could complicate the relationships between overloading and productivity. However, these factors may actually work to strengthen the conclusions in this section as they work to weaken the connection between overloading and cycle time and productivity rather than strengthen them. Hence, accounting for these factors may only make the conclusions of this section stronger.

3.5. SUMMARY

This research effort presents an understanding of the productivity of a global wheel loader fleet. The research used production data from more than twenty ultra-class wheel loaders to compare individual bucket production tonnage and cycle time data to determine each machine's productivity. The case study examined over three million bucket loads to determine if the machines were being subjected to a significant amount of overloading. Each individual wheel loader's results were compared against other loaders

in their respective class and against the design specifications. The data was also used to conduct ANOVA tests to determine whether there is a statistically significant difference in the productivity and cycle times of the same loader when the payload is Underload, Target Load or Overload.

Based on the results of the wheel loaders reviewed, the following general conclusions can be drawn:

- There is significant evidence to support the idea that higher payloads in the bucket increases the productivity of the loader even if the higher payloads lead to overloading of the bucket. In this work, all 17 loaders that had sufficient data to be tested for the effect of payload showed that payload affects the productivity of the loader.
- The evidence in support of the hypothesis that higher payloads lead to slower loading rate is not as clear as that in support of the hypothesis that higher payloads lead to higher productivity. Twelve of the 17 loaders used in the ANOVA tests showed that payload indeed affects cycle times. For the remaining five loaders, there was no statistically significant difference between the cycle times of the loaders with different classes of payloads.
- The analysis in this section confirms the general belief held by operators that they can produce more if the bucket is overloaded. However, the analysis also shows that overloading the bucket slows down loading rate and is detrimental to productivity in that regard.

- Overloading the bucket itself was not a major issue in any of the wheel loader fleets. Ninety percent (18 of 20) of the wheel loaders conformed to the overload policy.
- Most of the wheel loaders (14 of 20) were being under loaded, with the mode of bucket tonnage occurring in the bucket underload zone. The operator's ability to fill the bucket has the greatest effect on wheel loader productivity.
- Half the wheel loaders were operating within the machine target cycle time. The wheel loaders' bucket cycle time shows it has a secondary impact on the machine's productivity. The bucket weight and the cycle time are independent of each other.

4. EFFECT OF OVERLOADING THE BUCKET ON BUCKET FORCES EXERTED ON A WHEEL LOADER - A CASE STUDY

4.1. INTRODUCTION TO FORCES ON A WHEEL LOADER

This section focuses on the second objective of this dissertation. The work uses data from three ultra-class wheel loaders in mines in Australia and South America to examine the effect of overloading the bucket on forces exerted on the wheel loader structural components. The work uses only these three loaders because the hydraulic pressures data was recorded from the on-board vehicle monitoring system and these were the only units that useable data was obtained from the machines studied in the Section 3. Vehicle monitoring data overwrites itself on a four-hour loop and is typically not downloaded and stored unless the wheel loader has experienced a significant issue requiring further analysis.

The work evaluates the effect of overloading the bucket on the structural components of the wheel loader using hydraulic cylinder pressure data from three wheel loaders which were compared against the bucket overload dataset for the same time period. An instrumented wheel loader, for the OEM in this study, records large amounts of data on different channels while it is monitoring its systems. This work concentrates on the forces exerted on the lift arms structures (lift arms & bellcranks) because these structural components are more likely to be affected by overloading. This dissertation's objective is to examine hydraulic system pressures from the hoist cylinders during loading. The hydraulic pressure should be a direct indicator of the force (i.e., stress) exerted on the lift arm as the hoist cylinders support the lift arms (action and reaction) (Kong, 2014). Using a proxy (such as hydraulic cylinder pressures) is necessary because the wheel loader does not include pressure transducers, and in cases where the machines

have been instrumented the data is considered proprietary information. Data from the hoist cylinder pressure will be synchronized with the bucket payload data. Based on this data, the work assesses the magnitude of pressures recorded during overloads versus those recorded during normal or optimal loading events. The effect of overloading on the lift arm is characterized using this information.

The first step of this process identified wheel loaders with complete (all channel data) downloads archived. The next the data was synchronized with the production data used in the previous section for a given wheel loader. Next, the bucket hoist cycle was scrutinized to determine the maximum hoist cylinder base pressure and the time required to achieve it. The datasets were subjected to an ANOVA single factor test to evaluate whether the bucket hoist pressures were significantly different for overloaded and target load cycles.

4.2. FRAMEWORK FOR INSTRUMENTED WHEEL LOADER CHANNEL DATA REVIEW

Figure 4.1 shows the ultra-class lift arm and hydraulic cylinder configurations of these machines. The lift arm assembly is attached at four points to the wheel loader's frame: two connections at Point O (left and right sides) and two connections (again on both sides) to the hoist cylinders at Point P. The articulation of the bucket is manipulated through a set of hydraulic cylinders. Each cylinder is connected to a bellcrank and level link assembly. Hydraulic pressure in both the hoist and the bucket cylinders is used to accurately guide the bucket through the pile in order to load the bucket.

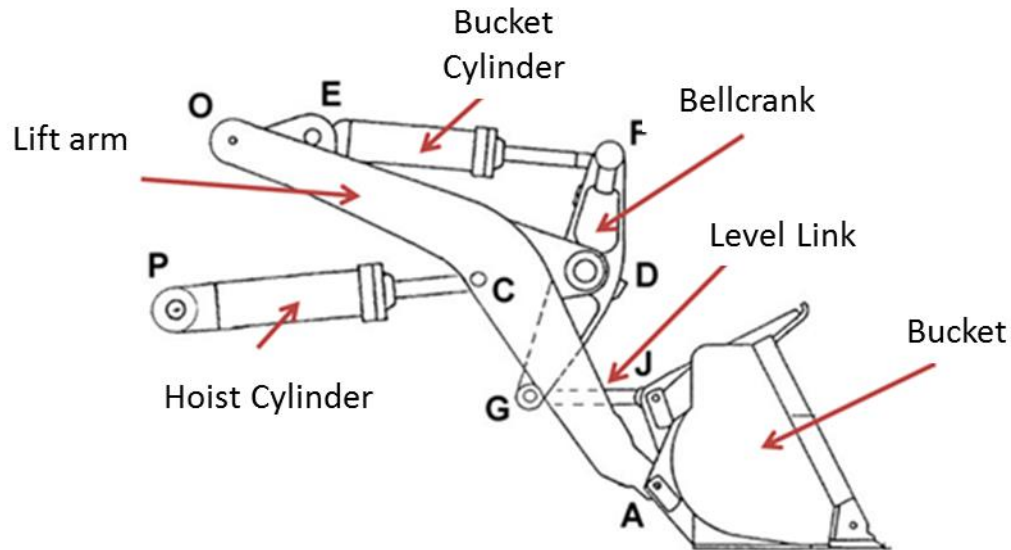


Figure 4.1. Typical Ultra-Class Wheel Loader Lift Arm Arrangement (Napadow, 2012)

All ultra-class wheel loaders are factory equipped with an on-board monitoring system. This on-board monitoring system records over one hundred data channels which are readings from various wheel loader systems' sensors (e.g., engine performance, electrical, hydraulic, etc.). Typically, the system's data logger is setup to log a sample every 20 milliseconds on a four hour continuous cycle loop (i.e., the channel data is recorded over every four hours.) The LINCS software allows one to isolate one to sixteen channels of data to be visually compared over time (LINCS, 2016).

This work focuses on the hoist cylinder's base pressure as a means to quantify the amount of force required to hoist a loaded bucket. In the analysis, three channels were examined to displayed, hoist cylinder base and rod pressures and hoist cylinder extension, to correlate the hoist cylinder base pressure in the hoist cycle interval. An example of a

plot showing the data from a complete bucket cycle for these three channels is shown in Figure 4.2.

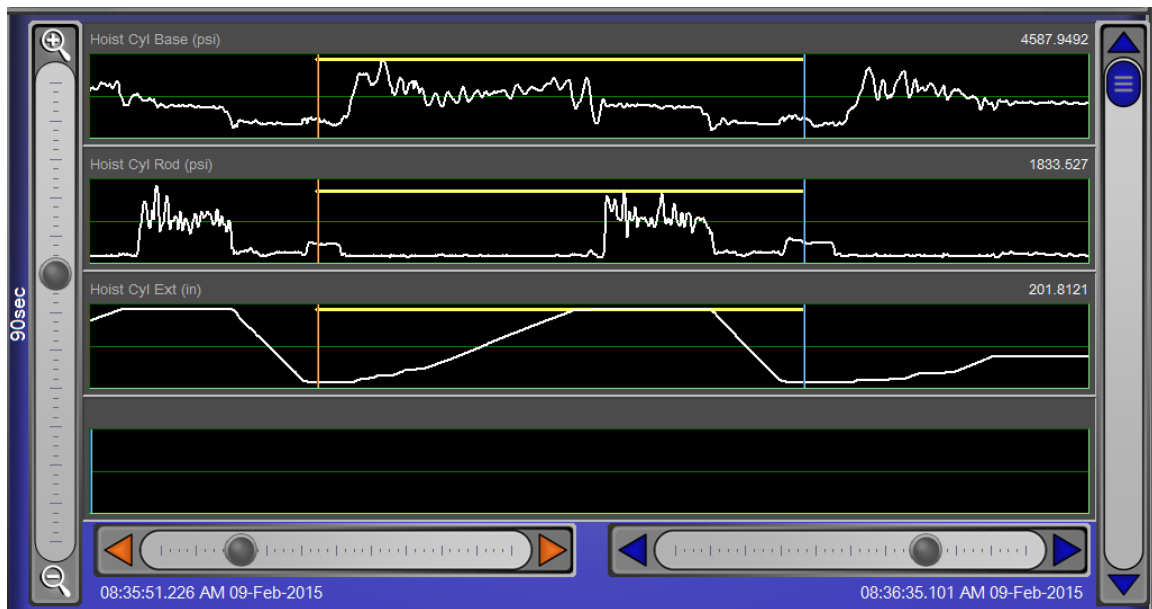


Figure 4.2. Example of Lift Arm Channel Data for Hoist Cylinders

The first channel displayed is the hoist cylinder base pressure (psi). This measures the pressure which is required to lift the bucket and its payload. Two distinct pressure peaks are usually observed in the hoist cylinder base pressure channel. The first pressure peak comes from the operator working the bucket to obtain a full bucket load or breakout. The second peak is from lifting the load to dump. The second channel shown was the hoist cylinder rod pressure (psi). The hoist rod pressure channel was used as check to ensure the bucket circuit was operating properly, and this channel's data is the opposite of the hoist cylinder base pressure (i.e., it is low when the machine is hoisting and high when the hoist cylinder) is being retracted to go into the pile for another bucket. The third channel shows the hoist cylinder extension, which is used to determine which of the two

pressure peaks is occurring. Loading the bucket is the first of these typically. The greater of the two pressure peaks comes in the first half of the bucket loading cycle. The second peak, resulting from lifting the payload, is generally marked by a pause in the hoist cylinder extension, indicating a transition from loading to hoisting. The hoisting portion of the cycle typically takes three to four times the length of the loading portion. Its peak frequently occurs in the last 25% of this cycle. The second channel shows hoist cycle rod pressure.

Figures 4.3, 4.4, and 4.5 show examples of the underload, target load, and overload signals, respectively. Examples of the different load types specified in Sections 3.3.1.1 are based on the bucket weight of the material actually loaded into the bucket.

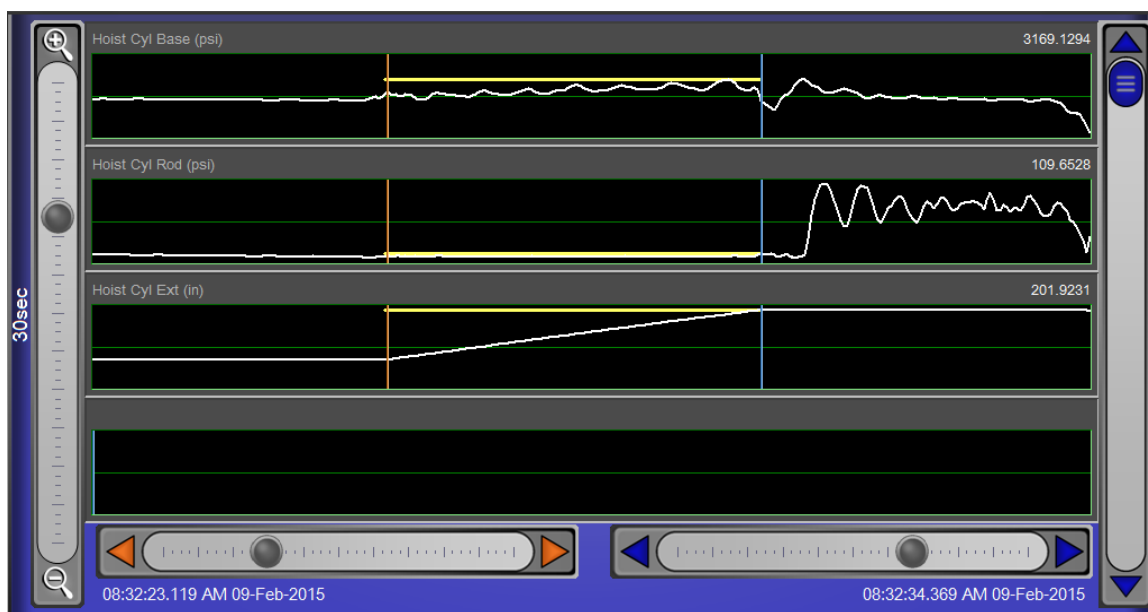


Figure 4.3. Channel Data from Hoist Cylinders Base Pressure - Underload

The maximum base hoist pressure reading for each of the three sample loads shown is displayed in the upper left corner of the top waveform. The hoist base pressure

can be calculated using Equation 4.1 (Milwaukee Cylinder, 2017). The middle waveform, maximum hoist rod pressure reading, should be minor because the pressure which is

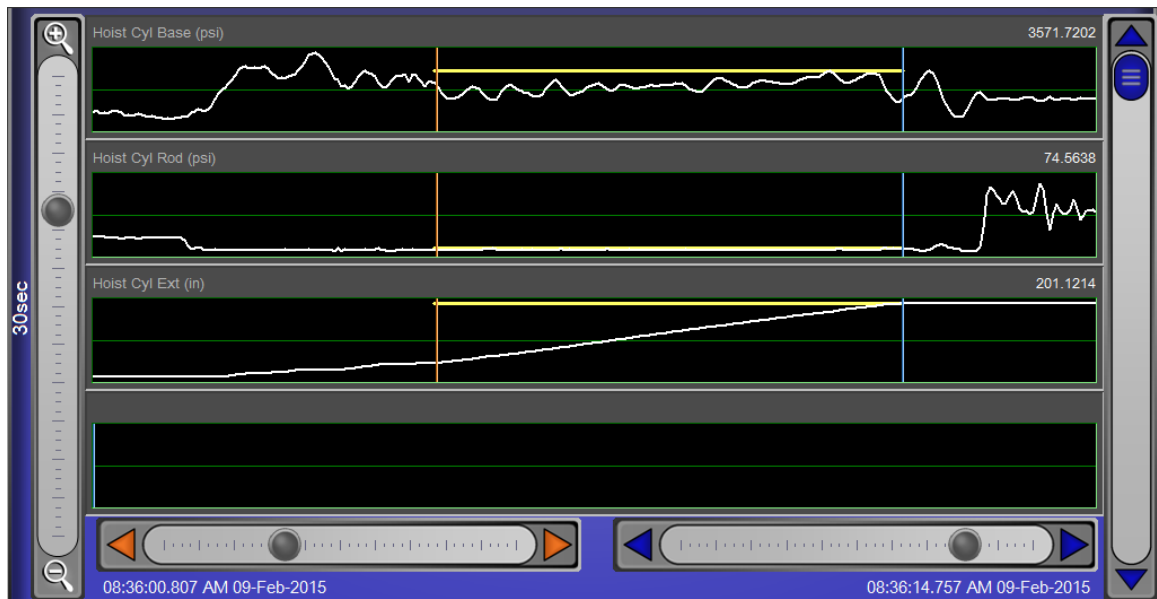


Figure 4.4. Channel Data from Hoist Cylinders Base Pressure - Target Load

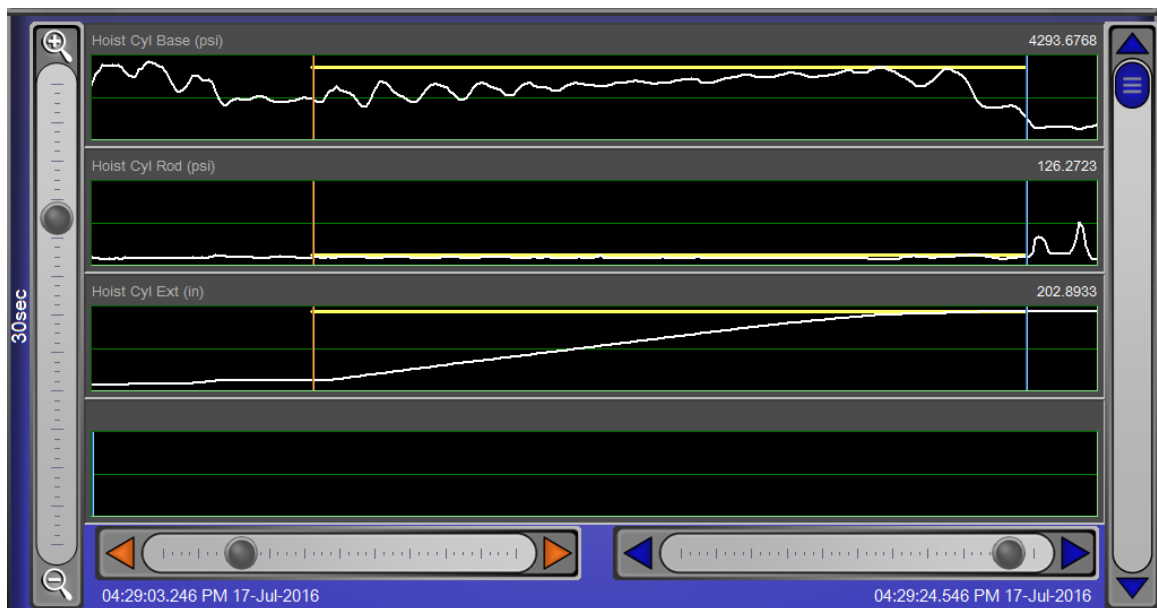


Figure 4.5. Channel Data from Hoist Cylinders Base Pressure - Overload

being exerted on the opposite side of piston, and is calculated by Equation 4.2 (Milwaukee Cylinder, 2017). The third waveform shows how far the cylinder is extending. Typically this should range between 83 - 202 inches, fully retracted to fully extended.

$$\text{FORCE} = \text{Pressure (psi)} \times \text{Net Area (in}^2\text{)} \quad (4.1)$$

$$\text{FORCE} = \text{Pressure (psi)} \times (\text{Net Area (in}^2\text{)} - \text{Rod Area (in}^2\text{)}) \quad (4.2)$$

4.3. DATA ANALYSIS & PROCEDURE

This section of the PhD study was designed to examine the effect of overloading the bucket on forces exerted on a wheel loader. On-board equipment monitoring data was collected from three 75 - 80 ton class wheel loaders for this study specifically to examine the effects of overloading on the hoist cylinder pressures, which is a proxy for the stresses on the lift arm. Two of the three wheel loaders (8002 and 8016) are part of the fleet used in the analysis in Section 3. Wheel Loader 8019 was added for this case study as it has completed a 2016 factory refurbishment / rebuild program. Loader 8019 is paired with a Loader 8016 operating at the same copper mine in South America.

4.3.1. Step 1: Compile the Wheel Loader Hydraulic Pressure Data. Data from the wheel loader's on-board equipment monitoring system was downloaded and synchronized with the production reports data used in Section 3. The maximum hoist hydraulic cylinder pressure - base data and duration to achieve maximum hoist pressure was added to the production data for analysis. An example of the combined data is displayed in Table 4.1.

Table 4.1. Example - Hydraulic Cylinder Pressures with Production Data
(weight is color coded by load type located in Table 3.7)

Event Type	Date	Hoist Cyl				
		Tons	Time (sec)	Prod (t/sec)	Base (psi)	Time (sec)
Production	8/1/16 11:30	78	70.2	1.11	4385	16.15
Production	8/1/16 11:30	78	50.6	1.54	4105	13.70
Production	8/1/16 11:31	77	47.6	1.62	3986	12.70
Production	8/1/16 11:32	76	49.2	1.54	4153	13.15
Production	8/1/16 11:33	70	46.3	1.51	3749	12.60
Production	8/1/16 11:34	80	89.2	0.90	4135	14.05
Production	8/1/16 11:35	67	54.9	1.22	3708	10.35
Production	8/1/16 11:36	73	49.1	1.49	3956	13.20
Production	8/1/16 11:37	77	50.6	1.52	4070	15.15
Production	8/1/16 11:38	68	48.3	1.41	3927	12.65
Production	8/1/16 11:39	78	84.1	0.93	4209	15.10
Production	8/1/16 11:40	81	56.4	1.44	4272	14.55
Production	8/1/16 11:41	75	49.3	1.52	4165	15.80
Production	8/1/16 11:42	77	52.6	1.46	3932	11.50

The wheel loader LINCS data was downloaded and sent via the CMMS system or transferred via memory sticks to the same Dell laptop used in the previous sections. Each of the datasets was downloaded, stored, and processed using the same protocol as the previous sections. Again, the data was added into the backup files from the other sections and the same procedure was followed.

4.3.1.1 Data quality control. The objective for this section was to determine if the maximum force exerted (as indicated by the maximum hoist cylinder pressure) generated on specific structural components is dependent to the amount of weight being hoisted by the wheel loader. Following the synchronization of the two datasets, each bucket load for a dataset was separated by bucket load type as shown in Table 4.2. This is the same breakdown used for the 75 - 80 ton wheel loaders in the bucket overloading wheel loader productivity study conducted in Section 3.

Table 4.2. Breakdown of the Bucket Load Weights by Bucket Load Type (Joy Global, 2015)

	Model	60 ton	55 ton	80 ton	75 ton
Bucket Load %	Bucket Load Type	Bucket Load Weight (st)			
0 - 85%	Underload	25 - 51	25 - 46	25 - 67	25 - 64
85 - 100%	Target Load	52 - 60	47 - 55	68 - 80	65 - 75
101 - 105%	Target Load	61 - 63	56 - 58	81 - 84	76 - 79
106 - 110%	Slight Overload	64 - 66	59 - 61	85 - 88	80 - 83
111 - 120%	Overload	67 - 72	62 - 66	89 - 96	83 - 90
120+%	Critical Overload	72+	66+	96+	90+

After the buckets in each dataset were classified by bucket load type, a data check was performed to ensure data quality. The time to achieve maximum hoist pressure was used to perform this data check. Typically, it should take 12 - 14 seconds to hoist a maximum payload bucket clear of the pile to maximum dump height. A ± 4 second window was added to account for variations in the starting elevation of the hoist, the site conditions, and the operator's ability. Bucket loads which did not reach their maximum hoist pressure between 10 - 18 seconds were eliminated from the dataset for analysis.

The hoist cylinder base pressure readings allow for a second analysis to compare the hoist base pressure value against the designed hoist circuit pressure for a specific load or group. The design hoist circuit pressure to hoist the maximum design payload of either 75 or 80 tons, depending on the loader's configuration, was estimated to be 4,000 psi (Richter, 2017). Table 4.3 exhibits the estimated hoist cylinder base pressures to hoist the bucket load types being studied. The hoist circuit typically requires a minimum pressure of 2,500 - 2,800 psi to operate with an empty bucket, and the pressure reliefs for the hoist circuit are set at 4,500 psi (Richter, 2017).

Table 4.3. Expected Hoist Pressure Readings (Richter, 2017)

Bucket Load %	Bucket Load Type	Hoist Pressure - Base (psi)
-85%	Underload	< 3400
85-100%	Target Load	3400 - 4000
101 - 105%	Slight Overload	4001 - 4200
106 - 120%	Overload	4201 - 4400
120+%	Critical Overload	> 4400

4.3.1.2 Overview of the data. The five ultra-class wheel loaders datasets consisted of 1 - 4 hours of event data. Table 4.4 displays when these downloads were collected.

The hoist base hydraulic pressure results are arranged by bucket load type which consists of underload, target load, and overload for the specified machines in this study. Loader 8002 is an 80 ton class wheel loader operating in Australia, while Loaders 8016 and 8019 are both 75 ton class machines operating at the same copper mine in South

Table 4.4. 75 - 80 ton WL Class Monitoring Data Collection Dates

Loader	Sample	Sample Collection Date	Sample Duration (min)
8002	1	February 9, 2015	120
8016	1	July 17, 2016	25
8019	1	August 1, 2016	90
8019	2	October 10, 2016	25
8019	3	October 22, 2016	45

America. The wheel loader's production statistics and hoist cylinder base pressure readings from the test datasets are shown in Table 4.5. The data presented in Table 4.5 shows the average hoist base pressure and the average time required from initiation of the hoist command to reaching the maximum pressure reading for each sample in dataset.

Table 4.5. 75 - 80 Ton WL Class Wheel Loader Performance Data

75 -80 ton Class Wheel Loader Performance

Loader	# of Events	Average			Avg. Hoist Cyl. Pressure (psi)	Avg. Hoist Cycle Time (sec)
		Tonnage	Time (sec)	Prod (t/sec)		
8002	16	49	58.0	1.02	3252	10.15
8016	52	66	64.3	1.20	4232	16.51
8019 S1	110	76	64.2	1.31	4137	14.00
8019 S2	17	60	50.3	1.23	3741	14.49
8019 S3	68	58	65.3	0.95	3722	15.13

The reader may observe that the performance results for the two wheel loaders' (Loaders 8002 and 8016) datasets presented in previous section are not similar to the large dataset averages shown in Table 3.16. These wheel loaders' productivity datasets

do, in fact, compare to individual short-time (i.e., 1 - 2 hours) periods from the wheel loaders' master datasets. Loader 8002 bucket's weight was 13 tons under its average while it was cycling 4 seconds slower than the targeted cycle time for the wheel loader during the period of the cylinder pressure sampling, resulting in an 18% decline in productivity. Loader 8016 results were better than the machine's average values with a bucket weight of 15 tons greater than its average, although its cycle time was 6 seconds slower, resulting in a productivity increase of over 7% during the period of the cylinder pressure sampling. Loader 8019 is not part of the data presented in Section 3.

The individual datasets here were further broken down into their respective bucket load types (i.e., underloads, target loads, and overloads, Tables 4.6 - 4.8). The results show that Loader 8002 was operating within its cylinder pressure ratings in the underload category per the guidance Table 4.3. Loader 8016 was operating with hoist cylinder pressures at the designed pressure for full bucket loads of 4,000 psi, while it was actually only hoisting payloads that are under the target payload of 63 tons. Loader 8019's cylinder pressures are in-between the other two while operating between 77% - 82% of the designed bucket weight. The hoist cycle times for the loads were within accepted published operating ranges (SAE (3), 1998).

The target load hoist cylinder base pressure results, given in Table 4.7, reveal the results of the target weighted buckets in the study. Loader 8002 did not record any target weighted buckets in the period of the cylinder pressure sampling. The average hoist cylinder pressures for Loader 8016 target weight buckets were in the overload pressure range at 4,258 psi and had a hoist time in the upper part of the range. Loader 8019 results

were as expected with the target load weighted bucket producing results in the target load hoist pressures and hoisting loads in the middle of the expected cycle time.

Table 4.6. Hoist Cylinder Base Pressure Dataset - Underload Results

Underloads

Loader	# of Events	Average			Avg. Hoist Cyl. Pressure (psi)	Avg. Hoist Cycle Time (sec)
		Tonnage	Time (sec)	Prod (t/sec)		
8002	16	49	49.0	1.19	3,226	9.70
8016	9	63	53.5	1.23	3,985	16.09
8019 S1	38	62	52.9	1.17	3,767	12.45
8019 S2	11	59	49.0	1.20	3,699	14.70
8019 S3	67	58	65.3	0.89	3,722	15.13

Table 4.7. Hoist Cylinder Base Pressure Dataset - Target Load Results

Target Loads

Loader	# of Events	Average			Avg. Hoist Pressure	
		Tonnage	Time (sec)	Prod (t/sec)	Base (psi)	Time (sec)
8002	-	No Target Loads in this dataset				
8016	42	67	59.3	1.20	4,258	16.77
8019 S1	51	75	60.0	1.26	4,034	13.54
8019 S2	6	66	54.4	1.21	3,842	13.96
8019 S3	1	67	66.0	1.02	3,953	13.09

All the datasets only yielded two overloaded weighted bucket pressure cycles. Loader 8016 had one data point (one cycle) with payload in the overload category. The maximum hoist pressure base was 4,145 psi and hoisting cycle time was 17.60 seconds.

Similarly, Loader 8019 also had one data point with payload in the overload category.

The maximum pressure was 4,192 psi and took 14.73 second to achieve it.

Table 4.8. Hoist Cylinder Base Pressure Dataset - Overload Results

Overloads

Loader	# of Events	Average			Avg. Hoist Cyl. Pressure (psi)	Avg. Hoist Cycle Time (sec)
		Tonnage	Time (sec)	Prod (t/sec)		
8002	-	No Overloads in this dataset				
8016	1	80	123.3	0.65	4,145	17.60
8019 S1	21	81	81.7	0.99	4,192	14.73
8019 S2	-	No Overloads in this dataset				
8019 S3	-	No Overloads in this dataset				

4.3.2. Step 2: Correlation Testing. This used the Pearson linear and Spearman and Kendall rank correlation coefficients to evaluate the strength of the relationship between the bucket weight and the maximum hoist cylinder pressures from the data sets. In these correlation tests, the bucket weight was set as the dependent variable and the hoist cylinder pressure was set as the independent variable (Keller, 1994).

The Pearson correlation is commonly used to express the strength of the relationship between two continuous variables. It generally assumes a linear relationship between the two variables, which are assumed to be normally distributed (Hauke & Kossowski, 2011; Chok 2010). This correlation is expressed with an r value between -1 and 1, with values towards 1 indicating a strong linear positive relationship, values around 0 indicating no linear relationship, and values moving towards -1 indicate a strong linear negative relationship (Rumsey, 2009). Hence, it is possible to obtain Pearson

correlation values near zero for variables that are related in a nonlinear manner or have a bivariate distribution that is not normal (Chok 2010). Also, the Pearson correlation coefficient is prone to wrong inferences in the presence of outliers (Hauke & Kossowski, 2011).

One can also use rank correlations, such as Spearman and Kendall, to measure the degree of association between two variables. Spearman's test is a rank-order correlation test that evaluates monotonic relationship between two variables (Hauke & Kossowski, 2011; Chok 2010). Additionally, it is recommended that Spearman's sample size be greater than 30 samples (Keller, 1994). The Spearman's correlation coefficient, r_s , ranges between -1 and 1, with values greater than zero indicating a positive monotonic relationship, values around 0 indicating no monotonic relationship, and values less than zero indicate a negative monotonic relationship (Chok, 2010). Hence, it is possible to obtain Spearman's correlation coefficient near zero for variables that are related in a nonmonotonic manner. However, the Spearman correlation coefficient can be 1 not only for variables that are linearly related but also for variables that are related by nonlinear monotonic relationships (Chok 2010).

Kendall's rank correlation is better suited for smaller datasets of 20 samples or less, because it is resistant to the effects of outliers, and it is not affected by monotonic transformations of either variable (Keller, 1994). The Kendall correlation coefficient, τ , is designed to measure the discrepancy between the number of discordant and concordant pairs in ordinal data. It can, however, be used for continuous variables. Similar to the other two coefficients, the values of the Kendall correlation coefficient ranges from -1 to 1 with values greater than zero indicating a positive monotonic relationship, values

around 0 indicating no monotonic relationship, and values less than zero indicate a negative monotonic relationship. However, the Kendall correlation coefficient is likely to give a value greater than zero for a wider range of monotonic relationships (Chok, 2010).

This research used all three correlations to take advantage of each tests strengths based on the number of data points within each dataset. Pearson’s correlation was chosen due to the belief there should be a linear relationship between the bucket weight and maximum hoist pressures based on scatter plots. The concern is the effect of outliers on the Pearson correlation especially with the number of concordance and discordance pairs observed in the distributions (Chok, 2010). The dataset from Loader 8016 has a majority of outlier events, exhibiting a 90-degree fan pattern versus the more linear patterns of the other datasets, observed in Figure 4.6. The number of outliers present in Loader 8016

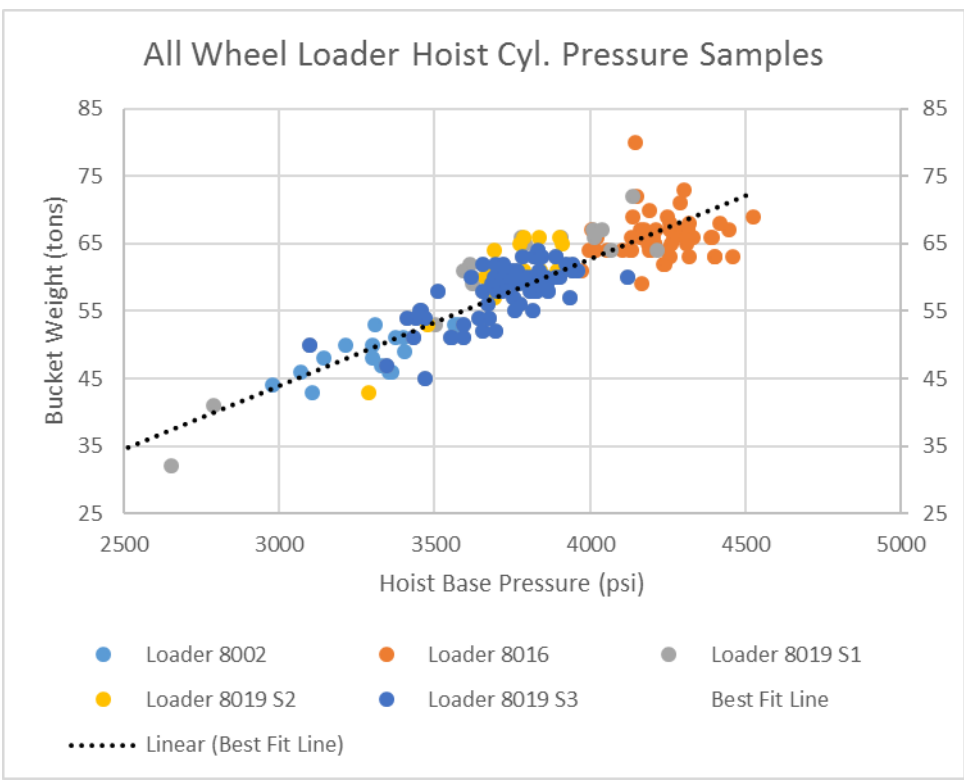


Figure 4.6. All Wheel Loader Hoist Cylinder Pressure Samples

dataset and their possible effect on Pearson correlation results was the reason to also include Spearman's and Kendall's correlations in the analysis (Chok, 2010). Both correlation methods were chosen based on number of samples in the respective datasets (Keller, 1994). The time to setup and run these tests was minimal and would allow for the interpretation of any discrepancies due to each tests limitations or limitations of the data. The Spearman and Kendall correlations results would be useful to compare and determine a confidence of the results.

Each hoist cylinder data sample was processed to organize the hoist cylinder maximum pressure during the hoist cycle and the weight of each bucket load for correlation testing. The data was plotted in a scatterplot to look for possible relationships between the variables (Rumsey, 2009). Figure 4.6 shows the relationship of all the hoist cylinder pressure data samples to bucket weight. Loader 8019 had three separate sampling events over a three month period (August - October 2016). These samples were combined into the same scatterplot events in Figure 4.7.

4.3.2.1 Pearson correlation analysis. Pearson's correlation coefficient, defined in Equations 4.3, measures the strength and direction of the linear relationship between two quantitative variables (Rumsey, 2009). In this work, Pearson was used to assess the linear relationship between hoist cylinder hydraulic pressure and bucket weight (payload). An assumption of Pearson's correlation coefficient estimates is that both variables should be normally distributed. Additionally, the data are linearly related and exhibit homoscedasticity (Rumsey, 2009).

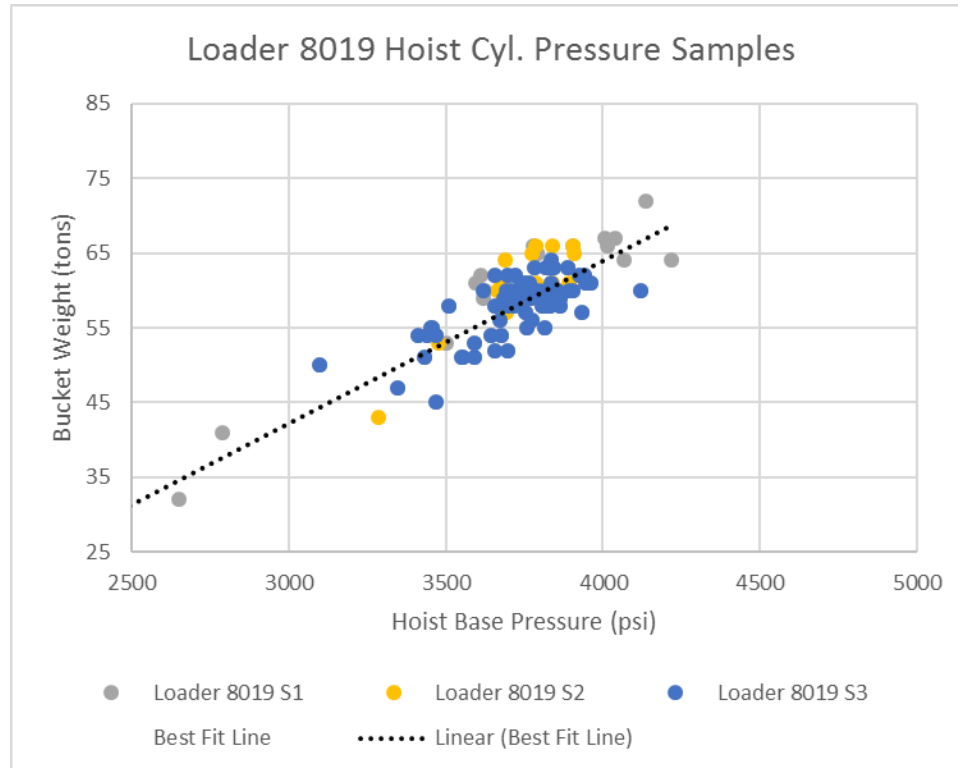


Figure 4.7. Loader 8019 All Hoist Cylinder Pressure Samples

$$r = \frac{(N \sum xy - \sum(x)(y))}{\sqrt{(N \sum x^2 - \sum(x)^2)(N \sum y^2 - \sum(y)^2)}} \quad (4.3)$$

For hypothesis testing, Equations (4.4) and (4.5) describe the null and alternate hypotheses. The hypothesis test estimates the test statistics, the critical value, and the p-value at a particular significance level. If the p-value is lower than the critical value, then there is enough evidence to reject the null hypothesis. Therefore we conclude that the correlation coefficient is non-zero at the specified confidence level. Otherwise there is not enough evidence to reject the null hypothesis. Hence, we have no basis to assume the correlation coefficient is not zero. We tend to then assume that there is no correlation between the variables.

$$H_0: r = 0 \quad (4.4)$$

$$H_1: r \neq 0 \quad (4.5)$$

The Pearson coefficient correlation analysis was performed using Matlab and the results are shown in Table 4.9. The r for Loaders 8002 and 8019 datasets showed a strong relationship (Rumsey, 2009). As hoist pressure increases so does the weight of the material being hoisted. Additionally, the p-value for these datasets indicate that there is enough evidence to reject the null hypothesis. Loader 8016's r value of 0.0903 was very low and the p-value is very high. Thus, we can infer, at even a confidence level of 90%, that there is no linear relationship between payload and hoist cylinder pressures for this dataset.

Table 4.9 Pearson Coefficient Correlation Results

Pearson Results

Loader	# Samples	rho	P-value
8002	16	0.7269	0.0014
8016	52	0.0903	0.5245
8019 S1	110	0.7270	0.0000
8019 S2	17	0.8771	0.0000
8019 S3	68	0.7087	0.0000

4.3.2.2 Spearman correlation analysis. The Spearman rank correlation also is a non-parametric test which measures the degree of association between two variables. The Spearman rank correlation test does not make any assumptions about the distribution of the data. Spearman's rho correlation assumption is that the date / time must be at least ordinal to the scores on the variable and must be monotonically related to the other

variable (Rumsey, 2009). The Spearman rank correlation formula is shown in Equation 4.6 while the null and alternate hypothesis of the test are shown in Equations 4.7 and 4.8.

$$\rho = 1 - \frac{6 \sum d_i^2}{n(n^2-1)} \quad (4.6)$$

$$H_0: \rho = 0 \quad (4.7)$$

$$H_1: \rho \neq 0 \quad (4.8)$$

The Spearman rank correlation estimates and hypotheses tests were completed using Matlab, and the results are reported in Table 4.10. The Spearman test results are similar to the Pearson coefficient correlation tests which were shown previously. The datasets of Loaders 8002 and 8019 display a strong positive relationship between the hoist cylinder pressure and the weight of the material being lifted. Additionally, the p-value for these datasets is low indicating that there is enough evidence to reject the null hypothesis. Loader 8016's p-value of 0.3142 indicates there is not enough evidence to reject the null hypothesis. We can thus infer that no relationship exists between hoist cylinder pressures and the payload for this dataset. This confirms the results of the hypothesis test for the Pearson correlation coefficient.

Table 4.10 Spearman Rank Correlation Results

Spearman Results

Loader	# Samples	r	P-value
8002	16	0.6509	0.0063
8016	52	0.1423	0.3142
8019 S1	110	0.6588	0.0000
8019 S2	17	0.6287	0.0069
8019 S3	68	0.6437	0.0000

4.3.2.3 Kendall correlation analysis. The Kendal rank correlation is similar to Spearman's rank correlation as a non-parametric measure of the correlation between two ranked variables. A positive correlation exists if both variables are increasing or decreasing, while a negative correlation occurs if one variable is increasing while the other is decreasing (Keller, 1994). This is illustrated in Equations 4.10 and 4.11. The difference of Kendall's Tau represents a probability that the observed data is the same order versus the probability that the data is not in the same order. The data was ranked low to high which was based on the maximum hoist cylinder base pressure to determine the number concordant pairs or discordant pairs present in the sample from the bucket weight. The probability was calculated using Equation 4.9 to determine tau value (statisticssolutions, 2017).

$$\tau = \frac{C-D}{C+D} \quad (4.9)$$

$$H_0: \tau = 0 \quad (4.10)$$

$$H_1: \tau \neq 0 \quad (4.11)$$

The Kendall rank correlation estimates and hypotheses tests were completed using Excel and the results are exhibited in Table 4.11. The Kendal test results are similar to both the Spearman rank correlation and the Pearson coefficient correlation tests. These results are compared in Table 4.12. The datasets of all loaders had a strong positive relationship between the hoist cylinder pressure and the weight of the material being lifted. This included a strong positive relationship for Loader 8016 to reject the null hypothesis.

Table 4.11 Kendall Rank Correlation Results

Kendall Results

Loader	# Samples	tau	z-value	P-value
8002	16	0.5833	3.1516	0.0008
8016	52	0.2232	2.3358	0.0098
8019 S1	110	0.5567	7.7256	0.0000
8019 S2	17	0.5441	3.0483	0.0012
8019 S3	68	0.525	6.3309	0.0000

Table 4.12. Summary of Correlation Results

Loader	# Samples	Spearman	Pearson	Kendall
8002	16	0.6509	0.7269	0.5833
8016	52	0.1423*	0.0903*	0.2232
8019 S1	110	0.6588	0.7270	0.5567
8019 S2	17	0.6287	0.8771	0.5441
8019 S3	68	0.6437	0.7087	0.525

* Not statistically significant at $\alpha = 0.05$

4.4. DISCUSSIONS

These examinations of hoist cylinder pressures versus bucket load weight data demonstrate a general relationship between them. Both the Pearson and the Spearman correlation tests confirm four of the five samples. For two of the three wheel loaders studied, they show a strong relationship where increasing the bucket weight leads to higher hoist cylinder pressures which were required to lift the load. Loader 8016 was the one loader for which there was no statistically significant correlation ($p > 0.3$) based on the Pearson and Spearman correlation tests. The Kendall results for Loader 8016 conflict with the Spearman and Pearson tests results, indicating that there was enough evidence to reject the null hypothesis. But even then, the correlation coefficient for the Kendall Tau is

still rather low (0.22). The results from the Kendall test indicates there may be a nonlinear relationship for Loader 8016, which the Pearson and Spearman test missed. A similar relationship between hoist cylinder pressures and the payload as seen in the other loaders datasets, though the relationship for Loader 8016 is not necessarily linear or monotonic. The scatter plot (Figure 4.6) of the Loader 8016 data was in fan type pattern versus the more linear patterns of the other loaders datasets.

These results indicate that as the wheel loader's bucket weight increases, it is likely to lead to higher hydraulic cylinder pressures. As higher cylinder pressures are indicative of higher forces on the lift arm. It is safe to assume that overloading the wheel loader is likely to lead to higher stresses (resulting from the higher forces) on the lift arm structure. Higher stresses are also transmitted to the other lift arm structures (i.e., the bellcranks, level links, and bucket). Additionally, the wheel loader's front frame sees these collective stresses being transmitted back through the machine.

Examining the differences in the hoist cylinder pressures of the three different bucket load classes (underloads, target loads, and overloads) explains further the relationship between the hydraulic pressure required to hoist greater bucket weights in the hoist circuit. Table 4.13 is a summary of the data presented in Section 4.3.1.2 for the three bucket load types. The results show that as the bucket weight increases so does hoist cylinder pressure required to lift it. Additionally, the average hoist cycle time required to lift the bucket load also increases as the weight of the bucket load increases. Overall the hoist cylinders and hydraulic circuit pressures behaved in accordance with the results of the expected hoist pressure readings in Table 4.3.

Table 4.13. Summary of the Hoist Cylinder Hydraulic Operating Data by Bucket Load Type

Ranges			
Bucket Load Type	Bucket Load Weight (tons)	Avg. Hoist Cyl. Pressure (psi)	Avg. Hoist Cycle Time (sec)
Underloads	< 64	3226 - 3985	9.70 - 16.09
Target Loads	65 - 79	3842 - 4258	13.09 - 16.77
Overloads	> 80	4145 - 4192	14.73 - 17.60

There are variations in the each of the individual wheel loaders datasets, and this transfers into the variability in the bucket load type data. For example, the 9.70 second average hoist cycle time for Loader 8002 is due to a combination of the fact that it loads smaller trucks (240 ton class haul trucks) and the inclusion of several clean-up / re-handle buckets in the 16 bucket dataset. Wheel Loader 8016 accounted for the highest average hoist cylinder pressure readings for the underload and target load bucket types, and they accounted for the highest average hoist cycle times in all three bucket load types.

There are several other factors that may be influencing the results and causing variances in the reported data. There are confounding factors in the analysis. These factors include the effects of operator skill, the wheel loaders hydraulic system, and the application, site / working conditions. This is a limitation of the analysis in this work because this analysis did not isolate the effects of these confounding factors. However, it is expected that isolating these confounding factors will actually increase the observed strength of correlation between payload and hoist cylinder hydraulic pressures.

4.5. SUMMARY

The research in this section evaluates the effect of overloading the wheel loader bucket on the structural components. The work evaluated the effect of overloading on the lift arm since it is the structural component most likely to be affected by overloading. The work uses the hoist cylinder pressures (force exerted) as a proxy for the stress events on the lift arm. The work presents an approach based on reviewing on-board vehicle equipment monitoring systems to extract data from hoist cylinder pressures and match them with production data for this analysis. Data from three 80 ton class wheel loader hoist systems was used to evaluate the effect bucket weight might have on the required hoist pressure.

Based on the results of this work, the following general conclusions can be drawn:

- The hoist pressure increases as the bucket weight increases.
- The majority of the hoist circuit pressure readings were within the expected operating ranges for the bucket loads lifted.
- Typically, the observed hoist circuit pressure readings tended to be on the higher side of the expected hoist pressure range for any given bucket.

The following recommendations are for future work which could improve and increase the body of knowledge from this research:

- Increase the amount of hydraulic system information by acquiring data from additional ultra-class wheel loaders to better understand wheel loader operating conditions.
- Examine individual operators in order to determine how individual operators affect the results.

5. EFFECT OF OVERLOADING THE BUCKET ON WHEEL LOADER STRUCTURAL COMPONENT RELIABILITY - A CASE STUDY

5.1. INTRODUCTION TO STRUCTURAL COMPONENT RELIABILITY

This section addresses the third objective of this dissertation. The goal of this section is to characterize the effect of overloading the bucket on wheel loader reliability. The work uses Weibull analysis to establish a time based point of reference for overloads in order to establish the reliability of the structural components. This was achieved by reviewing the data on wheel loader failure modes, along with the component hours, payloads, and other data relating to machine operation in order to build a failure dataset. Reliability analysis using a two-parameter Weibull Distribution Probability Density Function was performed using such a failure dataset in order to discover the mean time between failure (MTBF) and each structural components specific failure pattern (Moubray, (5), 1997). This was done with and without payload as a factor to examine the effect of accounting for payload in the reliability models.

First, the candidate identified the part numbers of the structural components to be included in the study and built a template to record information from the computer maintenance and management system (CMMS) cases. Second, each structural component's dataset was built from downloaded and reviewed cases from the CMMS database. The CMMS database was searched by part number and wheel loader serial number to ensure that all cases referenced were captured for this analysis. Third, Weibull frequency distribution analysis was performed on all structural component datasets that contained enough information to perform the analysis. Finally, Weibull results were analyzed to determine the general reliability of the ultra-class wheel loaders structural components in relation to the frequency of overloading.

5.2. EXPERIMENTAL EQUIPMENT & SITES

The experimental equipment fleet was expanded to include all current generation ultra-class wheel loaders. This expanded fleet also increased the number and types of mine sites from around the globe. The units in the study are performing production, stripping, stockpiling, and support roles in all the major mining sectors including coal, base and precious metals, industrial minerals, and gemstones (ParkerBayMining, 2016). Table 5.1 displays the number of wheel loaders by region in this study. Table 5.2 details the number of loaders in this study by the commodity they extract during their shift operations.

Table 5.1. Ultra-Class Wheel Loaders by Operating Class and Region

Class	Commodity				TOTAL
	Coal	Ind. Min.	Iron Ore	Metal	
55 - 60 ton	11	2	16	12	41
75 - 80 ton	2	0	18	14	34
TOTAL	13	2	34	26	

Table 5.2. Ultra-Class Wheel Loaders by Operating Class and Commodity

Class	Region					TOTAL
	Africa	Australia	Eurasia	S. America	N. America	
55 - 60 ton	3	7	2	19	10	41
75 - 80 ton	-	5	1	26	2	34
TOTAL	3	12	3	45	12	

5.3. DATA COLLECTION


This structural case failure data was collected from the CMMS system. The information was entered into the CMMS system to track product issues and process warranty claims by mechanics, field service engineer (FSE), factory service representative (FSR), service engineers, regional product support representatives, and factory service representatives as part of the maintenance and repair process to track issues with the fleet. It is the duty of these individuals to report initial observations of cracks or other structural defects as part of various inspection processes, which are conducted during preventative maintenance of the equipment. A report of a crack or “initial failure” or failure of a structural component begins the process to access and analyze / propose a solution, and to take action to correct the reported issue. All these elements are recorded in the CMMS system for each structural part. An example of CMMS data is shown for one of these structural cases in Figure 5.1.

Table 5.3 lists the structural components that were reviewed and used to build the reliability data in this analysis (highlighted components are shared between different model and wheel loader classes). Several of these structural components are used in multiple wheel loader classes. The front and rear frames along with the rear axle for both the 55 - 60 ton and the 75 - 80 ton class machines are the same. The roll-over protective structure (ROPS) structure is the same for all wheel loaders in this study. Additionally, the lift arms and the bellcranks are the same for the 55 ton and the 80 ton machines. The part numbers sharing components across two or more classes are highlighted with the same color. These results yielded thirteen unique structural component part numbers to begin building reliability datasets for analysis.

CASE Detail Edit Delete Clone Add/Change FLOC

Record Type	Machine/Component Failures [Change]
Case Type	Machine/Component Failures
Subtype	Structural
Reason	Quality Issue
Priority	High
Status	Closed
Case Origin	Email
Time of Incident	1/16/2016 9:17 PM
Potential Safety Issue?	<input type="checkbox"/>
Warranty Claim	Yes

▼ Description Information

Case Subject	Lift Arm Crack at LH Ball socket.
Case Description	Customer called about crack found on LH Lift Arm Ball socket. See pictures attached. A warranty will be submitted and we are busy with a parts list to accompany new set of Lift Arms.
Case Photos	

▼ Additional Information

Machine	Wheel Loader-2350-2217	Functional Location	No TOS Exists
Machine Serial Number	2217	FLOC Description	
Machine Tonnage		Failure Code	Material-Breakage
Machine Component Tonnage		Customer PO	
Machine Hours	13,020	Has This Issue Occurred Before?	Yes
Part Hours	13,020	Warranty	<input checked="" type="checkbox"/>
		CAPA Required	
		No CAPA Required Code	<input type="checkbox"/>
		CAPA Link	
		CCR ID	

▼ Case Resolution Details

Closed Reason	Other
Resolution Details	cloned case 188980
Tracking Department	<input type="checkbox"/>

▼ SAP Part Information

Part Number	R4267724	Division	9F
Serial Number of Part Added	866 EAG	Division Description	Surface Loaders LET
Component Serial Number	866 BYL	SAP Web Service Message	2016-10-03 14:41:33 OK
Part Description	STR LIFTARM G2 L18 HU/ L23 STD	SAP Web Service Manual Override	<input type="checkbox"/>
Procurement Type	F		
Procurement Description	External procurement		

▼ Warranty

In Service Date		SAP Notification Number	3934262
Customer Warranty Status		Sales Order Number	3930499
Internal Warranty Status	Rejected		

Figure 5.1. CMMS Structural Case Data Example (Joy Global, 2016)

Table 5.3. List of the Structural Components Examined

Structural Component	Wheel Loader Model Class			
	60 ton	55 ton	80 ton	75 ton
Front Frame	60 ton	55 ton	80 ton	75 ton
Rear Frame	60 ton	55 ton	80 ton	75 ton
Rear Axle	60 ton	55 ton	80 ton	75 ton
Lift Arm	60 ton	55 ton	80 ton	75 ton
Bellcrank (LH)	60 ton	55 ton	80 ton	75 ton
Bellcrank (RH)	60 ton	55 ton	80 ton	75 ton
ROPS	60 ton	55 ton	80 ton	75 ton

The CMMS data was downloaded and stored on the same Dell laptop used in the previous sections. The datasets were downloaded, stored, and processed using the same protocol as the previous sections. Again, the repair data was added to the data backup files the same as previous sections, and the same procedure was followed.

5.3.1. Step 1: Compile Wheel Loader Structural Component Failure Data.

The CMMS database was queried and searched multiple times to find all of the appropriate structural cases. First, the CMMS database was search for all current generation machines' structural cases via the Subtype field. Second, a list of part numbers was compiled for the structural components to be reviewed. This part number list was sorted to eliminate duplicates, as some structural parts are used on multiple wheel loader class machines. Each parts list was compared against the first as a check to confirm that all structural component reports were included in the dataset. Third, cases from the first two queries, those which reported multiple cases, or a parent / child case link, were traced to insure that all of the cases were present. Finally, the list of wheel loaders from Section 3 with their production data were double check against their individual machine history

cases to confirm that all structural cases were included in dataset. An example of the data gathered for a 55 - 60 ton class wheel loader rear axle is shown in Table 5.4 (see next page).

Typically, structural repairs are identified during various machine inspections. These inspections include but are not limited to the daily machine pre-shift walk around, daily maintenance inspection, engine oil service (250 - 500 hour), or a specific structural inspection. All of the wheel loaders in this study are scheduled to have structural inspections every 1,000 hours. The 1,000 hour structural inspections require that the wheel loader be cleaned, typically by power washing, to examine the frame at a predetermined number of points (>160) on the Structural Inspection Report Form. The report requires written notes and photographs for further review to better examine and determine how the structural component's health is changing.

During these inspections, the most common observations are to discover a crack in a structural component. The level of response depends on the crack's location and the specific size (length, width, and shape) and the affected component. A response may range from marking and monitoring the crack thus allowing the wheel loader to return to work, to schedule a weld / structural repair, or to withdraw the machine from operation for service. The specific structural component determines if it will be repaired or exchanged / replaced. The structural component's life varies from 25% - 100% of the wheel loaders life as shown in Table 5.5.

Typically, structural repairs are identified during various machine inspections. These inspections include but are not limited to the daily machine pre-shift walk around,

Table 5.4. Example of the Structural Component Dataset – 55-60 Ton Rear Axle

CASE	Subtype	Reason	Date of Failure	Machine	Machine Hours	Part Hours	Service Center	Load Material	55-60 ton Rear Axle	Failure Mode	Date Created	Report	Photo Available	Comments
211095	Structural	Wear and Tear	9/13/2016	1850-2204	28414	28414	Australia	Coal			9/13/2016		YES	2204-648 Rear Axle Cracking noted by BV via their normal inspection processes. I have ask the 14/3 to have a boiler maker look at it was verified through inspection that the front transition plate was ee oscillating axle on 1850-2207 had a set of 16" on the right side.
206350	Structural	Quality	7/27/2016	1850-2207	19991	19991	S. America	Iron ore		front transition plate cracking	7/27/2016		YES	During inspection a crack was found inside the rear axle in the are where the cable and hoses enter the axle, a ribb has been created in the Rio
197709	Structural	Wear and Tear	3/5/2016	1850-2208	25207	25207	Australia	Iron ore			4/29/2016		YES	On visual inspection of the rear axle, cracks were observed near oscillating axle near front ball on left and right sides.
191764	Structural	Customer Misuse	2/18/2016	1850-2225	8779	8779	Eurasia	Coal		Cracks near front ball	2/18/2016	YES		The crack was observed near front ball of rear oscillating axle on the left hand side. Please see the enclosed report for further details.
187902	Service and S	Application Question	11/4/2015	1850-2223	8952	8952	Eurasia	Coal			12/22/2015	YES		Fracture swing axle near right 80% of cross section.
185587	Structural	Quality	11/18/2015	1850-2069	32962	32962	S. America	Copper			11/19/2015		YES	loader 1850-2221 presented crack in the welding upper socket ball after 11,996 hours of operation.
161454	Structural	Quality	3/9/2015	1850-2221	11926	11926	S. America	Iron ore		Crack in welding upper socket	3/16/2015	YES		While disassembling this machine at Quinitette, it was noticed that there is a crack in the casting (see photos). We will have to fix this before re-
149883	Structural	Quality	1/11/2015	1850-2229	2554	2554	N. America	Coal		Rear Axle Box Cracking - Cable	1/11/2015		YES	During a planned outage on 2209 cracking was found on the rear axle box. The cracking originated out of the corners of the cable entry cut out hole.
149855	Structural	Wear and Tear	1/8/2015	1850-2209	14640	14640	Australia	Coal			1/8/2015		YES	We have three crack in our rear axle motor lead access hole coming out of the corners. When you look at it from the inside, the cut out is square (no
136982	Structural	Design Issue	3/4/2014	1850-2226	9291	9291	N. America	Copper			8/28/2014		YES	16/10/14 Richard Gray (NER Tech services) visited site and identified the loader requires GS9470, 463, 469, 471 and 511465. It was noted the
135942	Structural	Quality	8/15/2014	1850-2230	7870	2938	Australia	Coal			8/15/2014			Rear axle cracked in transition plate - left side front & rear. Known problem identified by Letoumeau product support. Osisko personnel are
126055	Structural	Quality	5/13/2014	1850-2218	14171	14171	N. America	Gold			5/13/2014			During a 1000 hour crack inspection we found a 4" and 1" crack in the rear axle rear ball. I have contacted Richard Williams for correct procedures
115455	Structural	Quality	3/15/2014	1850-2226	3294	3294	N. America	Copper			3/15/2014			10/16/13 Site carried out an NDT inspection and found a number of cracks in this machine that needed attention, especially concerning was 2 cracks
115314	Structural	Quality	2/17/2014	1850-2230	3900	3900	Australia	Coal			3/13/2014	YES		Crack on rear axle structure 2" in length
114848	Service and S	Application Question	3/4/2014	1850-2232	2781	2781	S. America	Coper			3/4/2014			
114322	Documentati	Service Documentation	12/5/2013	1850-2230	3900	3900	Australia	Coal			2/17/2014			in this machine that needed attention, especially concerning was 2 cracks
113973	Documentati	Service Documentation	12/5/2013	1850-2230	3900	3900	Australia	Coal			2/17/2014			

Parent / Child Cases

daily maintenance inspection, engine oil service (250 - 500 hour), or a specific structural inspection. All of the wheel loaders in this study are scheduled to have structural inspections every 1,000 hours. The 1,000 hour structural inspections require that the wheel loader be cleaned, typically by power washing, to examine the frame at a predetermined number of points (>160) on the Structural Inspection Report Form. The report requires written notes and photographs for further review to better examine and determine how the structural component's health is changing.

During these inspections, the most common observations are to discover a crack in a structural component. The level of response depends on the crack's location and the specific size (length, width, and shape) and the affected component. A response may range from marking and monitoring the crack thus allowing the wheel loader to return to work, to schedule a weld / structural repair, or to withdraw the machine from operation for service. The specific structural component determines if it will be repaired or exchanged / replaced. The structural component's life varies from 25% - 100% of the wheel loaders life as shown in Table 5.5.

Table 5.5. 55 - 60 ton Class Wheel Loader Expected Component Lives

Structural Component	Wheel Loader Est. Life by Component (Hours)			
	60 ton	55 ton	80 ton	75 ton
Front Frame	50,000	50,000	60,000	60,000
Rear Frame	50,000	50,000	60,000	60,000
Rear Axle	25,000	25,000	30,000	30,000
Lift Arm	25,000	25,000	30,000	30,000
Bellcrank (LH)	25,000	25,000	15,000	15,000
Bellcrank (RH)	25,000	25,000	15,000	15,000

5.3.2. Step 2: Validation of the Structural Case Sample Data. The review of the CMMS database yielded over 300 structural component records on thirteen individual component's parts numbers. Each component's (part number) dataset was then reviewed to identify and highlight duplicate cases. For example, parent / child cases in which two or more cases for the same wheel loader have been recorded for one event. Another example of multiple cases existing for the same repair occurs when two or more people enter information for an event and did not check to see if a case has already been created. Duplicate cases were marked in the dataset and a parent (master) case created for the analysis. Parent cases were assigned to the initial case event and all information was tagged back to the first case. Additional information from the child (subsequent) cases were added to the parent case so all the data from the event was contained there.

The opposite of the duplicate case occurs when a single case is used for multiple repairs. That is, a structural inspection finds a crack in two or more structural components but the service engineer or planner only opens one case. In this circumstance, if the case is open the repairs will be split, and a case for each component will track the repair or replacement of the component. Cases in which all the work has been completed for all of the individual components may appear multiple times in the various datasets to track all of the opened cases.

The data in each component dataset was reviewed to fill in any missing pieces (e.g., commodity being mined or updating failure modes from the comment section or attached reports). This review was to insure that as complete a picture as possible could be obtained from all the existing information. Next, each dataset was reviewed further to eliminate cases which did not contain enough information to be used in the Weibull

analyses. Examples of cases that were eliminated were instances where the component (part) hours were not recorded or the reason why the cases were created was not a failure or failure related.

After completing the review of all of these cases and the removal of non-failure, child, and missing information cases, the number of structural component failure cases was reduced to 176 total cases. A high-level breakdown of the quantity of structural component cases is shown in Table 5.6. The majority of the structural cases which passed validation for the models were in the 75 - 80 ton class wheel loaders. The ROPS structure was removed from the review because all of the cases in the CMMS database were for informational purposes.

Table 5.6. Quantity of Structural Component Cases by Component

Structural Component	# of Cases	55 ton class	60 ton class	75 ton class	80 ton class
Front Frame	6	1		1	4
Rear Frame	43	8	1	25	9
Rear Axle	43	14	1	21	7
Lift Arm	71	20		45	6
Bellcrank (LH)	9	3		2	4
Bellcrank (RH)	4	1		1	2
TOTAL	176	47	2	95	32
% of Cases by Class		96%	4%	75%	25%
% of Fleet Population		93%	7%	68%	18%

5.3.3. Step 3: Perform Weibull Analysis based on Failure Hours. The Weibull frequency distribution (probability density function) is widely used in instance like this because of it variety of shapes, which enable it to fit many kinds of data, especially data

relating to product (component) life. The distribution is defined by the shape parameter beta (β). The shape parameter defines the spread of the distribution and corresponds to the 63rd percentile of the cumulative distribution, characteristic life. Generally, Weibull distribution shapes for the shapes for $\beta=1$ is and exponential distribution, or random failures. When $\beta \geq 3.5$, it closely approximates a normal distribution and for $\beta \leq 1$ it tends to infant mortality to premature failures (Moubray (5), 1997, & Uptime, 2017). An example of Weibull frequency distribution for the 75 - 80 ton class wheel loaders rear axle dataset is shown in Figure 5.2.

A data summary for the 75 - 80 ton class wheel loader rear axle dataset and its corresponding Weibull analysis are displayed in Table 5.7. The dataset contained 40 cases which produced 28 validated cases on which the Weibull was based. The MTBF was calculated at 9,508 hours with a characteristic life expectancy of 10,666 hours. The shape parameter (β) equaled 1.7147 and the R^2 value was 0.9637 to determine the slope of the best fit line.

Table 5.7. Weibull Distribution Data - Example

75-80 ton class Wheel Loader

# of Cases	28
MTBF (hrs)	9,508
Beta	1.7147
Characteristic Life	10,666
R^2	0.9637

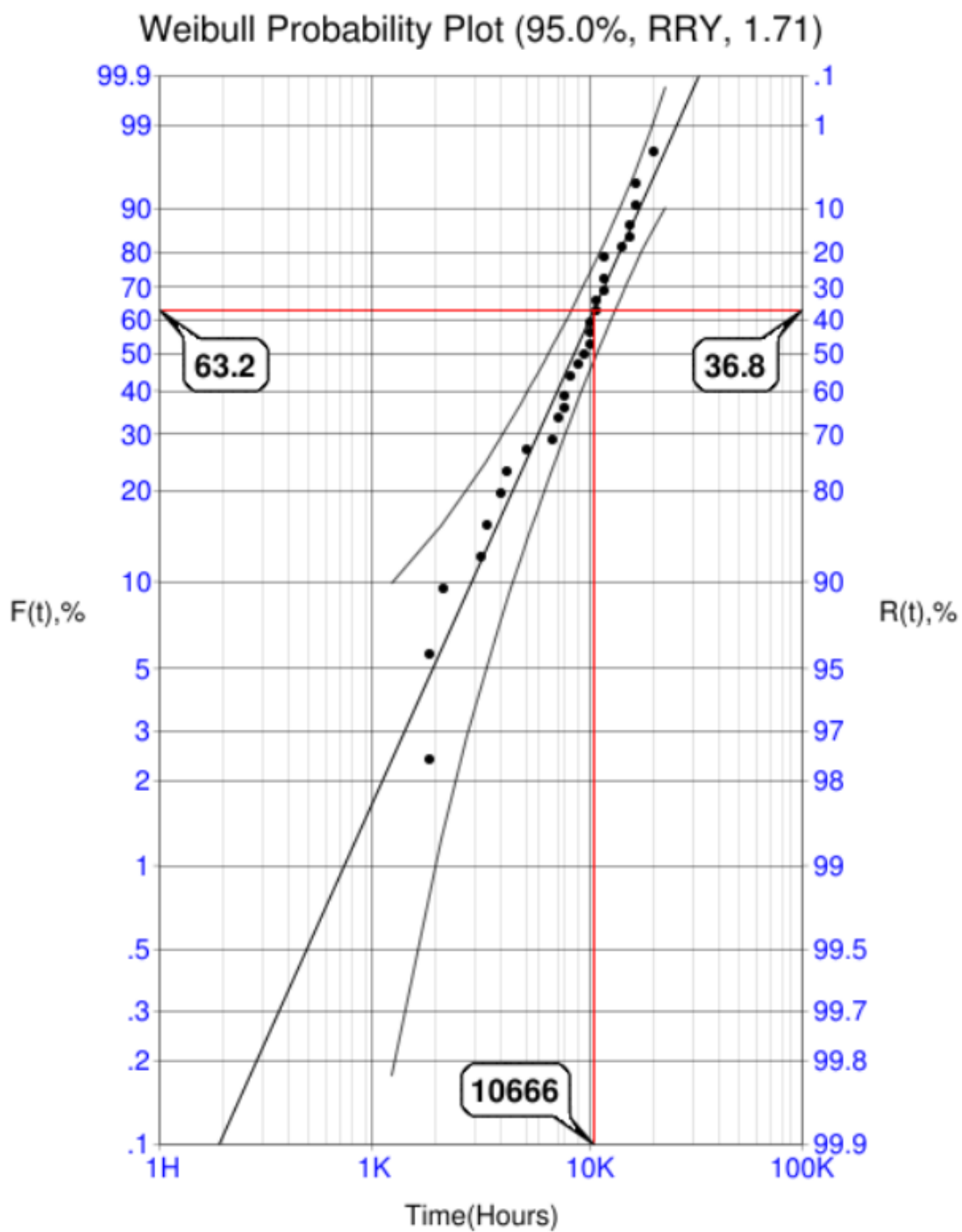


Figure 5.2 Weibull Probability Distribution Plot - Rear Axle 75-80 ton WL Class

The Weibull Reliability Plot and Probability Density Function are shown in Figures 5.3 and 5.4, respectively. The Reliability Plot calculates the failure time values based on the β from the Weibull Probability Distribution (with the selected parameters). These failure points represent the moving failure point left or right until they intersect the best fit straight line in the Weibull Probability Plot (Reliabilityanalyticstoolkit, 2017). The Probability Density Function, again based on the β value of 1.7147, is beginning to approximate a normal distribution, although it is skewed to the left which represents premature failure of the rear axle.

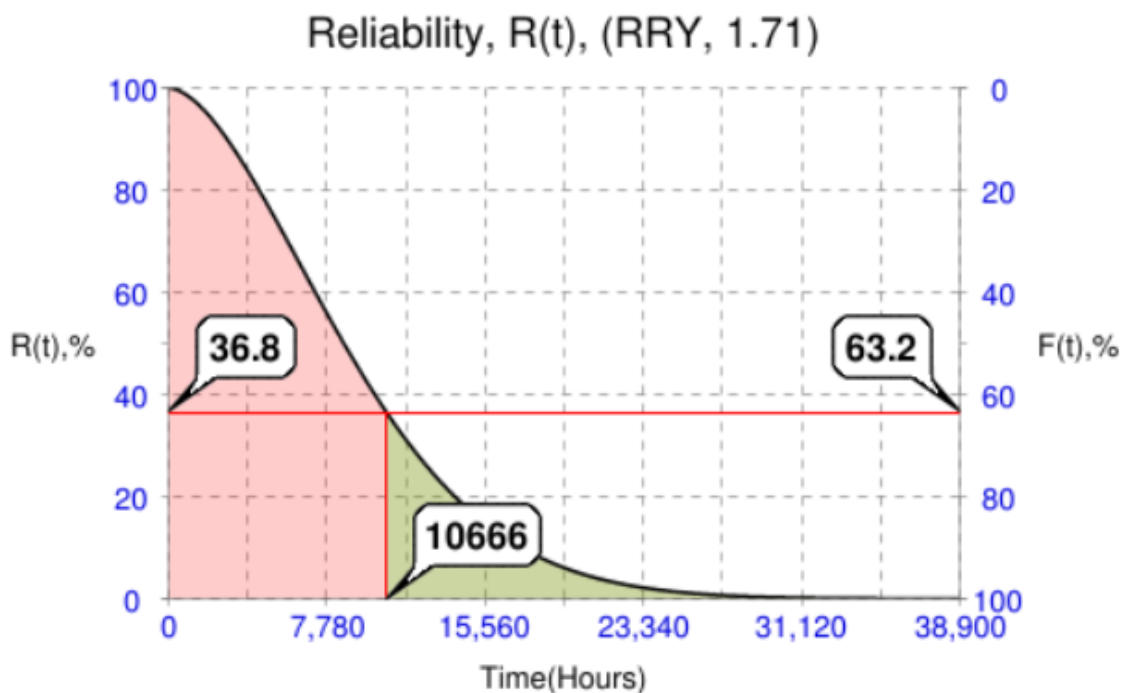


Figure 5.3 Weibull Reliability Plot - 75 - 80 ton WL Class Rear Axle

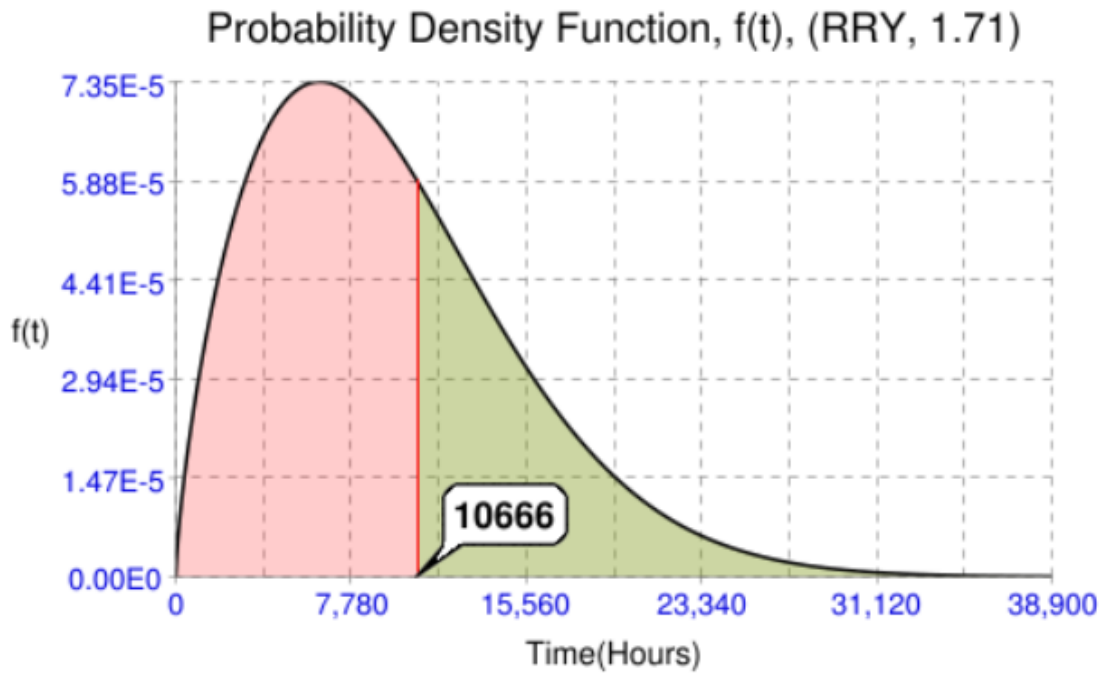


Figure 5.4. Weibull Probability Density Function Plot -
75 - 80 ton WL class Rear Axle

5.3.3.1 Presentation of 55 - 60 ton class wheel loader Weibull results. The results of the Weibull analysis of the 55 - 60 ton class wheel loaders' structural component cases are presented in Table 5.8. There was only a single case reported from the front frame and bellcrank (RH) and, hence, the candidate was unable to perform a Weibull analysis for these parts. The rear axle and lift arms produced a β value of ~ 1.23 exhibiting a random failure pattern. The bellcrank (LH) $\beta=1.81$ reveals that the failure pattern is beginning to normalize but may still fail prematurely over all. The rear frame record $\beta=3.49$, showing a normalized distribution of failures with the failure window occurring between 14,000 - 16,000 hour timeframe.

Table 5.8. Weibull Results Summary for 55 - 60 ton Wheel Loaders Class

**55-60 ton Class
Wheel Loader**

Structural Component	# of Cases	MTBF	Beta	Characteristic Life	R ²
Front Frame	1	14,000			
Rear Frame	9	14,018	3.4898	15,592	0.9225
Rear Axle	15	13,108	1.2275	14,034	0.9070
Lift Arm	20	15,758	1.2340	16,870	0.7317
Bellcrank (LH)	3	15,877	1.8116	17,862	0.9813
Bellcrank (RH)	1	24,189			
	49	14,198	1.5608	15,800	0.9310

Most of the data used in the analysis shown in Table 5.9 are cases from the 55 ton class wheel loaders. For the 60 ton class wheel loaders, with only three machines in the analysis, operating with this configuration, CMMS data search produced only two cases (one each for the rear frame and rear axle). Hence, the candidate is unable to run a Weibull analysis exclusively for the 60 ton class wheel loaders. However, it is possible to run an exclusive analysis for the 55 ton class loaders because there is adequate data.

For the 55 ton class wheel loaders structural components, the Weibull results are almost identical to the 55 - 60 ton class results (since most of the data is the same). As with the overall data, the front frame and the bellcrank (RH) had only one case each reported. The rear axle β value was slightly less at 1.18 vs. 1.23 for the overall group, while the lift arms β value of 1.23 remained unchanged. Both the rear axle and the lift arm still disclose a random failure pattern. The bellcrank (LH) $\beta=1.81$ stays the same along with its failure pattern beginning to normalize but may still fail prematurely over all. The rear frames β value increases to 4.5 tightening normalized distribution on

failures around 13,000 - 14,000 hours timeframe. The complete summary for all of the 55 ton class wheel loader components is displayed in Table 5.9.

Table 5.9. Weibull Results Summary for 55 ton Wheel Loaders Class

55 ton Class WL

Structural Component	# of Cases	MTBF	Beta	Characteristic Life	R ²
Front Frame	1	14,100			
Rear Frame	8	12,831	4.5196	14,052	0.9690
Rear Axle	14	13,058	1.1801	13,809	0.8941
Lift Arm	20	15,758	1.2340	16,870	0.7317
Bellcrank (LH)	3	15,877	1.8116	17,862	0.9813
Bellcrank (RH)	1	24,189			
	47	14,258	1.6039	15,915	0.9277

5.3.3.2 Presentation of 75 - 80 ton class wheel loader Weibull results. The results of the Weibull analysis of the 75 - 80 ton class wheel loaders structural component cases' are presented in Table 5.10. A summary of the results shows that all the components have random failure with β values ranging from 1.27 - 2.14. The MTBF and characteristic life values are approximately 67% of the 55 - 60 ton class wheel loaders, or in 9,000 - 12,000 hour timeframe.

Unlike the 55 - 60 ton class, the data was much more evenly distributed and therefore the candidate was able to conduct exclusive analysis for the 80 and 75 ton class loaders separately.

The 80 ton class wheel loaders structural components' Weibull outcomes were similar to the combined 75 - 80 ton class results. The rear frame and the lift arms had β

Table 5.10. Weibull Results Summary for 75 - 80 ton Wheel Loaders Class

**75-80 ton Class
Wheel Loader**

Structural Component	# of Cases	MTBF	Beta	Characteristic Life	R ²
Front Frame	5	10,524	1.1710	11,130	0.9526
Rear Frame	34	10,509	2.1422	11,867	0.9486
Rear Axle	28	9,508	1.7147	10,666	0.9637
Lift Arm	51	8,661	1.5379	9,622	0.9633
Bellcrank (LH)	6	9,330	1.3000	10,100	0.8600
Bellcrank (RH)	3	10,010	1.2900	10,807	0.8800
	127	8,956	1.5876	9,982	0.9703

values similar to the 75 - 80 ton class results, although the MTBF and the characteristic life windows increased between 2,000 - 5,000 hours, respectively. The front frame and the rear axle MTBF's and characteristic lives values decreased 2,000 - 3,000 hours while the β value remained relatively constant. The bellcrank (LH) β value was the most improved by over 100% to 2.61 with its MTBF and its characteristic life adding 2,000 - 3,000 hours. The bellcrank (RH) had only two cases reported, and the candidate was unable to perform a Weibull analysis. A complete summary for all the 80 ton class wheel loader components is given in Table 5.11.

For the 75 ton class wheel loaders, the candidate was only able to conduct Weibull analysis on three structural components: the rear frame, rear axle, and lift arms. The front frame and both of the bellcranks only had one or two valid cases which is insufficient to perform a Weibull analysis. The results of these components can be seen in Table 5.12. The rear axle has a β value of 1.75 and the MTBF and a characteristic life of 11,000 - 12,000 hours. The lift arms MTBF is 8,000 - 9,000 hours with a β value of 1.53.

For the lift arms this is relatively comparable to the 80 ton class. The 75 ton rear frame showed the closest results with the 80 ton class wheel loaders with a β value of 2.04 and a component life range of 10,000 - 11,000 hours.

Table 5.11. Weibull Results Summary for 80 ton Wheel Loaders Class

80 ton Class WL

Structural Component	# of Cases	MTBF	Beta	Characteristic Life	R ²
Front Frame	4	8,738	1.1437	9,181	0.971
Rear Frame	9	12,217	2.1528	13,795	0.9355
Rear Axle	7	6,572	1.6789	7,356	0.9788
Lift Arm	6	14,126	1.3153	15,332	0.8034
Bellcrank (LH)	4	11,556	2.6110	13,006	0.8398
Bellcrank (RH)	2	17,446			
	32	10,538	1.7565	11,834	0.9687

Table 5.12. Weibull Results Summary for 75 Ton Wheel Loaders Class

75 Ton Class WL

Structural Component	# of Cases	MTBF	Beta	Characteristic Life	R ²
Front Frame	1	15,714			
Rear Frame	25	9,990	2.0435	11,276	0.9348
Rear Axle	21	11,016	1.7519	12,370	0.9469
Lift Arm	45	8,159	1.5317	9,065	0.9516
Bellcrank (LH)	2	2,779			
Bellcrank (RH)	1	3,374			
	95	8,529	1.5561	9,491	0.9620

5.3.4. Step 4: Perform Standard Weibull Analysis of Structural Component

Failure Cases. The next step compared the component operating dates and failure dates/ time periods of the structural cases in Step 2 against the production data / time periods used in Section 3 to identify cases where structural component failures coincided with production data. The structural failure cases which overlapped both time periods were then selected for further analysis. These cases were rerun against the production databased in order to calculate the number of bucket loads, cycle time, and productivity for each of the failure cases. Each of the performance variables was further separated and analyzed by its bucket load type (underload, target load, and overload). A review of the structural cases for which there were both structural and production data is shown in Table 5.13. Only two of the wheel loader classes, 55 and 80 ton, had a sufficient number of cases to proceed with further analysis.

Table 5.13. Number of Structural Cases by Wheel Loader Class

Wheel Loader	# Cases
55 ton class	5
60 ton class	0
75 ton class	2
80 ton class	17

The Weibull analysis results for the 55 ton and 80 ton class wheel loaders are shown in Tables 5.14 and 5.15. Furthermore, two of the 80 ton class wheel loaders had enough data to perform individual Weibull analyses on these loaders. The 75 ton class

wheel loader presented only two cases covering the two datasets, while the 60 ton class wheel loader had no cases in common.

Table 5.14. 55 Ton Wheel Loader Class Weibull Results - Structural Cases

Wheel Loader	# of Cases	MTBF	Beta	Characteristic Life (hrs) Eta	R ²
6011	1	Insufficient data			
6012	1	Insufficient data			
6013	1	Insufficient data			
6014	0	Insufficient data			
6015	0	Insufficient data			
6016	2	Insufficient data			
6017	No cases found				
6018	No cases found				
TOTAL	5	1,212	2.2782	1,369	0.8464

The 55 ton class wheel loader analysis resulted in an MTBF of 1,212 hours, a characteristic life of 1,369 hours, and a β of 2.2782. The β value of 2.2782 indicates early wear-out failures of the 55 ton classes structural components (Meridium, 2015).

Table 5.15. 80 Ton Wheel Loader Class Weibull Results - Structural Cases

Wheel Loader	# of Cases	MTBF	Beta	Characteristic Life (hrs) Eta	R ²
8001	3	Insufficient data			
8002	7	1,186	2.1069	1,339	0.8623
8003	5	1,052	0.6460	1,216	0.9177
8004	0	Insufficient data			
8005	2	Insufficient data			
TOTAL	17	1,410	0.8510	1,294	0.9552

The 80 ton class wheel loaders analysis shows infant mortality failures for the fleet with a β value of 0.8510 (Table 5.15). This is also indicated by the characteristic life being lower than the MTBF at 1,186 hours and 1,052 hours respectively. Loaders 8002 and 8003 had sufficient cases to run Weibull analysis on the individual loaders. Loader 8002's MTBF was 1,186 hours and its characteristic life was 1,339 hours which produced a β of 2.1069 indicating an early wear-out failure pattern. Loader 8003 analysis produced a β of 0.6460, infant mortality failure with the MTBF and characteristic life values of 1,052 hours and 1,216 hours, respectively.

5.3.5. Step 5: Duty-Cycle Reliability Analysis. The overlapping cases' data examined to determine the severity of use, or the duty-cycle to which the wheel loader is being subjected to during the course of normal operations. The duty-cycle depends on the life stress relationship (LSR) of the wheel loader of the component being examined. Linear LSR was assumed to be the duty-cycle with the ratio of the load on the component. The duty-cycle can be expressed as the ratio of load on the component (V_2) to the rated load (V_1), which is shown in Equation 5.1 (Reliability HotWire, 2017).

$$d_c = V_2 / V_1 \quad (5.1)$$

The duty-cycle for each wheel loader was calculated in three categories: underloads and target loads together, overloads, and all loads. The recorded bucket weights were totaled (total production during the time between failures) and divided by the product of number of bucket loads and the designed bucket weight (i.e., the estimated production if each wheel loader excavated the rated payload for each cycle). Underloads and target load were combined because these loads did not exceed the design bucket

weight, thus returning values less than one. The overloads exceeded the design target and returned values greater than one. The results of the duty-cycle analysis can be seen in Tables 5.16 and 5.17 for the 55 ton and 80 ton class wheel loaders.

The last column in both Tables 5.16 and 5.17 shows the ratio of all loads for each given class compared against themselves. The wheel loader with the highest duty-cycle was set to 1.0000 and all remaining duty-cycle values were compared against this machine to produce their ratios (Hudak, 2011). Loader 6012 set as the hardest duty-cycle in the 55 ton class wheel loader group operates in a copper mine, while the other three loaders all work in coal mines. The four wheel loaders comprising the 80 ton class group all work in iron mines.

Table 5.16. 55 Ton Wheel Loader Class Duty-Cycle Based on Maximum Payload

Wheel Loader	Underloads / Target Loads (V_2 / V_1)	Overloads (V_2 / V_1)	All Loads (V_2 / V_1)	All Load Ratio (Top)
6011	0.7491	1.1823	0.7580	0.9322
6012	0.7974	1.1134	0.8131	1.0000
6013	0.6378	1.1051	0.6382	0.7849
6014				
6015				
6016	0.6135	1.2226	0.6143	0.7555
6017				
6018				
55 ton class	0.6817	1.1393	0.6822	0.8390

Table 5.17. 80 Ton Wheel Loader Class Duty-Cycle Based on Maximum Payload

Wheel Loader	Underloads / Target Loads (V2 / V1)	Overloads (V2 / V1)	All Loads (V2 / V1)	All Load Ratio (Top)
8001	0.7694	1.1657	0.8173	1.0000
8002	0.7294	1.147	0.7338	0.8978
8003	0.6912	1.1237	0.7468	0.9137
8004				
8005	0.7431	1.1209	0.7457	0.9124
80 ton class	0.7314	1.1463	0.7475	0.8978

5.3.6. Step 6: Perform Weibull Analysis Based on Duty-Cycle for Structural Component Failure Cases. The wheel loader duty-cycle ratio computed in the previous step was used to adjust the failure hours for each structural component case in Step 4. In other words, each time between failure is adjusted by using the duty-cycle values as a weighting factor per Equation 5.2. These new times between failure data points were used to run a second Weibull analysis for comparison. The results of the second Weibull analysis that account for the duty-cycle are shown in Tables 5.18 and 5.19.

$$t' = \frac{V_2}{V_1} t \quad (5.2)$$

The 55 ton class wheel loader results shows an MTBF of 1,054 hours and a characteristic life of 1,189 hours. Both the hours for the MTBF and characteristic life values are lower than the standard Weibull. This was expected due to the “All Load” ratio reducing the hours at failure in the calculation. The β value of 1.9697 decreased

from the previous analysis, but it still indicates early wear-out failures of the 55 ton classes structural components.

Table 5.18. 55 Ton Wheel Loader Class Duty-Cycle Weibull Results - Structural Cases

Wheel Loader	# of Cases	MTBF	Beta	Characteristic Life (hrs)	Eta	R ²
6011	1	Insufficient data				
6012	1	Insufficient data				
6013	1	Insufficient data				
6014	0	Insufficient data				
6015	0	Insufficient data				
6016	2	Insufficient data				
6017	No cases found					
6018	No cases found					
TOTAL	5	1,054	1.9697	1,189		0.9384

Table 5.19. 80 Ton Wheel Loader Class Duty Cycle Weibull Results - Structural Cases

Wheel Loader	# of Cases	MTBF	Beta	Characteristic Life (hrs)	Eta	R ²
8001	3	Insufficient data				
8002	7	1,065	2.1063	1,203		0.8624
8003	5	961	0.6455	1,111		0.9176
8004	0	Insufficient data				
8005	2	Insufficient data				
TOTAL	17	1,442	0.8907	1,365		0.9578

The 80 ton class wheel loaders' Weibull analysis based on duty-cycle still shows premature mortality failures for the fleet with a β value of 0.8907. The β value increased over the prior analysis presented in Step 4. This is also indicated by the characteristic life

being lower than the MTBF which is 1,442 hours and 1,365 hours respectively. Loader 8002's MTBF was 1,065 hours and its characteristic life was 1,203 hours, which produced a β of 2.1063 indicating an early wear-out failure pattern (Meridium, 2015). Loader 8003's analysis produced a β of 0.6455 with its infant mortality failure having an MTBF and characteristic life of 961 hours and 1,111 hours, respectively.

The results of the 80 ton wheel loader fleet and the individual machines show a tightening up of the results. This appears to be the result of applying the duty-cycle ratio. The β value for the fleet increased slightly by 0.0400 over the standard Weibull analysis β value. The individual loaders saw no significant change in their β values between the two separate Weibull analyses.

5.3.7. Step 7: Comparing the Standard and Duty-Cycle Weibull Analysis

Results. The last step of the process was to compare the results of both Weibull analyses to determine whether accounting for payload in the Weibull analyses improves the predictive power of the model. Weibull analysis can be compared based on their slope, "R²" value or Weibull modulus (Hudak, 2011). The 55 ton and 80 ton class wheel loader results are summarized in Tables 5.20 and 5.21 from Section 5.3.4 (Step 4) and 5.3.6 (Step 6). The 55 ton class wheel loader fleet shows a significant improvement with an increase of 0.0920 from a R² value of 0.8464 for the standard Weibull analysis to a R² value of 0.9384 from the duty-cycle based Weibull analysis. The 80 ton class wheel loader fleet R² results were 0.9552 for the standard Weibull analysis and 0.9578 on the duty-cycle based Weibull analysis, and improvement of 0.0026.

The results from the two 80 ton class wheel loaders, Loader 8002 and Loader 8003, show no difference in the Weibull R^2 values with both loaders results being within 0.0001 of each other. These loader results are shown in Table 5.22.

Table 5.20. 55 Ton Class Structural Cases Weibull Results - Comparison

Weibull Summary Results 55 Ton Class Wheel Loaders

	MTBF	Beta	Characteristic Life (hrs) Eta	R^2
Standard	1,212	2.2782	1,369	0.8464
Duty-Cycle	1,054	1.9697	1,189	0.9384

Table 5.21. 80 Ton Class Structural Cases Weibull Results - Comparison

Weibull Summary Results 80 Ton Class Wheel Loaders

	MTBF	Beta	Characteristic Life (hrs) Eta	R^2
Standard	1,410	0.8510	1,294	0.9552
Duty-Cycle (Top Down)	1,442	0.8907	1,365	0.9578

The higher R^2 values indicate that the Weibull distribution parameters determined by accounting for duty-cycle (based on payloads) provide a better fit to the observed time between failures than those parameters determined without regard to the duty-cycles. This confirms the research hypothesis that accounting for overloading (how hard the machine is worked with higher payloads) will lead to better predictions of failures.

Table 5.22. Individual 80 Ton Class Structural Cases
Weibull Results - Comparison

Weibull Summary Results Loader 8002

	MTBF	Beta	Characteristic Life (hrs) Eta	R ²
Standard	1,186	2.1069	1,339	0.8623
Duty-Cycle (Top Down)	1,065	2.1063	1,203	0.8624

Weibull Summary Results Loader 8003

	MTBF	Beta	Characteristic Life (hrs) Eta	R ²
Standard	1,052	0.6460	1,294	0.9177
Duty-Cycle (Top Down)	961	0.6455	1,111	0.9176

5.4. DISCUSSIONS

This examination of the global ultra-class wheel loaders' fleet structural component failure cases along with the subgroup of cases with additional production data sought to determine the severity of the wheel loaders duty-cycle and to show a general relationship between that and the reliability analysis. This highlighted subgroup of data illustrates the standard and the duty-cycle based Weibull distribution failure analysis between these groups. The results of the standard Weibull and the duty-cycle Weibull analysis were similar. The duty-cycle Weibull analysis showed an improvement in the slope modulus (R²) for both the 55 ton class and the 80 ton class wheel loader fleets. The limited number of cases and test samples in the subgroup is an area of concern. Additional samples added to the analysis (when available,) may significantly influence

the results. Additionally, several other factors may be influencing the results and causing variances in the reported data. These factors include operator skill, wheel loader / component manufacture, frequency of the wheel loader structural inspections, the maintenance and the repair operations of the wheel loader, and the application, and site / working conditions, such as pit geology, blasting relating to floor conditions and fragmentation of the pile, weather, road conditions and pit floor maintenance, etc.)

The complete OEM fleets reliability analysis results of the wheel loader fleets' structural components indicate that there may be random linear to early wear-out failure patterns for all of the components except for the rear frame of the 55 ton class machines. The Weibull β values for individual structural components ranged from 1.1710 to 2.1422. The failure pattern for the 55 ton class wheel loader rear frames was rapid wear-out failures based on a Weibull β value of 4.5196 with a failure time window occurring from 10,000 -14,000 hours.

5.4.1. Effect of Payloads on the Reliability of Structural Components.

Examination of the reliability analysis assessing the effect of duty-cycles on the performance of the structural components demonstrated mixed results in the fleet analyses. Two wheel loader fleets, 55 ton and 80 ton class machines, had sufficient data to perform duty-cycle reliability analysis. The results showed that both of these fleets had significantly reduced MTBF compared to the respective OEM fleet analyses. The 55 ton class wheel loaders' duty-cycle effected analysis had an MTBF of 1,212 hours between failures versus the OEM fleet average of 14,258 hours. The 80 ton class wheel loaders duty-cycle studied had an MTBF of 1,410 hours compared to the OEM fleet value of 10,538 hours. The β values results were also mixed for both fleets. The 55 ton class wheel loader's β value increased from 1.5608 (OEM) for the fleet to 2.2782 for the duty-

cycle based results. The 80 ton class wheel loaders β values decrease from 1.7565, early wear-out failure patterns in the OEM fleet to infant mortality failures with a β value of 0.8510 in the duty-cycle based analysis. Based on the OEM structural component failure data and duty-cycles, these results give the impression that the duty-cycle wheel loader samples were less reliable compared to the entire OEM fleet. The limited number of test samples (22) and the short time duration (i.e., less than one year) could be affecting the results.

5.4.2. Effect of Accounting for Payload Duty-Cycle on the Reliability of Structural Components. The duty-cycle analyses for both the 55 ton and the 80 ton class wheel loaders were adjusted by applying a duty-cycle ratio as a weighting factor to account for increased (overloading) loading of the machines. The 55 ton and 80 ton wheel loader classes results show that applying the ratio to the failure hours linearized the failure rates predicted by the Weibull analysis. The Weibull results for both wheel loader classes had their respective β values approaching a β value of 1, a linear failure rate. The 55 ton class wheel loader's β values are decreasing towards a β value of 1, while the 80 ton wheel loader class machines β values were increasing to the linear β value.

The Weibull results for the 55 ton and 80 ton class wheel loaders were mixed based on adding duty-cycle ratio comparison. The results of the 55 ton class wheel loaders showed a decrease in MTBF from 1,212 hours to 1,054 hours for adjusted duty-cycle ratio comparison, with the β value decreasing from 2.2782 to 1.9697, respectively. The 80 ton class wheel loaders MTBF results increased from 1,410 hours to 1,442 hours for the duty-cycle ratio tests. The β values for the tests also increased from 0.8510 to 0.8907 for the duty-cycle ratio tests.

The ability to determine the wheel loaders' duty-cycle ratio allows for better maintenance planning by adjusting the structural components inspection interval from a one-size fits all approach to a customized approach based on the wheel loaders duty-cycle. The ability to split out sections of the structural inspections by structural component allows us to gather data on these sections to plan repair actions before failure (see the Point-Failure curve), but eliminate recreational maintenance (Collis, 2017) items, where no changes are occurring over the inspection interval. This allows the ability to plan tasks; that is, schedule repair crews and parts, while decreasing the number of machine down hours required for maintenance inspections which allows for additional availability / production time.

This research into the severity of use of the structural components could be extended to additional equipment systems such as hydraulic cylinders and circuits and drive line components. These systems are designed based on the wheel loader's target load to cycle a number of times per hour (e.g., every 45 seconds for a hoist cylinder or 80 times per hour or to be utilized at a specified duty-cycle, the engine operates above 1,650 rpm 45- 55% of the time). This analysis of the equipment's duty-cycle evaluates how severely the machine is being operated (above, below, or within its design parameters). The equipment duty-cycle detail brings an added dimension to the reliability analysis and provides additional context to the analysis based on current delineations by model, configuration, region, and commodity being handled.

Additionally, this allows the ability to evaluate reliability centered maintenance (RCM) plans to revise the individual tasks or adjust individual intervals to keep the programs optimized for the plans or groups based on the schedule. Also, this provides a

means to re-evaluate these systems and adjust the maintenance hours or the tasks to maximize operating hours and minimize downtime. The analysis results can point to other RCM plans, bringing in new engineering solutions to modify or redesign components / systems to extend life expectancy and simplify maintenance tasks and reduce maintenance time thus improving machine availability.

5.4.3. Analysis Limitations. There are certain limitations to this analysis. These include the fact that the analysis does not explicitly account for all the structural repairs for each of the wheel loaders in the study. A majority of the structural cases presented were factory involved repairs. As such this level of repairs provides additional procedural controls, observations, and documentation. Regional or mine level repairs may have been done to allow the wheel loader to operate until such a time proper repairs were possible. Additionally, the analysis does not overtly account for the effect of the type of commodity the loaders operate in, operator skill, bucket configuration, or application due to the limited samples. Any or all of these components could complicate the relationship between overloading the bucket and the failure of any of the structural components.

However, the candidate believes these factors actually work to reinforce his conclusions in this section as they strengthen the connection between overloading and structural component failures. Hence, accounting for these factors will only make the conclusions of this study stronger.

5.5. SUMMARY

This research effort presents a methodology to account for wheel loader overloading (duty-cycles) into structural component reliability analysis. The case study of 8 wheel loaders, four 55 ton and four 80 ton class machines, structural component

failures comprising over 20 cases was examined to determine the effects of adding the duty-cycle to the analysis. The results of Weibull analysis on these two methods show an improvement in the predictive power of the models.

Based on the results of the eight wheel loaders reviewed, the following general conclusions can be drawn:

- The Weibull shape modulus for the standard analysis and the duty-cycle based analysis showed little variance. The failure method expressed by the shape of the Weibull distribution for the standard analysis was repeated in the duty-cycle based Weibull analysis.
- Applying the duty-cycle ratio to the failure hours linearized the data for the Weibull analysis. This is shown in the β value of the 55 ton class wheel loaders decreasing while it increased in the 80 ton class wheel loaders. The results of both wheel loader classes are approaching a β value of a linear failure rate of 1.
- The accuracy of the duty-cycle based Weibull analysis was increased over the standard analysis for both the 55 ton and the 80 ton class wheel loaders as shown in the R^2 , the slope variable of the Weibull plot.

The candidate makes the following recommendations for future work, which could improve and increase the body of knowledge in this area:

- Conduct a similar study with more extensive datasets to evaluate whether these conclusions to hold true with more extensive data.

- Use cumulative damage models analysis to study the effect of ever increasing overload cycles and determine if their effects on the reliability can be quantified (Weibull, 2012).
- Study the use of accelerated life tests and life models on the structural components in order to determine the differences in overstressing the machine by progressive stress, cyclic stress and / or random stress in order to reduce the failure threshold (Pulido, 2015) and move the failure models' curves to long - duration constant failure modes.
- Look at changing the Weibull analysis time parameter from hours to bucket loads and specifically bucket overloads.

6. CONCLUSIONS AND RECOMMENDATIONS FOR FUTURE WORK

6.1. SUMMARY

A wheel loader's productivity is affected by multiple factors including its working conditions, the operator's skill level, and the health of the machine. The operator's skill and practices affect the material weight handled and the machine's cycle time, which in turn controls the machine's productivity. The bucket weight and the cycle time may each influence the wheel loader's performance independent of the other.

This research examined the effect of overloading the bucket on a wheel loader's productivity and its reliability through tracking the total number of bucket overloads and the failure of the wheel loader's structural components. These bucket overloads (excessive duty-cycle) contribute to premature aging and wear of a wheel loader's structural components. The long lives of the wheel loader's structural components and the limited fleet size was challenging to this research. This research provides a basis to update RCM plans based on the likelihood of a structural component failure and encourage replacement prior to failure.

The goal of this research was to determine the effect of overloading the wheel loader's bucket on the machine's productivity and reliability. In accordance with the overall goal of this research, the specific objectives were:

1. Examine the effect of overloading the bucket on wheel loader productivity.
2. Examine the effect of overloading the bucket on forces exerted on a wheel loader.
3. Investigate the effect of overloading the bucket on the reliability of the structural components of a wheel loader.

The first objective determined the productivity of the wheel loader and discovered the amount of overloading which is occurring in the global fleet of a major OEM. The wheel loader classes were also compared against their OEM specified operating parameters. The candidate used an ANOVA test to investigate the hypothesis that bucket payload class (underloaded, target and over load) had a significant impact on cycle time and productivity.

The second objective examined the effect of payload on the forces placed on the wheel loader by examining its hydraulic system, (i.e., the hoist cylinder pressures). Again, the candidate collected data and examined Spearman and Pearson correlations to check test the hypothesis that payload was correlated to the hoist cylinder pressures.

The final objective was achieved by first establishing the reliability of the structural components for the global fleet using a standard Weibull analysis. Second, the case study's fleet Weibull analysis dataset hours were adjusted based on each wheel loader's duty-cycle (based on payloads), and the Weibull analysis was run again to show the effect of the duty-cycle on the structural components reliability.

6.2. CONCLUSIONS

Based on the work done in this dissertation several conclusions are drawn:

1. With respect to the first objective (evaluate the effect of overloading the bucket on wheel loader productivity):
 - a. The evidence in support of the hypothesis that higher payloads lead to slower loading rate (higher cycle times) is not as clear as that in support of the hypothesis that higher payloads lead to higher productivity.

- b. The analysis in this dissertation confirms the operators' general belief that they can produce more if the bucket is overloaded. However, the analysis also shows that overloading the bucket slows down the loading rate and is detrimental to productivity in that regard.
 - c. Overloading the bucket itself was not a major issue in any of the wheel loader fleets considered in this work. Most of the wheel loaders (14 of 20 or seventy percent) were being underloaded.
 - d. Half of the wheel loaders were operating within the machine's target cycle time. The wheel loaders' bucket cycle time shows it has a secondary impact on the machine's productivity. The bucket weight and the cycle time are independent of each other.
2. With respect to the second objective (examine the effect of overloading the bucket on forces exerted on a wheel loader):
 - a. The work shows that the maximum hoist pressure during the wheel loader cycle increases as the bucket weight increases.
 - b. The majority of the hoist circuit pressure readings were within the expected operating ranges for the bucket loads lifted. However, the machines in the study appear to be operating in the upper range of the expected hoist cylinder pressures.
3. With respect to the third objective (investigate the effect of overloading the bucket on the reliability of the structural components of a wheel loader):
 - a. The Weibull shape modulus for both the standard analysis and the duty-cycle based analysis showed little variance. The failure method

expressed by the shape of the Weibull distribution for the standard analysis was repeated in the duty-cycle based Weibull analysis.

- b. The effect of applying the duty-cycle ratio to the failure hours linearized the data for the Weibull analysis. This is shown in the β value of the 55 ton class wheel loaders decreasing while it increased in the 80 ton class wheel loaders. The results of both wheel loader classes are approaching a β value of a linear failure rate of 1.
- c. The accuracy of the duty-cycle based Weibull analysis was increased over the standard analysis for both the 55 ton and 80 ton class wheel loaders as shown in the R^2 of the slope variable of the Weibull plot.

6.3. CONTRIBUTION OF THE PHD RESEARCH

The results of this research advance the understanding of the wheel loader maintenance and reliability by using empirical equipment generated performance data in conjunction with maintenance data to understand structural component lives. The goal of this research was to increase wheel loader productivity and structural component lives by emphasizing the effects of overloading the bucket and focus operations towards the use of proper operational techniques. The research: (i) expands the research frontier by furthering our understanding of the effect of overloading on the reliability and the productivity of a wheel loader's structural components; and (ii) contributes to mining engineering in relation to optimization of maintenance practices for wheel loaders. The research results will be broadly disseminated to facilitate its adoption in industry and further research based on these findings.

6.3.1. Expansion of Research Frontier. This research has expanded our understanding of the effect of overloading the wheel loader's bucket on productivity and the effect of this excessive duty-cycle of the machine's structural component lives. This research confirmed the hypothesis that higher bucket payloads lead to a slower loading rate (high bucket cycle times) and the general belief that the loader will be more productive if the bucket is overloaded.

Correlations showing the connection between hydraulic system pressures presented and wheel loader payload do not exist in the literature. This research shows the expected result that the hydraulic pressure increases to lift greater bucket weights. While the hoist cylinder hydraulic pressure reading was still in the operating range, it was in the higher end of the range. The results presented were for a handful of wheel loader all of one class. However, they show the existence of such correlation and should prompt further studies with more wheel loaders and wheel loaders in other operating classes. Additionally, other studies examining the duty-cycle of the hydraulic cylinders would be beneficial in determining if other components (cylinder or drive components) show the same correlation. These would serve as better indicators to accelerate maintenance activities based on harder duty-cycle usage.

6.3.2. Contributions to Mining Engineering Practices. Mining engineering practices should see two primary areas for improvement maintenance plans based on multiple data inputs (i.e., machines / component hours and machine cycles / duty-cycles), and operating training / follow-up / retraining. The failure of a structural component leads to lengthy and costly repairs. The ability to understand the wheel loader's duty-cycle is primary to determine usage based on application and an operator's skill level. The ability

to add in a secondary measure, (i.e., duty-cycle) to establish, confirm, and validate inspection and maintenance intervals is paramount to improving the overall maintenance plan. Knowledge and understanding of the wheel loader's duty-cycle allows for the customization of the wheel loader's reliability centered maintenance (RCM) plan. This includes the ability to adopt individual maintenance plans for the mine and even down to the machine level. In the future, constant monitoring of the duty-cycle may also lead to refining the plan based on changes to the duty-cycle in addition to time based reviews. This new approach may conceivably lead to additional improvements in maintenance department operations with a more proactive approach to equipment health monitoring.

The other main contribution involves training of the equipment operators. Operator training, evaluation, and re / follow-up training focusing training resources to improve operator training / retraining to a more consistent loading of the bucket, including reinforcing general housekeeping at the working face and mine site. This technique will incorporate using performance metrics to evaluate operator productivity (Awuah-Offei, 2016) and the effect that bucket overloading has on overall equipment health. This research assimilates the ability to link unhealthy operations practices (bucket overloading) to increases in downtime and repair costs, through shortened structural component rebuild and the replacement lives with expansion of this concept to encompass the complete wheel loader.

6.3.3. Dissemination of Research Results. The results from this research will be disseminated to relevant peer groups within Komatsu Mining Corp., specifically the Wheel loader Engineering and Product Support Groups. Additionally, the results may be used by the Life-Cycle Management (LCM) groups to update component lives in fleet

management contracts. The information will be used to update RCM plans and as discussion points for future RCM workshops. There are plans to publish in the future to encourage better maintenance plans and repair activities with customers and with the industry. Additionally, there are opportunities to continue this research with additional follow on / follow-up equipment and maintenance research opportunities to advance the results presented in this dissertation.

6.4. FUTURE WORK

The following recommendations for future work have the capability to improve and to add to the body of knowledge from this research:

1. This research should be continued in order to track the studied fleet of wheel loaders and to add data from other machines in the current fleet and future OEM builds. The results of these additions will allow a better understanding of how wheel loader payloads (duty cycle) affects the structural reliability of a wheel loader.
2. This research project should be expanded to include other wheel loader systems, i.e., major components, hydraulics, and other systems. Similar methodology would be used to compare how overloading the wheel loader affects the reliability of these components and systems. Further analysis should examine the usefulness of the wheel loader's duty-cycle to supplement time-based maintenance intervals.
3. Further research should develop and incorporate this process into an IPSECA workflow model, and the research results shared with design engineers. This

will facilitate updated / new designs to increase the target lives of the structural components.

4. This research project should be expanded to examine the relationships between productivity and structural component lives, presented in this dissertation, to other loading tools, (i.e., electric cable shovels, draglines, and hydraulic excavators).
5. In the longer term, further research should attempt to develop rigorous parametric and non-parametric reliability models for mining loading equipment which directly accounts for the duty cycle. For example, such work could follow the example of Adekpedjou, et al. (2010) who formulated models for hospital visits (same as machine breakdowns) where the nature of previous visits are incorporated into estimates of the next visit. The analogy here is that the equipment history (beyond the time between failures), such as the history of overloads, can be incorporated into the reliability.

BIBLIOGRAPHY

1. Abdi Oskouei, M., & Awuah-Offei, K. (2015), A method for data-driven evaluation of operator impact on energy efficiency of digging machines, *Energy Efficiency*, 1-12. <https://doi.org/10.1007/s12053-015-9353-3>.
2. Adekpedjou, A., Peña, E. A., & Quiton, J. (2010), Estimation and efficiency with recurrent event data under informative monitoring, *Journal of statistical planning and inference*, 140(3), 597-615.
3. Akgü.; F., Senoğlu, B., & Arslan, T. (2016) An alternative distribution to Weibull for modeling the wind speed data: Inverse Weibull distribution, *Energy Conversion and Management*, 114 (2016) 234-240, <http://dx.do.org/10.1016/j.enconman.2016.02.026> 0196-8904/.
4. Akhavian, R. (2013), Simulation-Based Evaluation of Fuel Consumption in Heavy Construction Projects by Monitoring Equipment Idle Times, *Proceedings of the 2013 Winter Simulation Conference*, IEEE, pp. 3098-3108.
5. Allen, F., Hawkes, P., & Noy, M. (1999), "Bucket Fill Factors - A Laboratory and Field Study with Implications for Blasting," *"Explo '99"* Kalgoorlie, WA, pp. 43-46.
6. Allison, L. (2017), The Arizona Geological Survey, http://www.azgs.az.gov/minerals_kingcopper.shtml.
7. Australian Government - Geoscience Australia (2017), <http://www.ga.gov.au/scientific-topics/energy/province-sedimentary-basin-geology/petroleum/onshore-australia/bowen-basin#heading-2>, May 2017.
8. Awuah-Offei, K. (2016), Energy efficiency in mining: A review with emphasis on the role of operators in loading and hauling operations. *Journal of Cleaner Production*, pp. 89-97. Elsevier Ltd. <https://doi.org/10.1016/j.jclepro.2016.01.035>.
9. Awuah-Offei, K., & Frimpong, S. (2011), Efficient Cable Shovel Excavation in Surface Mines. *Geotechnical and Geological Engineering*, 29(1), 19-26. [https://doi.org/10.1007/.](https://doi.org/10.1007/)
10. Awuah-Offei, K., & Frimpong, S. (2007), Cable shovel digging optimization for energy efficiency, *Mechanism and Machine Theory*, 42, 995-1006, <https://doi.org/10.1016/j.mechmachtheory.2006.07.008>.

11. Awuah-Offei, K., & Frimpong, S. (2011), Efficient Cable Shovel Excavation in Surface Mines. *Geotechnical and Geological Engineering*, 29(1), 19-26, <https://doi.org/10.1007/>.
12. Awuah-Offei, K., Frimpong, S., & Askari-Nasab, H. (2009), Formation excavation resistance modelling for shovel dippers, *International Journal of Mining and Mineral Engineering*, 1(2), 127-146, <https://doi.org/10.1504/ijmme.2009.023131>.
13. Barabadi, A. (2013), Reliability model selection and validation using Weibull probability plot- A case study *Electric Power Systems Research*, 101, 96-101.
14. Barksdale, R. D. (1996), The Aggregate Handbook, National Stone Association, Washington D. C., USA, pp. 7-16 - 7-21.
15. Baqerin, M. H., Shafahi, Y., & Kashani, H. (2016), “Application of Weibull Analysis to Evaluate and Forecast Schedule Performance in Repetitive Projects,” *Journal of Construction Engineering Management*.
16. Barabady, J., & Kumar, U. (2007), Reliability analysis of mining equipment: A case study of a crushing plant at Jajarm Bauxite Mine in Iran, *Reliability engineering & System Safety*, 93(4), 647-653.
17. Beganovic, N., & Söffker, D. (2017), Remaining lifetime modeling using State-of-Health estimation, *Mechanical Systems and Signal Processing*, 92 (2017) 107-123.
18. Bise, C. (1992), Chapter 12.8, “Equipment Maintenance”, pp. 1260, Hartman, H. (1992), SME Mining Engineering Handbook, Society of Mining, Metallurgy, and Exploration, Inc. Denver, CO.
19. Braasch, G. (2013), “The Daily Climate,” www.scientificamerican.com. December 9, 2013.
20. Bundy, E. (1988), “Optimum Design Basis of Digging Equipment of Earth Moving Machines on Example of a Backhoe Attachment”, Institute of Building Mechanization and Rock Mining, Warsaw, Poland, pp. 387-396.
21. Cassanelli, G., Mura, G. Fantini, F, Vanzi, & Plano, B. (2006), Failure Analysis-assisted FMEA, *Mircoelectronics Reliability* 46 (2006) 1795-1799, Doi:10.1016/j.microrel.2006.07.072.
22. Caterpillar Performance Handbook (1), (1996) (27th Edition), Caterpillar Inc., Peoria, Illinois, USA, pp 19-8.

23. Caterpillar Performance Handbook (2), (1996) (27th Edition), Caterpillar Inc., Peoria, Illinois, USA, pp 19-40.
24. Caterpillar Performance Handbook (3) (1996) (27th Edition), Caterpillar Inc., Peoria, Illinois, USA, pp 12-30 - 12-41.
25. Caterpillar Performance Handbook (1), (2014) (44th Edition), Caterpillar Inc., Peoria, Illinois, USA, pp. 23-11 & 23-12.
26. Caterpillar Performance Handbook (2), (2014) (44th Edition), Caterpillar Inc., Peoria, Illinois, USA, pp.7-38.
27. Caterpillar Performance Handbook (3), (2014) (44th Edition), Caterpillar Inc., Peoria, Illinois, USA, pp. 25-44 & 25-45.
28. Caterpillar Performance Handbook (4), (2014) (44th Edition), Caterpillar Inc., Peoria, Illinois, USA, pp. 23-222 - 23-224.
29. Caterpillar Performance Handbook (5), (2014) (44th Edition), Caterpillar Inc., Peoria, Illinois, USA, pp. 28-1.
30. Caterpillar Performance Handbook (6), (2014) (44th Edition), Caterpillar Inc., Peoria, Illinois, USA, pp. 25-3.
31. Caterpillar Aggregates Machine Applications (1998), "Job evaluation - Analysis," Caterpillar Inc., Peoria, Illinois.
32. Chanda, E. K., & Hardy, R. J. (2011), "Selection Criteria for Open Pit Production Equipment-Payload Distribution and the '10/10/20' Policy," *35th APCOM Symposium*, Wollongong, NSW, pp. 351-364.
33. Chok, N. S. (2010), Pearson's versus Spearman's and Kendall's correlation coefficients for continuous data (Doctoral dissertation), University of Pittsburgh.
34. Collis, H. (2017), Personnel Communication, March 23, 2017.
35. Colorado Geological Survey, Coal (2017), <http://coloradogeologicalsurvey.org/energy-resources/coal-2/how-does-it-form/>.
36. Colorado Geological Survey. Surface Mining (2017), <http://coloradogeologicalsurvey.org/energy-resources/coal-2/mining-methods/surface-mining/>.

37. Corbetta, M., Sbarufatti, C., Manes, A., & Giglio, M. (2014), Continuous crack growth monitoring and residual life prediction under variable-amplitude loading conditions, XVII International Colloquium on Mechanical Fatigue of Metals (ICMFM17), *Procedia Engineering* 74 (2014) 343-345.
38. Corbetta, M., Sbarufatti, C., Manes, A., & Giglio, M. (2015), Real-time prognosis of random loaded structures via Bayesian filtering, A preliminary discussion, *Engineering Fracture Mechanics*, 145, <https://doi.org/10.1016/j.engfracmech.2015.07.008>.
39. Corke, P., & Sukkarieh, S. (2006), "Tracts in Advanced Robotics", *Field and Service Robotics*, Springer, Germany, pp 592-602.
40. Das, K. (2008) A comparative study of exponential distribution vs Weibull distribution in machine reliability analysis in a CMS design, *Computers & Industrial Engineering*, 54(1), 12-33.
41. Debelec, C. (2014), "On Modelling of Bucket Oscillations for a Wheel Loader", *RJAV* vol XI issue 2/2014.
42. Dhillon, B. S. (2008), Mining equipment reliability, maintainability, and safety, Springer Science & Business Media.
43. Dubberly, J. (2017) *Personnel Communication*, June 15, 2017.
44. Fernando, S. (2011), "Large Mining truck - Truck Overload Policy "10/10/20," February 13, 2011.
45. Fine, J. (2017), *Personnel Communication*, June 20, 2017.
46. Fleet, M. (2017), *Personnel Communication*, May 21, 2017.
47. Fredriksson, G. & Larsson, H. (2012), An analysis of maintenance strategies and development of a model for strategy formulation - A case study, Master of Science Thesis, Department of Product and Production Development, Chalmers University of Technology, Göteborg, Sweden, 2012.
48. Frimpong, S., Hu, Y., & Awuah-Offei, K. (2005), Mechanics of cable shovel-formation interactions in surface mining excavations, *Journal of Terramechanics*, 42, 15-33, <https://doi.org/10.1016/j.jterra.2004.06.002>
49. Garvey, D. R., John, M., & Baumann, J. (2010), Nonparametric life consumption modeling of high end drilling tools, In *Proceedings - Annual Reliability and Maintainability Symposium*, <https://doi.org/10.1109/RAMS.2010.5448034>.

50. Gehloff, M. (2013), PF Curve 101 - Keeping it simple, The Maintenance Phoenix, Allied Reliability Group, October 2013.
51. George, M. (2003), Lean Six Sigma for Service, McGraw-Hill, New York, pp 286.
52. Grida, M., & Zaid, A. (2012), Optimization of Preventive Maintenance Interval, IEEE, 978-1-5090-5284-4/17.
53. Golbasi, O., & Deniral, N. (2015), "Investigation of stress in earthmover buckets using finite element analysis: a generic model for draglines," *The Journal of the Southern African Institute of Mining and Metallurgy*, 115(7), pp. 623-628.
54. GSWA (2017), Geological Survey of Western Australia, <http://www.dmp.wa.gov.au/Geological-Survey/Geology-of-Western-Australia-1389.aspx>.
55. Gui, J., & Li, H. (2005), "Penalized Cox regression analysis in the high-dimensional and low-sample size settings, with applications to microarray gene expression data," *Bioinformatics*, 21(13), pp. 3001-3008.
56. Gurganli, H. (2016), Personnel Communication February 24, 2016.
57. Hauke, J., & Kossowski, T. (2011), Comparison of values of Pearson's and Spearman's correlation coefficients on the same sets of data, *Quaestiones geographicae*, 30(2), 87.
58. Hartman, H. (1992) SME Mining Engineering Handbook, Society for Mining, Metallurgy, and Exploration, Littleton, CO, USA, 1992, pp.1327-1330.
59. Herberich, E., Sikorski, J., & Hothorn, T. (2010), "A Robust Procedure for Comparing Multiple Means under Heteroscedasticity in Unbalanced Designs," *PLOS ONE*, 5(3), e9788.
60. http://www.cat.com/en_US/support/maintenance/condition-monitoring.html. April 2017.
61. <http://www.joyglobal.com/services/life-cycle-management>. July 2017.
62. <http://www.joyglobal.com/search-results?indexCatalogue=site%2Dsearch&searchQuery=PreVail&wordsMode=0>. April 2017.

63. <http://milwaukeeecylinder.com>. November 2016.
64. <http://parkerbaymining.com/mining -equipment/wheel-loaders.htm>. July 2017.
65. <http://psych.unl.edu/psycrs/handcomp/hcspear.PDF>. March 2017
66. http://reliabilityanalyticstoolkit.appspot.com/weibull_production_future_number_of_failures. April 2017.
67. <https://statistical-research.com/wp-content/uploads/2012/09/kendall-tau1.pdf>, October 2017.
68. <http://www.statisticssolutions.com/correlation-pearson-kendall-spearman/>. March 2017.
69. Huang, W. (2013), "The Total Life-Cycle Management of Building Engineering Systems," Advanced Materials Research, ISSN: 1662-8985, Vols. 671-674, PP 3055-3058, Trans Tech Publications, Switzerland.
70. Hudak, D. and Tiryakioglu, M. (2011), "On Comparing the Shape Parameter of Two Weibull Distributions", *Materials Science and Engineering A*, v. 528, pp 8028-8030.
71. Hutton, A. (2009), "Geological Setting of Australasian Coal Deposits. In R," Kininmonth & E. Baafi (Eds.), *Australasian Coal Mining Practice* (pp. 40-84), 15-31 Pelham Street, Carlton Victoria 3053, The Australasian Institute of Mining and Metallurgy, pp 56-60.
72. Jafary, B, Nagaraju, V., & Fiondella (2017), Impact of Correlated Component Failure on Preventive Maintenance Policies, *IEEE Transactions on Reliability*, Vol. 66, No. 2, June 2017, pp. 575-586.
73. Joy Global, (1) (2016), P&H Wheel Loader LeTourneau - Series Service Manual, Longview, TX, USA, pp. 1-1-3.
74. Joy Global, (2) (2016), P&H Wheel Loader LeTourneau - Series Service Manual, Longview, TX, USA, pp. 2-1-35.
75. Joy Global, (3) (2016), P&H Wheel Loader LeTourneau - Series Service Manual, Longview, TX, USA, pp. 2-1-68.

76. Joy Global, (4) (2016), P&H Wheel Loader LeTourneau - Series Service Manual, Longview, TX, USA, pp. 6-4-1-2.
77. Keller, G., Warrack, B., & Bartel, H. (1994), Statistics for Management and Economics, Duxbury Press, Belmont, California, USA, pp. 669-673.
78. Komatsu Specifications and Applications Handbook (1), (1998) (19th Edition), Komatsu Ltd. Training & Materials Group, Product Support Group, pp 3A-93.
79. Komatsu Specifications and Applications Handbook (2), (1998) (19th Edition), Komatsu Ltd. Training & Materials Group, Product Support Group, pp 13A-7.
80. Komatsu Specifications and Applications Handbook (2009) (30th Edition), Komatsu Ltd. Training & Materials Group, Product Support Group.
81. Kolte, S. (2015), "Optimization of Loader Arm of Wheel Loading Shovel", International Journal of Engineering Research & Technology, Vol. 4 Issue 4, April, 2015.
82. Kong, Y. S., Omar, M. Z., Chua, L. B., & Abdullah, S (2014), "Fatigue life prediction of parabolic leaf spring under various road conditions," *Engineering Failure Analysis*, 46, 92-103.
83. Krupa, P. & Myers, J, (2004), Data Mining Root Cause Analysis Findings, IEEE, 978-1-509-5284-4-/17.
84. Lall, P., Mirza, K., Harsha, M., Suhling, J., & Goebel, K. (2013), Damage precursor based assessment of impact of high temperature storage on reliability of leadfree electronics, In *Proceedings - Electronic Components and Technology Conference*, <https://doi.org/10.1109/ECTC.2013.6575668>.
85. Li, Y, & Frimpong, S. (2008), Hybrid virtual prototype for analyzing cable shovel component stress, International Journal Advanced Manufacturing Technology (2008) 37:423-430, DOI 10.1007/s00170-007-0985-0.
86. Li, Y, Liu, W., and Frimpong, S. (2015), Compound mechanism modeling of wheel loader front-end kinematics for advance engineering simulation, International Journal Advanced Manufacturing Technology 78:341-349, DOI 10.1007/s00170-014-6640-7.

87. Lobo-Guerreo, A. (2008), "Geological Overview of the Carajas Mineral Province (Brazil) and its iron oxide-copper-gold mineralization," Geological Association of Canada and the Mineralogical Association of Canada, Quebec City, Quebec, Canada, May 2008.
88. Lowrie, Raymond L (2002), SME Mining Reference Handbook, Society for Mining, Metallurgy, and Exploration, Littleton, Colorado, pp. 383-385.
89. Luppens, J and Scott, D. (2013), "Assessment of the Coal Geology, Resources, and Reserve Base in the Powder River Basin, Wyoming and Montana," Fact Sheet 2012-3143, www.pubs.usgs.gov/fs/2012/3143/fs-2012-3143.pdf, U. S. Geological Survey, U. S. Department of the Interior, February 2013.
90. Ma, X, Wu, X, & Zhang (2014), Research on Maintenance Strategy of Coal Mining Vehicle Based on RCM, *Applied Mechanics and Materials*, Vols. 543-547 (2014) pp 126-129. Doi: 10.4028/www.scientific.net/AMM.542-547.126.
91. Maquez, A. (2005), "Modeling critical failures maintenance: a case study for mining," *Journal of Quality in Maintenance Engineering*, Vo. 11 No 4, 2005, pp. 301- 317.
92. Montenegro, I. & Lellis, M. (2003), "Planning and Modelling Maintenance Activities for High Effectiveness," *Mine Planning and Equipment Selection*, Kalgoorlie, WA. April 2003.
93. Mitchell, Z. (1998), A Statistical Analysis OF Construction Equipment Repair Costs using Field Data & The Cumulative Cost Model, Virginia Polytechnic Institute and State University, Blacksburg, VA, pp. 229-231.
94. Miziula, P. and Rychlik, T. (2014). "Sharp Bounds for Lifetime Variances of Reliability Systems With Exchangeable Components," *IEEE Transactions on Reliability*, Vol. 63, No.4, IEEE December 2014.
95. Morris, R. C. (1998), "BIF-hosted iron ore deposits - Hamersly style," *AGSO Journal of Australia Geology and Geophysics*, 17(4), 2017-11.
96. Moubray, J. (1), (1997), Reliability-centered Maintenance (2nd Edition), Industrial Press, New York, New York, pp. 6-16.
97. Moubray, J. (2), (1997), Reliability-centered Maintenance (2nd Edition), Industrial Press, New York, New York, pp. 16-18.

98. Moubray, J. (3), (1997), Reliability-centered Maintenance (2nd Edition), Industrial Press, New York, New York, pp. 163-165.
99. Moubray, J. (4), (1997), Reliability-centered Maintenance (2nd Edition), Industrial Press, New York, New York, pp. 77-80.
100. Moubray, J. (5), (1997), Reliability-centered Maintenance (2nd Edition), Industrial Press, New York, New York, pp. 241-243.
101. Multitrode (2008), "Maintenance Strategies: Predictive Maintenance vs "Run to Fail," September 2008.
102. Muhammad R., and Frimpong, S. (2013), "Cable Shovel Stress & Fatigue Failure Modeling - Causes and Solution Strategies Review", *Journal of Powder Metallurgy & Mining*, January 2013.
103. Napadow, G. (2013), Energy Study of Bucket Positioning Systems on Wheel Loaders, Division of Industrial Electrical Engineering and Automation Faculty of Engineering, Lund University.
104. Nordman, D.J., & Meeker, W. Q. (2002), "Weibull Prediction Intervals for a Future Number of Failures," *Technometrics*, 44, 1523.
105. Noppe, N., Iliopoulos, A., Weijtjens, W., & Devriendt, C. (2016), Full load estimation of an offshore wind turbine based on SCADA and accelerometer data, *Journal of Physics: Conference Series*, 753(7), <https://doi.org/10.1088/1742-6596/753/7/072025>.
106. Oskouei, M. A., & Awuah-Offei, K. (2014), Statistical methods for evaluating the effect of operators on energy efficiency of mining machines, *Mining Technology*, 123(4), 175-182, <https://doi.org/10.1179/1743286314Y.0000000067>.
107. Palczynska, A., Pesth, F., Gromala, P. J., Melz, T., & Mayer, D. (2014), Acquisition unit for in-situ stress measurements in smart electronic systems, In *2014 15th International Conference on Thermal, Mechanical and Multi-Physics Simulation and Experiments in Microelectronics and Microsystems, EuroSimE 2014*, <https://doi.org/10.1109/EuroSimE.2014.6813795>.
108. Pulido, J. (2015), Life Data Analysis Using the Competing Failure Modes Technique, *IEEE*, 978-1-4799-6703-2/15.

109. Rasimarzabadi, R., & Joseph, T. G. (2016), Particle flow mechanism into cable shovel dippers, *Journal of Terramechanics*, 64, 10-22, <https://doi.org/10.1016/j.jterra.2015.12.003>.
110. Raza, M. A. & Frimpong, S. (2013), "Cable Shovel Stress and & Fatigue Failure Modeling - Causes and Solution Strategies Review," *Journal of Powder Metallurgy & Mining*.
111. Reliability User Course #1503 (2015), Meridium, Inc., V3.6.0 DT-SQL, pp 55-58.
112. Reliability HotWire (2007), "Using Duty Cycle is System Reliability Analysis," Issue 74, April 2017.
113. Richter, Eric, Personnel Communication January 26, 2017.
114. Riddell, R. (2014), P-F Curve Reliability, www.sca.com, July 2017.
115. Rosiere, C. and Chemale Jr., F. (2000), "Brazilian iron formations and their geological settings," *Revista Brasileira de Geociencias*, January 2000.
116. Ross, J. R., and Vlok, P. J.(2015), *Lean Approaches in Asset Management Within the Mining Industry*, Springer International Publishing, Switzerland, pp. 101-118.
117. Roux, C. (2011), "Crafting a Reliability Strategy to Improve Equipment Uptime," *Engineering & Mining Journal*, November '11, pp. 129-131.
118. Rumsey, D. (2009), Statistics II for Dummies, Wiley Publishing, Inc., Indianapolis, Indiana, USA, pp. 58-60.
119. Ryan, J. (2016), Personnel Communication, January 31, 2017.
120. Saderova, J. & Bindzar, P. (2014), "Using a model to approach the process of loading and unloading of mining output at a quarry", *Gospodarka Surowcami Mineralnym - Mineral Resources Management*, Vol. 30 Issue 4, pp. 97-112.
121. SAE Handbook (1), (1998), Society of Automotive Engineers, Volume 3 On-Highway Vehicles and Off-Highway Machinery, Standards Development Program, Warrendale, PA, pp 40.90 to 40.92.
122. SAE Handbook (2), (1998), Society of Automotive Engineers, Volume 3 On-Highway Vehicles and Off-Highway Machinery, Standards Development Program, Warrendale, PA, pp 40.130 to 40.131.

123. SAE Handbook (3), (1998), Society of Automotive Engineers, Volume 3 On-Highway Vehicles and Off-Highway Machinery, Standards Development Program, Warrendale, PA, pp 40.422 to 40.424.
124. Samanta, B., Sarkar, B., and Mukherjee, S. (2004), Reliability modelling and performance analyses of an LHD system in mining, *The Journal of The South African Institute of Mining and Metallurgy*, January/February 2004.
125. Sarata, S., Hisashi, O, Hirai, Y. & Matsushima, G. (2006), Trajectory Arrangement of Bucket Motion of Wheel Loader, *National Institute of Advanced Industrial Science and Technology*, Tsukuba, Japan, pp.135-140.
126. Sarata, S, Hisashi, O., Kawai, Y., Tomita, F., (2004) Trajectory Arrangement based on Resistance Force and Shape of Pile at Scooping Motion, *Proceedings - IEEE International Conference on Robotics and Automation*, v 2004, n 4, p 3488-2393, 2004.
127. Scott A. (1991), "Potential Role of Technology in Improving Open Cut Coal Mining Performance," "*Proceedings Queensland Coal Symposium*", pp 31-36.
128. Schmid, M. & Hothorn, T. (2008), "Flexible boosting of accelerated failure time models," *BMC bioinformatics*, 9(1), 269.
129. Silverman, M. & Johnson, J. (2013), RME on FMEA, IEEE, 978-1-4673-4711-2/13.
130. Shields, S. (2017), Personnel Communication, March 27, 2017.
131. Smith, A. M. and Hinchcliffe, G. H. (2004), RCM Gateway to World Class Maintenance, Elsevier Butterworth-Heineman, Burlington, MA, USA. pp. 112-116.
132. Song, L. & Cooper, C. (2009), "Real-time Simulation for Look-ahead Scheduling of Heavy Construction Projects".
133. Song, W., Jacobsen, H.-A., Xia, X., Ye, C. and Ma, X. (2017), Scientific Workflow Mining in Clouds, *IEEE Transactions on Parallel and Distributed Systems*, Vol. 28, No. 10, pp 2979-2992, October 2017.
134. Stephen, K. (2013), Asset Management and Today's Mining Industry, *Canadian Mining Journal*, Oct. 2013, 124, 8, ProQuest, pp. 22 -31.

135. Stephens, R. I., Fatemi, A., Stephens, R. R., & Fuchs, H. O (2001), Metal Fatigue in Engineering, (2nd Edition), John Wiley & Sons Interscience, New York, New York. pp. 277-281.
136. Suchan, D. (2016), Personnel Communication, August 10, 2016.
137. Dodinov, M. T. (2009), Limitations of the Weibull disruption related to predicting the probability of failure initiated by flaws, *Safety, Reliability and Risk Analysis, Theory, Methods and Applications - Proceedings of the Joint ESREL and SRA-Europe Conference Volume 2, 2009*, Pages 1655-1662 Joint ESREL (European Safety and Reliability and SRA-Europe (Society for Risk Analysis Europe) Conference, Valencia, Spain, 22 September 2008 through 25 September 2008.
138. Tomlinsong, P. D. (1), (1998), Equipment Management, Kendall/Hunt Publishing Company, Dubuque, IA, USA, pp. 419.
139. Tomlinsong, P. D. (2), (1998), Equipment Management, Kendall/Hunt Publishing Company, Dubuque, IA, USA, pp. 308-309.
140. Tomlinsong, P. D. (3), (1998), Equipment Management, Kendall/Hunt Publishing Company, Dubuque, IA, USA, pp. 74.
141. Tomlinsong, P. D. (4), (1998), Equipment Management, Kendall/Hunt Publishing Company, Dubuque, IA, USA, pp. 235.
142. Sun, J., Zuo, H., & Liang, K. (2015), Remaining useful life estimation method for the turbine blade of a civil aircraft engine based on the qar and field failure data, *Jixie Gongcheng Xuebao/Journal of Mechanical Engineering*, 51(23), <https://doi.org/10.3901/JME.2015.23.053>.
143. Sun, Y., Li, X. S., & Guo, H. (2014), "Enhance Mining System Reliability Through System Integration Approach," *CSIRO Earth Science and Resource Engineering*.
144. Usta, I., & Kanter, Y., (2012), Analysis of some flexible families of distributions for estimation of wind speed distributions, *Applied Energy*, 89 (2012) 355-367, doi:10.106/j.apenergy.2011.07.045.
145. Van Noortwijk, J. M., van der Weide, J. A., Kallen, M. J., & Pandey, M. D. (2007), Gamma processes and peaks-over threshold distributions for time-dependent reliability, *Reliability Engineering & System Safety*, 92(12), 1651-1658.

146. Waghmode, L. Y. & Sahasrabudle, A. D. (2010, January), A Comparative Study of Life Cycle Cost Analysis of Pumps, ASME 2010 International Design Engineering Technical Conferences and Computer and Information in Engineering Conference (pp. 491-500), American Society of Mechanical Engineers.
147. Wenz, C. (2013), "Maintenance Life Cycle Planning - An Introduction," TMMG, Chesapeake, VA.
148. Wheelan, C. (2013), naked statistics, W. W. Norton & Company Inc, New York, NY, USA, pp. 201-202.
149. Wiley, M. (2002), Chapter 21. "Maintenance and Inventory," pp. 383, Lowrie, R. (2002), SME Mining Reference Handbook, Society of Mining, Metallurgy, and Exploration, Inc. Denver, CO.
150. Williams, T. Ribadeneira, X. Billington, S. and Kurfess, T. (2001), "Rolling Element Bearing Diagnostics in Run-To-Failure Lifetime Testing," Mechanical Systems and Signal Processing (2001) 15(5), 070-003.
151. Wu, X. and Cao, L. (2014), "Research on Management System of Coal Mine Equipment Maintenance Based on RCM," Applied Mechanics and Materials, Vols. 687-691, pp. 4844-4847.
152. Zhang, Y. M., & Lui, Q. L. (2002), "Reliability-based design of automobile components," *Proceedings of the Institution of Mechanical Engineers, Part D: Journal of Automobile Engineering*, 216(6), 455-471.

VITA

Eric Raymond Achelpohl has received B.S. and M.S. degrees in 1997 and 2001 in Mining Engineering from the Missouri University of Science & Technology, formerly the University of Missouri-Rolla (UMR). He received his PhD in Mining Engineering from Missouri S&T in May 2018.

Eric has specialized in the areas of equipment reliability, maintenance, mine planning, and explosives. At present he works for Komatsu Mining Corp, formerly Joy Global, as a Reliability Engineer in the Wheel Loader Product Support Group, where he has tracked wheel loader performance and monitored component lives in order to improve their reliability and productivity. Previously, he has worked for the Vulcan Materials Company, Zemex Industrial Minerals, and Peabody Energy in operations, maintenance, project management and engineering roles.